Simulating urban growth and its impact on the potential crop production of a coastal area in Greece

Msc.Thesis

Final report

Student name / Student number:

Georgios Konstantinidis / 8745577

g.konstantinidis@students.uu.nl

Supervisor:

Judith Verstegen

Responsible Professor:

Ron van Lammeren

Contents

Abbreviations used

LULC: Land Use and Land Cover

UGM: Urban Growth Model

PUA : Peri-Urban-Agriculture

FAO: Food and Agriculture Organization of the United Nations

CA: Cellular Automata

GIS: Geographic Information System/s

BAU: Business as usual

APR: Agriculture preservation

EEA: European Environmental Agency

RSA: Regulatory (or Strategic) Plan of Athens

CAP: Common Agriculture Policy

RS: Remote-Sensing

Acknowledgments

Throughout the writing of this work, I have received a great amount of help and assistance. I would like to give special thanks to my supervisor Judith Verstegen for her guidance, patience and effort during the whole process of this thesis. Her critical feedback and remarks together with inspiring ideas helped me overcome different obstacles and finalize this study.

Abstract

Peri-urban space and agricultural activities have proven to be critical in supplying urban population with healthy and proximate food. The special characteristics of peri-urban areas are a challenging parameter to consider when it comes to planning policies and strategies. As urban growth has historically proven to affect agricultural peri-urban areas it is important to assess its potential impacts and evaluate certain policies and plans.

Scenario-based, urban growth simulation models are widely used to test policies and plans for exploring potential impacts of future changes. Cellular Automata (CA) models are popular amongst others in modelling urban growth and land use and landcover changes, due to their ability to mimic complex real-world phenomena and interactions in an inherently spatial manner with simplicity and controllability. Furthermore, they are commonly used with Geographic Information Systems (GIS) and Remote Sensing (RS) data

This study uses the SLEUTH urban growth model (UGM) to simulate urban growth in the metropolitan region of Attica Greece under two scenarios of change towards 2050, to assess the total potential crop production loss of 12 selected crop classes. The scenarios implemented are based on policies mentioned in the Master Plans of Athens (former and newer version) for protecting and enhancing peri-urban space and agricultural areas. The business-as-usual BAU scenario represents current growth trends, while the agriculture-preservation APR scenario implements restrictive to urbanization measures on agricultural areas and a zoning system to preserve harvested area and production. Using SLEUTH's outputs together with crop spatial data, both scenarios are assessed and examined.

Keywords: Urban-growth-modelling, SLEUTH, Cellular-Automata scenario-based modelling, peri-urban agriculture, crop production, food security, Geographic Information Systems, regional planning, urban planning

1 Introduction

Urban growth historically affects agricultural peri-urban and rural areas, causing direct or indirect pressures which can lead to potential environmental degradation and socio-economic challenges (García-Nieto, et. al. 2018). Urban and peri-urban agriculture has been defined by Van Veenhuizen & Danso, 2007 as “the growing of plants and the raising of animals for food and other uses within and around cities and towns, and related activities such as the production and delivery of inputs, processing and marketing of products”. Moreover, it is believed that it can positively affect food security, local and national economy and the maintenance of landscape and biodiversity (Van Venhuizen et.al., 2007). According to Cecchini et.al., 2019, peri-urban cropland areas and tree crops have been considered for a long time, as “land waiting for urbanization” The worldwide swift towards sustainability and natural resources preservation has given peri-urban agricultural areas and tree crops a new meaning, especially in terms of the spreading demand of fresh and proximal food by urban population (Cecchini et.al., 2019). Peri-urban agriculture contributes in the development of local food systems, creates new support networks and can shape healthier dietary habits for urban dwellers with a positive environmental impact. In addition, it provides labour and housing opportunities (El Bilali et.al., 2013). Moreover, peri-urban areas provide products and high-value goods at minimum transportation costs, both financial and environmental (Moissidis & Duquenne, 1997). Follmann, et.al. 2020 underline that the continues urban growth and conversion of fertile agricultural land into built-up areas is a key challenge for food security and sustainability of urban and peri-urban areas.

As the process of urbanization continues, it is important to model and project urban sprawl patterns to estimate potential consequences and develop sustainable plans and strategies at different spatial scales (Jat et.al., 2008). Numerous of models have been developed to examine urban growth and LULC changes from different views and approaches such as Cellular Automata (CA), Artificial Neural Networks (ANN), fractal, linear or logistic, agent based, decision trees, etc (Santé et.al.2010, Berling-Wolff & Wu, 2004, Chen & Lin, 2009, López et. al., 2001, Rajan & Shibasaki, 2001 Shafizadeh-Moghadam et.al., 2017). Among those, CA models have been widely used as they are able to capture bottom-up phenomena successfully relying on neighborhood operations on defined grid cells (Triantakonstantis & Mountrakis, 2012, Syphard et.al., 2005, Musa et. al., 2017). CA have grown popular in urban growth modelling as they are easy to integrate with Geographic Information Systems (GIS) and able to incorporate spatio-temporal dimensions of urban growth processes with simplicity, flexibility and controllability (Yeh et.al., 2021).

1.1 Problem statement

There is evidence that urban areas tend to expand on the most productive soils, which is critical for agricultural activities and food production (Gardi et.al., 2015). The conversion of arable land into built-up areas creates indirect pressures in other locations too, as agricultural areas are forced to relocate elsewhere in a usually less productive soil (Cecchini et.al., 2019, Gardi et.al., 2015, d’Amour et.al., 2017, Martellozzo et.al 2018).

Plonka & Sroka, 2021, mention in their study that, peri-urban agriculture (PUA) areas can be sustained only if they are included in the regional and urban planning processes and policies. Furthermore, they outline that among different policies and tools that are nowadays implemented in many developed countries such as France, Canada, USA and Great Britain, zoning policies and agricultural buffers are of great importance. As Sarker et.al.2019 mention, incorporating urban (PUA) policies into spatial planning processes can minimize different threats to food supply in metropolitan areas which are related with climate change, land availability, water, oil, etc., as well as enhance regional economies. Thus, food production should be considered as an urban development concern, as functional food urban systems are an important component of sustainable development. Furthermore, Sarker et.al.2019 notice that urban planning in recent decades does not consider production systems, as a consequence of the swift from local to global production.

1.2 Research Aim

This study aims to simulate future urban growth in Attica region Greece, to assess the potential production loss due to urban expansion towards 2050 under two scenarios of change: a business-as-usual scenario (BAU) and an agriculture preservation scenario (APR). Hereto, a CA model of urban growth will be applied. The BAU scenario will project future changes, assuming the growth continues based on current trends. The APR scenario will simulate based on the implementation of sustainability policies and plans. Furthermore, agricultural areas are going to be examined together with crop data from different sources, to quantify the actual crop production and estimate potential future changes. The outcome of this study will provide a method for quantifying the impact of urban growth on crop production and harvested area in a temporally dynamic and spatially explicit way. The results can provide assistance to the responsible authorities, which can implement policies and plans for securing the annual crop production, control urban growth and ensure the future sustainability of the region.

1.3 Research questions

The main research question is:

- What is the impact of future urban growth in the Attica region up to 2050 on the potential total production of different crops under two scenarios of change: a business-as-usual scenario (BAU) and an agriculture preservation scenario (APR)?

The sub-questions arising are:

1. What are the drivers of change and how can spatial strategies and policies be integrated into an UGM?
2. What measures can be taken to protect and enhance peri-urban agriculture?

1.4 Limitations

This work will focus mainly on the expansion of built-up areas over agricultural without considering other LULC changes. Thus, the model will not estimate crop production loss as a result of other LULC changes. An important limitation to mention is the fact that due to lack of data, a global dataset for actual yield and harvested area provided the information about the crop production in the research area. Therefore, the data have lower spatial resolution, while having high statistical accuracy. Furthermore, both the estimation of potential yield and harvested area changes, is not included in this research and thus the latest available data will be used for future simulations.

2 Theoretical Background

2.1 Urbanization and urban growth

Urban growth is considered to be one of the most significant anthropogenic alterations of landscape (Patra et.al. 2018). Urban growth and LULC change are proceeding with higher rates in developing than in developed countries (Mohan et.al., 2011). In 2017, 4.1 billion people lived in urban areas and it is projected that by 2050 this number is going to increase up to 6.7 billion, representing the 67% of the global population which is expected to reach up to 9.8 billion. The term “urbanization” is widely used to describe the transition of people from rural into urban areas (Ritchie & Roser, 2018). Nowadays, more than half of the global population lives in urban areas, while this rate is estimated at 85% for the European countries (Ritchie & Roser, 2018). Urban growth on the other hand is the growth that intensifies the use of land for the construction of buildings and artificial surfaces. Urbanization is mainly expressed through urban growth, which can appear as a result of population growth, rural to urban migration and reclassification of urban and rural system (Hope, 1998). Across the Mediterranean basin peri-urban areas, sea coasts and lowlands have the highest population growth (Zitti, et.al.,2018). It is estimated that one third of the total population in the Mediterranean basin, is concentrated near coastal areas. The coastal population on those areas grew for more than 50% between 1980 and 2005 reaching up to around 150 million and it is projected to reach 200 million by 2030 (UNEPMAP QSR, 2021).

2.2 Peri-Urban space and agriculture

As mentioned before PUA involves by its definition activities related to food production near or inside the urban fringe. Whether peri-urban agriculture is considered similar with urban agriculture has been debated in terms of population densities and urban area patterns. Opitz et. al. 2016 describes peri-urban agriculture as a residual form of agricultural activities around the urban fringe of growing cities. Those areas are described as transition zones between the rural and urban district, where population and built-up densities are lower than inside the city. Although, those areas suffer from urban pressures, they also benefit due to the proximity with the urban fringe, market and culture. In developed countries these areas often consist of mixed land uses of urban and rural activities. Those vary from residential housing, small to medium scale agricultural activities (e.g. horticulture and semi-rural uses such as practice fields or a horse-riding camp (Wynne et. al 2016). According to Wynne et. al 2016 peri-urban areas have a critical role in providing healthy food to urban populations, especially when it comes to perishable food such as vegetables, eggs, fruits etc. It is also mentioned that those areas require a special attention, when it comes to planning processes, due to their characteristics, which discriminate them from both urban and rural systems. Moreover, it is underlined that planning mechanisms often are insufficient in protecting land uses such as agricultural production.

2.3 Managing peri-urban space

Shaw et.al., 2020 on their extended review on scientific literature on the peri-urbanization process in Europe have found that, due to their multifaced character peri-urban areas cannot be examined under a generic approach, but require a multidimensional approach to address both their spatial and socio-economic aspects, including all stakeholders involved in the planning process. According to the European Environmental Agency (EEA) the most significant drivers of artificial surface expansion on open areas are related to development. Those are: 1) housing services and recreation, 2) transport infrastructure, 3) industrial and commercial sites 4) construction sites, 5) dumping sites, mines and quarries (EEA, 2019). Spyra et.al (2021) refer to six examples of regional policy making for protecting peri-urban open space at a regional level. It is found that often policy making at a regional level is either rural or urban oriented in terms of actions and strategies, while ignoring undervalued open space. Furthermore, they refer to several policy instruments that were assessed during their research and found applicable based on both qualitative and quantitative findings. Some of those are :

- Promotion of compact settlement structures
- Encouraging the development of Natura2000 areas and other similar areas
- Long term sustainable governance methods based on supportive government environment

Other important findings indicate that policy improvements suggested for protecting peri-urban space, are related with changing the existing land use zoning systems, creating green corridors, developing sustainable activities, promoting the awareness of ecosystem services and their protection and others. In relation to that, the European Observation Network for Territorial Development and Cohesion (ESPON) describes in its main report several densification, regeneration and containment interventions for promoting sustainable urbanization and development (SUPER, 2020). Those include a total of 11 separate interventions on different countries. Some of those that have been found relevant are :

- The “Huerta de Valencia Spatial Plan” (2018) in Spain, which enhanced the protection of traditional Huerta (vegetable cultivations) by combining the protection of rural areas with support for agricultural activities
- The “Stockholm Urban Containment Strategy” (2017) in Sweden, which focused on controlling urban expansion by adopting a comprehensive perspective that gives attention to all sustainable development pillars, namely economic, social and ecological. This strategy gives special attention to rural land and the provision of affordable housing.
- The “Sustainable urbanization procedure” or Ladder Dutch strategy (2014), which is a rule that enable urban expansion on all zoning plans after arguing about its importance and examines the optimal solution, if the selected developed area is a greenfield and can be relocated elsewhere. Citizens can challenge those development plans in court.

A common characteristic found in several of those interventions, was the implementation of zoning criteria and a bottom-up approach, in terms of planning and policy making, where different aspects of the peri-urban space are examined.

2.3.1 The Master Plans of Athens

The urban expansion patterns in the metropolitan region of Athens have significantly changed since the postwar development from compact, to uncontrolled sprawl, polycentricism and nowadays a more regulated by planning policies system (Asprogerakas, 2016, Zitti, et.al.,2018, Colantoni et.al., 2016). Spatial planning system in Greece consists of numerous laws and regulations, which are not efficiently monitored and control. As a result, the spatial planning system responds slowly to changing circumstances. Out of these the Athens Master Plan , known as the Regulatory (or Strategic) Plan of Athens (RSA) describes both visually (with maps) and with an extended report all physical planning structures of the production sector, the transportation system, the technical infrastructure, as well as of the land and residence policy for the metropolitan region. Furthermore, it encompasses plans and policies for areas of special interest or special problems and it plays a coordinating role in development projects and studies related to the spatial planning.

There are two versions of RSA: 1) the former version, which was enacted initially in 1985 with Law 1515/1985 (Greek Government, 1985) and lasted until 2014 after many revisions, and the newer version for 2015-2020 (Asprogerakas, 2016). The main strategic objectives applied to both of these Master Plans are : a) balanced economic development and strengthening of the international role of Athens, b) sustainable spatial development, effective protection of the environment and cultural heritage and adaptation to climate change, and c) improvement of the quality of life by balancing the distribution of resources and the benefits of development. In practice though, both the former and the newer plan have shown deviations during implementation and bypassing phenomena were noticed. For example, during the preparations for the Olympic projects, major contradicting transformations of the urban fringe occurred, opposing to the regulations of the former Master Plan that further promoted urban sprawl. The new RSA directs towards the “compact city” as the main policy tool, aiming of climate change adaptation and ecological footprint reduction through lower planning levels (Asprogerakas, 2016).

The new RSA makes an extensive report on measures to be taken for urban expansion areas in Law 4277/2014, Chapter 4, Article 12 (Greek government, 2014). It is strongly oriented towards the “compact city” approach and this particular article outlines how new urban expansion areas are examined and developed. The policies are setting a clear restriction in diffusive growth and irregulated building (constructions outside the predefined urban extend from “Local Spatial Plans”), allowing the urban expansion only on areas, which are integrated into Local Spatial Plans (former municipality level Urban Plans) and underwent all the appropriate controls. Furthermore, the importance of the peri-urban area protection as a “vital” parameter of sustainable development, ecological balance and quality of life for the residents of Attica region, is underlined. The protection from urban sprawl phenomena should be regulated by urban spatial plans and building coefficients (coefficients that derive after research and act as a multiplier on defined surfaces for building activities, to indicate the maximum allowed surface and height of new buildings).

In addition to the abovementioned, in Chapter 5 of the Law 4277 (Greek government, 2014), the new RSA refers in detail on protection policies and measures to be taken for protecting the environment and biodiversity of the region, adapting to the problems of the climatic change. Forests and areas of high ecological value are protected strictly and land-use changes in those areas are not allowed. Moreover, the land uses of high productivity agricultural areas are not allowed to change, with the exception of cases of national interest. The agricultural land is referred as an important environmental and production resource and thus a zoning system based on the land-productivity is being implemented under the cooperation of three ministries.

Since Greece became a member of the European Union, there has been a constant effort to adopt European policies and regulations on development processes and spatial planning. Although many times in the past the practical implementation of Master Plans has shown deviations from the strategic goals set, it can be concluded that the metropolitan region of Athens has a regulated regional strategy, which is bottom-up oriented. As Asprogerakas, 2016 also underlines, Master Plans have a regulatory character and therefore they often don’t meet their goals as policy and planning processes tend to take a lot of time and undergo many changes until they are finally implemented. Although both of the Athens Master Plans outlined the need for the revision of Local Spatial Plans (e.g. General Urban Plans) of the municipalities in Attica, only recently have those plans been finalized in their majority. It can be concluded that although urban planning in Greece is traditionally weak (Asprogerakas, 2016), urban expansion is expected to continue in a regulated way with visible informalities.

2.4 Cellular Automata Modelling

Cellular automata (CA) are spatially and temporally discrete, abstract computational systems (Fransesco & Tagliabue, 2021). In a CA, a sub portion of the natural world is represented by a two-dimensional grid of cells. Cells are the smallest units within the system that display characteristics of adjacency or proximity. Each cell is characterized by its state, with all cells and their states being updated at frequent predefined intervals, commonly referred to as time steps (Fransesco & Tagliabue, 2021). Ilachinski (2001) pinpoints the five characteristics that, independently of each CAs specific purpose and unique configuration, are ever present within such a model. These are:

- The CA consists of a discrete n-dimensional lattice of cells.
- Cells exhibit homogeneity.
- Each cell takes on one of a finite number of predetermined states.
- Each cell can alter its own state based on itself and its neighbors
- Cells update their states according to a rule or a set of rules that take into account the aforementioned defined neighbors

The degree of success and popularity CA have achieved as a modeling and simulation tool is widely accredited to their ability to mimic complex real-world phenomena and interactions in an inherently spatial manner while maintaining a conceptually simple structure and design (Coulthard & Van De Wiel, 2013). The wide usage of such models to explain geographic phenomena results in continuous improvements and refinements to their design and implementation. Since the conception of CA, the earliest studies of which are largely accredited to John von Neumann in the late 1940s, continuous efforts have been made to refine CA, expand their capabilities and apply them in numerous fields of study. Several researchers (Kyparissas & Dollas, 2019, Zhang & Wang, 2021, Zaitsev, 2017) have proposed innovative and efficient ways in which one can expand the local neighborhood that affects a cell's state within a CA, allowing for more refined predictions that take into account interactions and rules of a more globally oriented nature. Earlier applications of CA usually focused on ecological theory and species interactions and behavior.

Study case examples include Caswell & Etter (1993) who aimed to identify the advantages of using CA as opposed to traditional competition and predation models when trying to simulate species behavior in a study area, Hogeweg (1988) who looked at the possibilities of utilizing CA functionalities to model the expansion of vegetation, and Chen et. al. (2002) who designed a CA to qualitatively and quantitatively model and assess underwater species growth in a Lake environment. As is true for all models and methodological frameworks linked to GIS and remote sensing technologies, the development of CA is greatly affected by advancements in soft- hard- and data ware, as well as improvements and refinements in conceptual models and theoretical foundations.

Development of new application is at the moment quite vibrant, with new cellular automata models being designed for an immense variety of phenomena of geographic interest, with a simultaneous growth in their utilization as a testing ground for theory, practice, policy and prediction (Torrens, 2009). Land use change modeling, quantification and simulation is an exceptionally fertile ground for the use of CA. Li and Gong 2016, mention about the wide use of Cellular Automata Urban Growth Models (CA-UGM) thanks to its simplicity, flexibility and intuitiveness. Some commonly used examples are mentioned such as the logistic-CA model, the Slope, Land cover, Excluded, Urban, Transportation and hill shade layer (SLEUTH) model and the neural network model. Scenario-based prediction CA models is believed to be one of the most promising applications in spatial planning and has been applied to simulate policy implementation (Feng et.al., 2019).

2.5 Cellular Automata and LULC change

CA-UGM are able to simulate and forecast LULC changes, as they assume that past trends of urban growth will affect future development, triggered by local and regional interactions (Aburas et.al., 2016). Several land use change and regional planning researchers have used CA, on its own or in combination with other modelling frameworks. Yang et. al. (2012) combined an ant colony optimization (ACO) probabilistic algorithm with Markov chains and CA models. ACO and CA were integrated in order to manage the spatial distribution of land use change and take into account the natural and socioeconomic factors driving it, while Markov chain analysis was employed to make long term forecasts. In Abdullahi's and Pradhan's work (2018) the merits of combining CA and weights-of-evidence functionalities to assist urban planning were outlined. The model designed proved highly effective in adhering to existing real world land use trends in the study area in a dynamic and spatially explicit manner, with the resulting prediction maps proving to be highly reliable compared to similar maps created by expert knowledge. Combining CA and artificial neural networks, Islam et. al. (2018) modelled and predicted changes in vegetation within a wildlife sanctuary, identifying slope, elevation and distance from the road and water networks as some of the main driving factors for the loss of vegetated land. To model land use, change efficiently and define the most prevalent amongst conflicting driving factors affecting the phenomenon, Feng and Tong (2017) used regression methods to accurately identify the most statistically significant driving factors to be taken into account when designing their CA. This allowed them to tackle multicollinearity issues and arrive at results that were free of data redundancy.

All aforementioned research cases took advantage of the conceptually simple principles of CA. A cell's state is converted based on a predefined set of rules. In the case of land use change CA, cells are converted according to the ultimate potential of the modelled area, the spatial and socioeconomic suitability of each land use at any given cell and the overall influence of surrounding land uses. General (global) rules can also be applied to all cells within the model's grid. By adjusting the extent of the local neighborhood as perceived by the model, researchers can extend the area of effect of all implemented rules or parameters.

Nevertheless, shortcomings in the performance and accuracy of CA land use change models can also be identified. Hu et. al. (2018) place the emphasis on the high dependency of a CA model's accuracy on the weight value of spatial variables, thus making it hard to explicitly account for complex spatially autocorrelated parameters. Regarding the need to simultaneously simulate past and future changes, Yang et. al. (2016) mention the complicacies arising from trying to account for past trends while at the same time predicting future developments. This is further emphasized by Kyparissas and Dollas (2020), who identify the need to design the optimal framework so as to configure a cell's state to depend also on its state in previous generations, by expanding a system and storing in every cell information from previous states. Finally, Pan et. al. (2010) look into the different aspects that represent scale in a CA (i.e. spatial extent, cell size and neighbourhood size) and the influence they have on each model's results, and emphasizing the negative impact different combinations of these aspects can have on a model's accuracy. For instance, changing the neighborhood shape (from scope to ring) and size (e.g. from 7x7 to 9x9) resulted in a significant shift in the model's accuracy. Based on the above, it is made evident, that CA land use change models need to be assessed, in terms of input datasets, procedures and results, so as to report the quality of each simulation and ensure that the model succeeds in reliably reproducing complex spatial patterns (Tong & Feng, 2020).

2.6 Study cases around the world on LULC change and agriculture

Studies at different scale of analysis have attempted to assess and predict urban growth and its impact on agricultural and natural areas (Zhou et. al.,2019, Martellozzo et. al., 2018, Liang et. al. 2020, Maithani et. al., 2007). Particularly in China, this field is very well documented, as extensive population and urban growth threatens food security (d'Amour et.al., 2017, van Vliet et.al. 2017). Cui et. al., 2019 study the impact of ongoing urban growth in China on cropland areas and food security applying the Markov-chain technique to simulate future cropland changes due to urban growth. Their results have shown that although China is still on an ongoing urbanization process the cropland areas are not expected to decrease sharply until 2030 and mentioned other important factors, which also imply food security problems, such as the spatial distribution of croplands and urban expansion on newly arable lands. Qui et. al. 2020, examines the cropland loss due to urbanization at a national level and the pressures observed from a city scale analysis of different magnitude (Mega-city, town and village) across China, to examine how unbalanced urbanization processes lead to cropland losses and food security problems.

At a European level, Barbosa et.al. 2017, modelled the land-take phenomenon across Europe in delineation with the milestone set by Commission on the Roadmap to Resource Efficient Europe (RERM) for no net land take by 2050 (Lavalle et.al., 2013). Verzandvoort et.al. 2009, estimated in their study that by 2030 Europe's prime agriculture area will be decreased by 20 Mha, and underlined that there is an increasing interest on prime agricultural land, due to the increasing demand of food and biomass production.

In Greece Zambon et.al., 2018, investigated in their study the role of fallow land in the metropolitan region of Attica considering their findings from environmental/agronomic and regional scientific aspects. An empirical analysis was carried out to investigate the complex relationship between spatial distribution of fallow land, agricultural landscape characteristics and urban sprawl, which indicated a relation between urban growth/containment, conservation of rural biodiversity transitions and fallow land as possible areas for urban expansion. A variety of related studies has been carried out in the Metropolitan Region of Attica. Colantoni et. al. 2016, studied about the urbanization driven land take processes in the Athens Metropolitan region for over twenty years. Their results indicated that built-up areas in Attica grew sharply, while cropland areas declined more than any other land use type. In relation with UGM, Gounaridis et.al. 2018, developed a CA-UGM, coupled with random-forest method (RF) to explore future LULC changes and dynamics in Attica region. Their results indicated that agricultural areas will decline for about 20% in the next 20 years (by 2040). Another study by Triantakonstantis & Stathakis 2015, modelled the urban growth of Athens, Artificial Neural Networks (ANN) to explore past trends of urban growth and provide future estimations for assisting planning policies for future scenarios.

3 Methodology

3.1 Overview

A schematic framework of this work is provided in Figure 1. This chapter outlines the tools and methods to be used for answering the research questions of this study. After studying related studies and literature, a scenario-based simulation method for projecting urban growth will be identified and applied. The results of the model will then be evaluated. Hereafter, an impact assessment will estimate potential crop production loss due to urban growth.

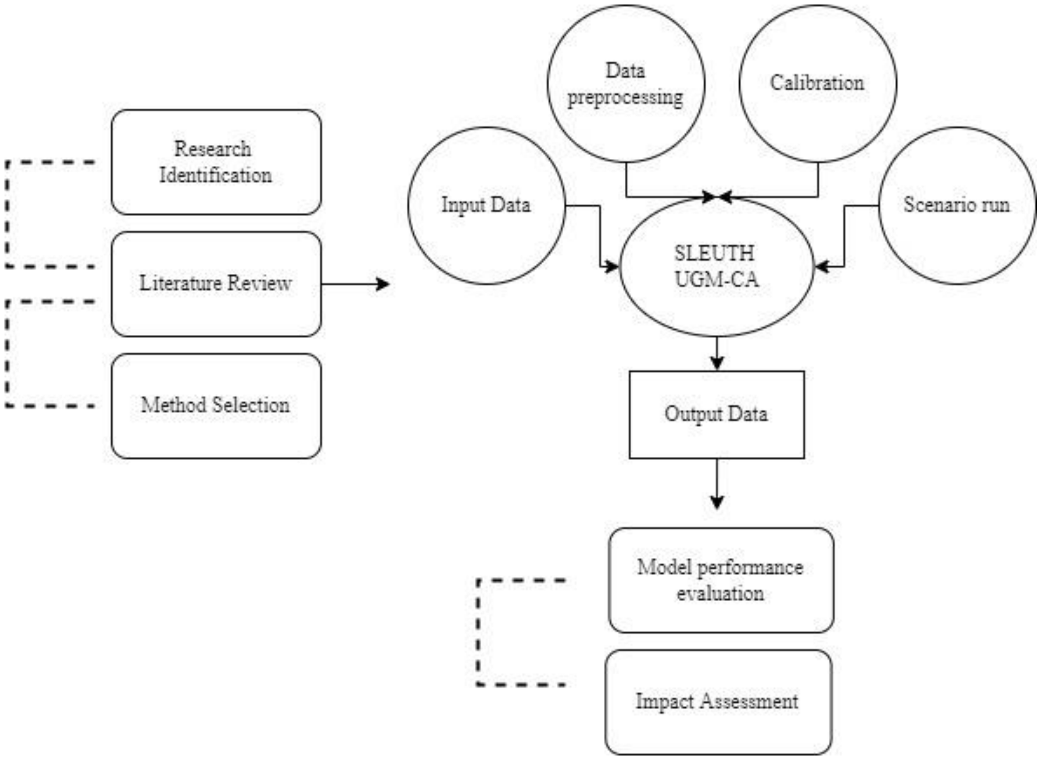

Figure 1: Schematic framework of study workflow

3.2 The SLEUTH urban growth model

In this research, SLEUTH is used to simulated urban growth. The SLEUTH CA based UGM, developed by (Clarke et. al., 1997) has been widely used among researchers its documentation and source code have been free for use since 1999, leading to multiple revisions and modifications. The SLEUTH model simulates urban growth by transition or growth rules (Table 1) that influence the cell state in a CA environment as a set of nested loops. The outer loop executes Monte-Carlo iterations, while the inner loop simulates the urban growth rules (Chaudhuri & Clarke, 2013). SLEUTH represents an acronym for the input layers required for the model to run. Those layers are: Slope, Land use, Excluded from urbanization, Urban, Transport and Hill shade (Sandamali et.al. 2018). For each iteration, diffusion, breed, spread, slope and road coefficients determine the behavior of the CA (Zhou et.al., 2019). Based on Silva & Clarke, 2002 and Clarke et.al., 1997 four different types of growth can derive, namely spontaneous, diffusive, organic and road-influenced.

Growth cycle order	*Growth type*	*Growth Coefficients*	*Description summary of transition rules*
1	spontaneous	Dispersion/diffusion	Selection of potential new growth cells
2	Diffusive	Breed	Growing new urban centers as a result of spontaneous growth
3	Organic	spread	Urban centers trigger additional growth
4	Road-influenced	Road – gravity, diffusion, breed	New urbanized cells tend to grow and expand towards the roadnetwork
During all	Slope resistance	Slope	Slope resistance on potential urbanized cells
During all	Excluded layer	User defined	Areas specified by the user to be resistant on urban growth

Table 1: Summary of growth types simulated by the SLEUTH model

The diffusion coefficient indicates the overall dispersiveness of the distribution both in the single grid cells and in the growth of new urban areas outward through the transportation system. The breed coefficient determines the probability of a random area to become urban and begin its own growth cycle. In this step the model selects if any of the newly generated urbanized cell, will become a new spreading center, by controlling if a newly urbanized cell has at least two neighboring urbanized cells. The spread coefficient determines the outward expansion of urban systems towards their edges. It is also called “edge-influence” growth. The road gravity coefficient influences urban growth towards transportation systems. In this step growth is triggered by the existing transportation network as well as the recently urbanized cells from the last three steps. The slope coefficient controls the probability of urban growth on steeper slopes. According to common knowledge lower slopes are easier to build upon than steeper. The steeper the slope the more unlikely for an area to be suitable for urbanization. The slope coefficient is applied for all the above-mentioned growth steps throughout each growth cycle. Last but not least, the excluded layer is used as a policy layer through every simulation step, it is user-defined and can determine areas that are excluded from urbanization even if they meet all other criteria. In addition to the beforementioned growth coefficients the model uses a second level of growth rules to respond on rapid or depressed growth rates, which are the sum of all four different types of growth and they are called ‘self-modification parameters.

This work is going to follow the SLEUTH method in developing the UGM, as it was found suitable for the research purpose in simulating scenario-based projections due to certain reasons. First of all SLEUTH is a CA model that was originally developed to simulate urban growth and no other LULC changes, making it very reliable on that specific subject. As Sakieh et. al. 2015, outlines the SLEUTH model is easy to apply compared to other LULC change simulation models such as the Conversion of Land Use and its Effect (CLUE) (Veldkamp & Fresco 1996), thanks to less data required. Furthermore, SLEUTH incorporates CA, which is capable of simulating complex urban phenomena and LULC changes and it is widely used for projecting different scenarios for policy implementation (Saxena & Jat, 2019). Huang et.al. 2008 , also outline that the SLEUTH model is robust in simulating urban growth, as it takes into consideration four different types of growth and has been used effectively for assisting urban management applications. As Yin et.al. 2018, also underline, a high advantage of the SLEUTH model is that it can relate the exclusion layer to a specific land-use or policy constraint and thus it is a legit method for simulating urban growth in a scenario-based approach.

3.3 Calibration of SLEUTH model

The calibration of SLEUTH is arguably the most important and time-consuming step of the model application, as it captures the urban growth uniqueness and achieves the model future simulation (Bihamta et.al. 2015). During the calibration phase the model compares the known historical data to simulated, in an effort to find those coefficient values that best model urban growth through time. The SLEUTH performs "brute-force" Monte Carlo runs through the historic data using every possible combination of the user defined coefficient values ("Project Gigalopolis", 2005). The calibration of SLEUTH includes three separate stages. Those are "coarse", "fine" and "final". The coefficient combinations computed during each calibration phase result into 12 metrics as described by Silva & Clarke, 2002, which are all written in the output directory. Some of those metrics are described in Table 2.

Selecting coefficient ranges between every calibration phase is also challenging. The Optimal Sleuth Metric (OSM), developed by Dietzel & Clarke 2007 was selected for this study to narrow down the coefficient range, as it is proven to be more effective than other methods used before. After each phase of calibration, the OSM code downloaded from ("Project Gigalopolis", 2005) can be run using the control_stats.log to calculate the "top 50" best fit values. This application sorts the coefficient values of the calibration phase, according to specific metrics that describe their optimal values.

In each stage the model is calibrated using a hierarchical spatial resolution method (Dietzel & Clarke, 2007). This means that each calibration stage, sequentially narrows the coefficient value ranges, while increasing the spatial resolution of the data. Therefore, the primary dataset to be used for the simulation should be resampled two times, namely one at ½ and one at ¼ of its own resolution. For the coarse calibration the coefficient values are set from 0 to 100 with a 25-step unit. Each combination of the parameters was simulated under 4 Monte Carlo iterations resulting into *n* number of runs. For the "fine" calibration stage the ½ resolution data are used. Based on the output of the "coarse" stage a new narrowed coefficient range, with a finer step is chosen and the calibration runs using 8 Monte Carlo iterations resulting into *n* amount runs. In the final calibration stage, the beforementioned steps are followed for the data at their initial resolution on 10 Monte Carlo iterations resulting into *n* number of runs.

After running the OSM code, the "top 50" text file sorts the values in a descending order based only on the OSM metric. Next the top 3 scores are chosen and the coefficient ranges for the fine calibration are selected. In the final calibration, only the top score of the "top 50" text file is selected and the corresponding values are chosen as the best-fit coefficient values. If a coefficient remains the same in all top scored simulations a finer user defined range must be selected

Using the best-fit coefficient values that derived after the final calibration step, the simulation from year 2015 to 2050 is initiated. The model will run for this timeline on 100 Monte Carlo iterations for each timestep of both simulated scenarios. SLEUTH simulates growth based on percentage probabilities scaling from 50% percent to 95%. For this study all probabilities above 50% are selected. The model creates output maps for each simulation year

Index	***Description***
Product	A composite index which is the result of all scores multiplied together
Compare	Comparison of modeled final urban extent to real final urban extent
r^2	Least square regression score of modeled urbanization compared with actual
Population (Pop)	urbanization for control years
Edge r^2	Least square regression score for modeled urban edge count compared with actual urban edge count for control years
R^2cluster	Least square regression score for modeled urban clustering compared with known urban clustering for control years
Leesalee	A shape index, a measurement of spatial fit between the modeled growth and the known urban extent for control years
Average Slope r^2	Least square regression of average slope for modeled urbanized cells compared with average slope of known urban cells for control years
X - r^2	Center of gravity[x]: Least square regression of average x values for modeled urbanized cells compared with average X values of known urban cells for control years
Y - r^2	Center of gravity[y]: Least square regression of average y values for modeled urbanized cells compared with average y values of known urban cells for control years
Rad	Least squares regression of standard radius of the urban distribution, i.e normalized standard deviation in x and y

Table 2: A selection of metrics produced by the SLEUTH model as described by (Silva & Clarke, 2002, Dietzel & Clarke 2007)

3.4 Evaluation of SLEUTH's performance

For the evaluation of the model performance the study followed the approach of Diezel and Clarke (2007), which indicates that out of the 12 metrics produced by each calibration phase, only 7 are needed to determine the goodness-of-fit of the model. This is proved in the study of Diezel and Clarke (2007), where 3 datasets were calibrated with all the 12 metrics that describe the goodbess-of fit of the model. The OSM metric is the product of those 7 metrics and has proven to be the most effective among others, such as the Leesalee metric, which was often used to narrow down the coefficient ranges during each calibration phase and select the best-fit coefficient values for future simulations. Those metrics are: compare, population, edges, clusters, slope, X-mean, and Y-mean metrics. To derive the OSM top 50 scores, the seven metrics ranging from 0 to 1, are multiplied together and the iterations are then sorted on a descending order, starting from the best scores calculated.

The Cohen's Kappa coefficient (Cohen, 1960) and its many revisions have been widely used for comparing two categorical datasets such as LULC maps and assess their similarities between observed and simulated/expected results (Equation 1).In essence Kappa is based on the percentage of agreement between to categorical datasets, corrected for the fraction of agreement that can be expected by chance. P(A) stands for the observed fraction of agreement, P(E) for the expected fraction of agreement given the distribution of class sizes and P(max) for the maximum fraction of agreement given the distribution of class sizes. Hagen (2002), refers in his article to two distinct statistics, namely K-histogram and K-location that explain both the similarities of location and the similarities in quantity. Kappa is now a product of K-histogram and K-location, as these metrics considerably improved the Kappa assessment for categorical maps. (Equations 2, 3, 4). Kappa can take values from perfect agreement 1 to no agreement at all -1. Values approaching 0 are an indication that the agreement equals the agreement that is expected by chance.

$$K = \frac{P(A) - P(E)}{1 - P(E)}$$

Equation 1: Cohen's Kappa

$$\mathrm{Khisto} = \frac{P(\max) - P(E)}{1 - P(E)}$$

Equation 2: Kappa histogram

$$\mathrm{Klocation} = \frac{P(A) - P(E)}{P(\max) - P(E)}$$

Equation 3: Kappa location

$$K = \mathrm{Khisto} * \mathrm{Klocation}$$

*Equation 4: Kappa as a product of Khisto * Klocation*

Van Vliet et. al, 2011 realized that the distribution of class sizes is not a meaningful reference level for models that simulate from an original LULC map. Applications, which model an area with fewer changes/transitions, yield better results than others. This high agreement though is not realistic as it does not prove an accurate simulation. Using the K-location and K-histogram, Van Vliet et. al, 2011 developed the K-transition and K-transloc (Equation 6). The first expresses the agreement of quantity of LULC transitions, while the second accounts for the degree to which the transitions agree in their allocations. Thus, they extended the Kappa coefficient to incorporate the distribution of class transitions starting from an original map (Equation 5)

$$K_{\mathrm{Simulation}} = \frac{p_o - p_{e(\mathrm{Transition})}}{1 - p_{e(\mathrm{Transition})}}$$

Equation 5: Kappa simulation

$$K_{simulation} = K_{transition} * K_{transloc}$$

Equation 6: Kappa-simulation as a product of K-transition and K-transloc

K-simulation provides a more meaningful reference level for assessing LULC such as an UGM, as it accounts for class transition and not just the size. K-simulation values that approach to 0 now are showing no or few transitions and high values are both depending on the agreement of both the class size transition and allocation, which is harder to achieve. In this study only two classes exist, namely "urban" and "non-urban", out of which, only one changes through time.

At this point, it must be mentioned that due to lack of time and data for this study, an independent validation of the model was not feasible. The original map used for this study is the starting year of the calibration, namely the urban layer of 1975. The evaluation period will be from 1975 to 2015, which is the last year of the model's calibration. To avoid any misunderstanding, word validation here is used as a reference to the process of assessing the parameter set during the calibration with an independent dataset. An independent validation would require a third map at a given timestep, which is not used during the calibration of the model. Hereafter, the simulated results would be compared with the third map at the given timestep (Van Vliet et. al, 2011).

Visser & De Nijs, 2006 developed "the Map Comparison Kit", which is an application that incorporates different map comparison algorithms. This application will be used to interpret the results of the evaluation and apply K-simulation after SLEUTH's calibration.

3.5 Impact Assessment

After running and evaluating the simulation of SLEUTH, the impact of urban growth on the potential crop production is going to be assessed. The crop production of a certain crop can only be calculated by knowing the yield y_i of this crop and its harvested area h_i (Equation 7). The total crop production P_{sum} is the weighted sum of the production P_i of each crop class i (Equation 8). Crop yield values of all crops will remain constant throughout this process as related parameters (i.e agroecological) will not be considered. Furthermore, the harvested area of the selected crops will not expand in future simulations. Thus, the latest data (2015) on harvested area will be used for the estimation of future impacts. The harvested area of all crops will be reduced over time as a direct effect of urban growth on agricultural areas.

$$P_i = h_i * y_i$$

Equation 7: Production for each crop class

$$P_{sum} = \sum_{i=1}^{n} (P_1 + P_2 + P_3 + \cdots + P_n)$$

Equation 8: Weighted sum of all crop's individual production

SLEUTH produces outputs for each simulation year, which are then overlayed on the total crop production to estimate the fractional change of production over time given a known yield starting from year 2015. Iterating this process for all model outputs in both scenarios, will provide information on the total harvested area and production loss during the 35 years span. Other statistical results will be calculated, such as the mean loss per year and a comparison of both scenarios will be implemented to underline similarities and differences.

In this study only the weighted total production of all 12 crops is assessed. By the same method, individual crop production of each crop selected can be computed too.

3.6 Study Area

The region of Attica is known for its high urban pressure as it includes the metropolitical area of Athens. The population of Attica region is estimated around 3.8 million and a total area of around 3000km^2 (ELSTAT,2020). Attica includes originally eight regional units but from those, the regional unit of "Islands" is excluded from this research, as it refers to island and specific coastal areas, which have significantly different development policies and plans from the rest of the mainland regions Figure 7.

The metropolitan region is economically oriented towards traditional and advanced services, public administration, manufacture and construction industries. Moreover, the population density of urban municipalities exceeds 5000 inhabitants/km, making it the most densely populated region in Greece (Salvia et.al., 2020). The geomorphological characteristics of the region determined the availability of land and urban expansion, especially after the postwar years. The plain where Athens city is located is surrounded by four mountains (Egaleo,Parnitha,Penteli and Hymmetus) with a maximum elevation around 1350 m and Marathonas, Thriasian and Messoghia plain (Gounaridis et.al.2018). According to national statistics, the total cultivated area in 2018 amounted around 3.220 ha (ELSTAT-Table 01,2018).

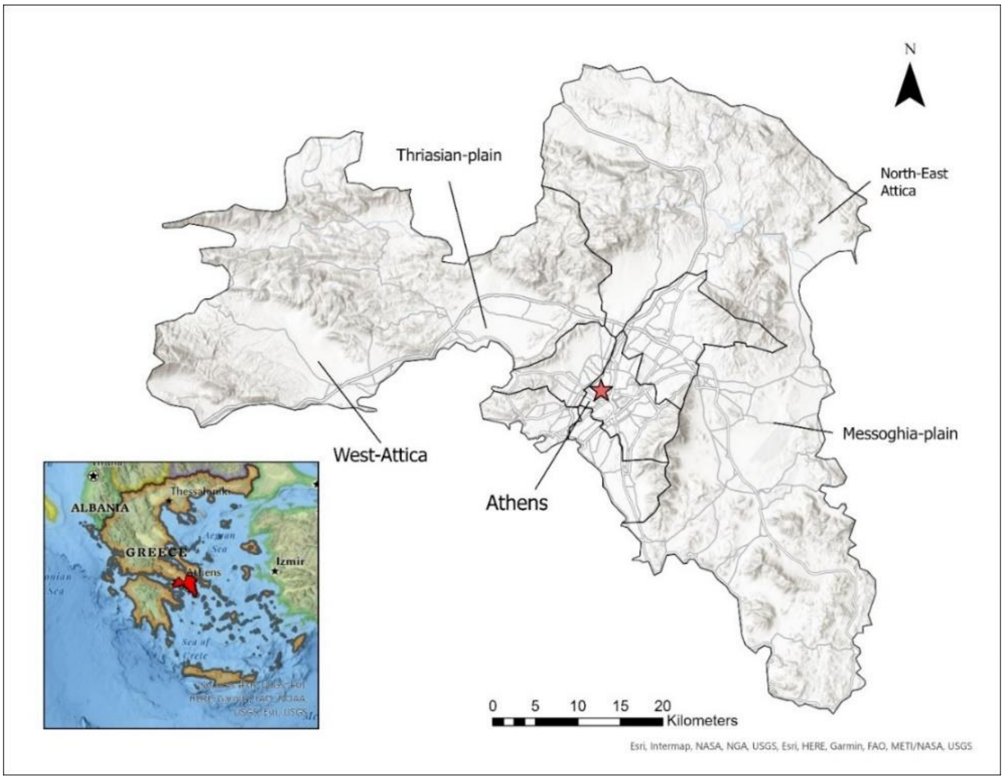

Figure 2: Map of the study area

The postwar development of Athens urban area has been wide examined under different scopes and views, as it encompasses an example of a transformation from compact growth to sprawl and polycentrism (Gounaridis et.al., 2018, Moissidis & Duquenne, 1997). Athens is a characteristic case of land-take processes. The wider metropolitan area experienced multiple waves of growth in the last two decades with dense and discontinues urban areas expanding over primary agricultural and natural land (Zitti, et.al.,2018, Colantoni et.al., 2016). The economic crisis in 2008 has vastly impacted Greece's economy and especially urban areas such as Athens. Aggregate food retail sales decreased sharply, while the total expenditure on food has increased its share of the total household consumption budget, showing critical signs of food poverty (Skordili, 2013).

3.7 Scenario Development

3.7.1 The Business As Usual (BAU) scenario

The BAU scenario assumes that the historical growth patterns of urban growth continue over the upcoming years. In different researches (Sakieh et.al., 2015, Goodarzi et.al., 2017, Wu et. al., 2010) this scenario is applied for projecting future urban growth based on the values of the growth coefficients that derived during the calibration phase. Thus, the BAU scenario will project future growth and potential crop production based on historical growth patterns in the study area together with certain constraints that describe the current policies and urban growth management. Those will be exclusion areas where urban expansion is not likely to appear in the future such as natural protected areas, forests and water bodies.

Sayas, 2006, describes the housing construction regimes in the Metropolitan area of Athens since the postwar era. In his study, he refers to the findings of other researches to set the scene for the urban expansion in the area. According to his study the wider region of the Athens Metropolitan Area underwent numerous changes, showing clear signs of uncontrolled sprawled development, which led to polycentricism. Furthermore, it is underlined that the urban development in the region is by no means linear. As mentioned before, Athens Metropolitan Area experienced multiple waves of urbanization in the last decades, resulting into the expansion of continues and discontinues urban areas over primary agriculture and natural land (Zitti, et.al.,2018, Colantoni et.al., 2016).

As forest and natural areas are protected by Greek law and policy regulations, according to Article 11, Law 1515/1985 (Greek Government, 1985) only agricultural areas expect to change as a result of urban expansion, although it is important to mention that those are also included in regulating and protection policies of Law 4277/2014 (Greek government, 2014), but are more vulnerable for bypassing. This scenario will assume that urban growth is allowed without restrictions on agricultural areas, while natural and forest areas will be partially or completely excluded. The BAU scenario will be used as the BAU excluded layer of SLEUTH and will be explained in Chapter 3.9

3.7.2 The Agriculture Preservation scenario

This scenario will give high priority on the implementation of strategies and policies that focus on controlling irregular urban expansion, while protecting and enhancing urban and peri-urban agricultural areas.

Summarizing the abovementioned findings (Chapter 2.3.1), the future urban growth in this scenario is considered to be a sustainable development strategy, which includes the driving forces of the BAU scenario together with new parameters, such as protection measures for high value agricultural areas. This scenario will focus on compact growth, which suggests that future urban development should take place adjacent to existing urban structures (Jabareen, 2006). Forest and natural areas will be completely excluded from urbanization. In delineation with the new RSA, agricultural areas will also be excluded partially. Unfortunately, due to the lack of data, it was not possible to include the zoning criteria on agriculture productivity, but instead this scenario will implement an urban expansion zoning system, by allowing urban expansion up to a defined distance from the existing urban areas as a compact city measure. The APR scenario will be used as the APR excluded layer of SLEUTH and will be explained in Chapter 3.9

3.8 Software to be used

SLEUTH is an open-source model, widely used, allowing an easy access to previous studies applied with detailed documentation ("Project Gigalopolis", 2005). The software selection for preprocessing and re/classifying the data is ArcGIS Pro and QGIS 3.16.3. The QGIS 3.16.3 proved very useful for downloading the road data from OSM, while it is also used as a controlling mechanism for certain tools and data preprocessing deriving from the ArcGIS Pro software. For the model development the open-source code of SLEUTH is going to be used ("Project Gigalopolis", 2005). The latest release (6/2005) SLEUTH3.0beta_p01 LINUX alongside with the Optimum Sleuth Metric (OSM), a small application for assisting the calibration process, will be downloaded. All files and applications run using the open software Cygwin ("Cygwin", n.d.), a large collection of GNU and Open-Source tools which provide functionality similar to a Linux distribution on Windows.

For evaluating the model's performance the 'The Map Comparison Kit" (MCK) software (Visser & De Nijs, 2006) is be used. The MCK is able to perform different map-comparison techniques and is especially used for categorical or nominal maps, such as LULC maps.

For the impact assessment step, the open-source PCRaster software (Karssenberg et.al., 2010) is used, to create a dynamic model which estimates the impact of future urban growth on crop harvested area and production both visually and statistically. PCRaster is a GIS which consists of computer tools for storing, manipulating, analyzing and retrieving geographic information. PCRaster contains also a scripting model development environment, which supports scripting languages such as PCRcalc and Python. All scripts will be developed inside the Spyder computational notebook using Python programming language.

3.9 Data and Preprocessing

In Table 3, the data to be used for this study are presented. Following the SLEUTH method, the layers needed for running the model are slope, land use, excluded from urbanization, urban, transport and hillshade. Thus, the known data for the model's input are elevation, land use and land cover (LULC), built up areas, road and exclusion areas, which are mostly data regarding natural protected areas, water bodies, forests, etc.

Data to be used for the impact assessment are also mentioned in Table 3. Those are related with crop data on yield and harvested area. Those data will be used to create the crop maps and estimate the total production of certain crop classes based on the yield and harvested area values of different crops.:

Type	***Dataset***	***Source***	***Description***
	Data to be used for SLEUTH		
Elevation (Slope, Hillshade)	EU-DEMv1.1	Copernicus	Elevation dataset at 25m spatial resolution for all European countries,will be used for slope and hill shade layers.
Built-up (Urban) data	GHS_BUILT (Corbane et.al., 2018).	Global Human Settlement Layer (GHSL)	Built-up data from 1975, 1990, 2000, ,2015
Road data	Open Street Maps	OSM	Road network data for at least 2 different periods: present & past
Excluded layer data, Land Use and Land Cover data (LULC)	Natura 2000 dataset & Corine Land Cover (CLC) (2018)	European Environmental Agency (EEA) Copernicus	Natura 2000 and protected areas
	Data to be used for the impact Assessment		

Agricultural data	GAEZv4 ,2015 (Frolking et.al, 2020) Actual yield & harvested area data per 5-arcminute grid cell	Harvard Dataverse	Data on crop measurements for different yields (yield, harvested area, actual production)
Other statistical data	Regional data on actual production & harvested area Food supply quantity per capita for year 2015	Hellenic Statistical Authority, 2015 FAO,2015	Crop harvested area and production based on the national statistical database of Greece Food supply per capita per year (kg/capita/year) based on FAO statistics for Greece in 2015

Table 3: Data and datasets used in this study case.

In order to reduce the amount of data and create the excluded from urbanization layers for SLEUTH, a reclassification process of the CLC classes is needed. The CLC dataset is only used for the development of SLEUTH's exclusion layers, as policy implementation layers. The reclassification process is about aggregating classes with similar characteristics to a larger class. Table 4 shows the reclassification of the CLC classes into aggregated new classes.

LULC aggregated class	***CLC level 2 class***
Built up areas	Continuous urban fabric, Discontinuous urban fabric, Industrial and commercial, Port areas, Airports, Mineral extraction sites, Dump sites, Sport & Leisure facilities
Roads	Roads
Arable land	Non & permanently irrigated arable land
Permanent crops	Vineyards, Fruit trees and berry plantations, Olive groves, Complex cultivation patterns and Land principally occupied by agriculture
Semi-Natural areas	Pastures, Natural grassland, Transitional woodland-shrubs, sparsely vegetated areas, Inland marshes, Salt marshes,
Water bodies	Water bodies, Coastal lagoon, Sea and Ocean
Forest & natural areas	Broal-leaved forest, Coniferous Forest, Mixed Forest, Burnt areas*, Sclerophyllous vegetation, Green urban areas*

Table 4: Reclassification of CLC classes of the Corine landcover 2018, Natura 200

*Burnt areas and green urban areas are classified as Forest & Natural as they are expected to be protected and preserved.

For the development of the urban growth model, the built-up layer is going to derive from the Global Human Settlement Layer GHS-BUILT dataset (Corbane et.al., 2018). The data from GHSL are going to be preprocesses and resampled to match the attributes of the other input layers of the model and will act as an independent layer during the development step. This layer will be the active layer of the model, which will simulate urban growth.

Computing the total crop production of the study area requires spatial and statistical data about harvested area and yield of existing crops in the research area. GAEZv4 provides a grided dataset of 5 arc-minute (almost 10km) resolution (Frolking et.al, 2020) including 26 different types of crops. The decision to apply this dataset for this study is made as it has the highest spatial resolution on a variety of different crop products, it is free for use and is the most recent (2015) among other datasets that were examined such as MAPSPAM (2010) and is based on data from FAO. Moreover, it provides a spatial distribution of the actual yield and harvested area of each crop, which will be used to create production maps. To assess the accuracy of the selected dataset, GAEZv4 data are compared with national statistical data from the same year.

Table 5, provides an overview of the selected 12 products for the research area, after reviewing local statistics from the Hellenic Statistical Authority for the year 2015, that were matching with the data included in the GAEZv4 dataset.

Crop classes from GAEZv4 dataset	
1.Barley	7.Olives
2.Cotton	8.Other cereals**
3.crops NES*	9.Potato & sweet potato
4.Fodder crops	10.pulses
5.Maize	11.sugar beet
6.wheat	12.vegetables

Table 5: Selected crop classes from the GAEZv4 dataset based on local evidence from the Hellenic Statistical Authority,2015

* Crops NES are crops that are not listed in the 25-crop list of GAEZv4. It includes all other crops from FAOSTAT production domain

**Other cereals include: Buckwheat, canary seed, mixed Grain, oats, corn, quinoa, rye, triticale

The preprocessing step involves the estimation of each crop production using the total harvested area (rainfed & irrigated) and the mean yield (rainfed & irrigated) of the GAEZv4,2015 as shown in Equation 7. The resulted crop production layers are then compiled together into a single total production layer based on Equation 8. Because all other data where resampled into 100 m grid cells it was important to estimate the per hectare values of both raster layers. To do so, the 5 arc-minute grid cell had to be converted from degrees into meters given a known latitude & longitude. By approximation this resulted into 9297 meters grid cell given the fact that the initial values indicated 0,08333 degrees and 1 degree is approximately 111.000 meters. Knowing the approximate size of each grid cell for that particular region, allowed the calculation of the fractional value of total harvested area per hectare between 0 and 1. This will allow to compute the approximate total production value per hectare and the potential loss after the simulation for both scenarios. All preprocessed layers can be viewed in Appendix A.

After preprocessing the GAEZv4 data (Frolking et.al, 2020) for the total harvested area and production for the first year of the simulation (2015) were compared with national statistical data (Hellenic Statistical Authority, 2015) from the same year to evaluate their statistical accuracy. The total amount of harvested area of the selected 12 crops corresponded to more than 90% of the total harvested area of all crops existing in the study area, which makes them a solid sample for analysis (Table 6). Moreover, the total amount of harvested area and production of the GAEZv4 data agree to more than 80% and 74% respectively with the same amount reported in the national statistical data for the 12 selected crops. Those results of a relative high agreement indicate a relatively good representation of the actual statistical data in the modelled data.

Total harvested area of Attica in 2015 for all crop classes (National statistics)	Total harvested area of Attica in 2015 for the selected 12 classes (National statistics)	Relative amount of total harvested area of the selected 12 crops to the total of all crops existing in the study area (National Statistics)	Total harvested area of Attica in 2015 for the selected 12 classes (GAEZv4 data)	Agreement of GAEZv4 data with the National statistics for the harvested area of the selected 12 crops in 2015	Total production of Attica in 2015 for 12 selected crop classes (National statistics)	Total production for 12 selected crops for 2015 (based on GAEZv4 data)	Agreement of GAEZv4 data with the National statistics for the production of the selected 12 crops in 2015
40974.3 ha	37043.8 ha	90.4%	29675 ha	80.2 %	198017 tonnes	267898.9 tonnes	74%

Table 6: The table shows the comparison between the national statistics and the GAEZv4 data in terms of harvested area and production for the total amount of the selected 12 crops (Barley, Cotton, crops NES, Fodder crops, Maize, Olives, Other cereals, Potato & sweet potato, pulses, sugar beet, vegetables, Wheat). Furthermore, the table provides an overview of the total amount of harvested area for the 12 crops selected in comparison to the total amount of harvested area of all crops existing in the region, based on the national statistical data.

3.9.1 Preparing the SLEUTH model

The SLEUTH urban growth model requires 5 input data layers to run. Those layers must be compiled as grayscale .gif image files. For all the input data layers, 0 is an inactive value, while 0 < n < 255 is an active value. Furthermore, all input data layers must have the same extend (same number of rows and columns 933x802), spatial resolution (same cell/pixel size 100x100) and projection to address the model's requirements. The resolution of the input datasets was resampled at 100 m (x and y) and all data where re-projected to "GGRS 1987" geographic coordinate system, which is the national projection system of Greece. Moreover, the data have been further resampled, two and four times the size of the chosen resolution (100 x 2 = 200m, 100 x 4 = 400m) to address the requirements of the calibration step. Hereafter, the data are clipped inside the research area boundaries. Data outside the clipped area have been assigned with a non-existent value. For statistical reasons , at least four urban and two road time periods must be used. All input data layers derived from the preprocessing step can be viewed in the Appendix A.

The slope and hillshade layers derived from, the European Digital Elevation Model (EU-DEMv1.1). Although the hillshade layer acts only as a background layer and does not affect the simulation, slope is considered a critical parameter for urban growth in the model. The model cannot urbanize cells on slopes greater than 21% by default and therefore, after some research on the study area this, critical slope value was increased to 51%.

SLEUTH requires the urban extend data of at least four different time periods, in order to derive a sufficient estimation of the research areas urban dynamics during the calibration. For this purpose, the multitemporal dataset GHS_BUILT (Corbane et.al., 2018) was used, which includes data from 1975, 1990, 2000 and 2015. The model simply requires a binary classification of urban/non-urban areas with 0 being non-urban and 0 < n < 255 urban.

The road network layer can greatly affect the development of the region as road influenced growth included in SLEUTH simulates the attraction of urban growth towards increased accessibility locations. For calibration purpose, the model requires at least two road data layers of different time periods. The road network layer can be either binary, same as the urban layer, or have relative values. First one assigns the same accessibility value to the whole network, while the second one allows the user to categorize the network with different values. In this case a binary representation of the road network was selected for the time periods 1990 and 2021.The road data were downloaded using the QuickOSM tool in QGIS 3.16.3. This tool provides the user with the ability to extract spatial units from the OSM. To derive the road network of an earlier time period, a high-resolution image of 1990 was downloaded using the Google Earth Pro software. This image acted as a background reference layer, which was used to subtract those road segments that weren't present at that time and derive the earliest road network layer for SLEUTH

3.9.2 Excluded / Scenario layers

The excluded layers are used to indicate locations that are partially or completely resistant to urbanization processes and act as policy layers for the scenario implementation. All preprocessing outputs can be viewed in Appendix A. The excluded layer in SLEUTH is assigned with values that range from 0 to 255. Locations that do not contain any restriction measures have a value of zero. The development of the BAU scenario followed the approach of Oguz, et al., (2007) by assigning on the data layer, probabilities of exclusion or levels of protection. Values ranging from 0% to 100% can be assigned to the excluded layer, in case the user chooses to represent partially exclusion locations with values > 99% being completely excluded. For the calibration of the model the BAU excluded layer was used. Locations with low or no resistance are presented with darker pixels. The brighter the pixel, the more resistant to urbanization. For the creation of this layer, the latest CLC (2018), the Natura 2000 and the latest GHSL_BUILT (2015) datasets were merged and reclassified based on Table 4. The derived classes were assigned resistance values scaling from 0 to 100 percent (values >99% received the value 255). More specifically, Table 6 presents the resistance values assigned to each class for the BAU scenario. The Natura 2000 protected areas were merged together with the re-classified LULC classes. The merged locations of the two datasets were assigned the added value of both.

It is important to mention at this point, that the reclassified CLC(2018) built-up class does not overlap with the GHSL_BUILT urban class. Thus, it was decided to keep both of these classes in the excluded layer as urban and available for urbanization. The UGM of SLEUTH though, will simulate the urban expansion only based on the GHSL_BUILT dataset, as it is far more accurate than the classified CLC(2018) Built-up class. This means that urban expansion can be simulated on locations indicated as built-up too. This area will present potential open space that is neither urban or agriculture and is available for urbanization.

Excluded layer classes	**Resistance Value %**
Built up areas +open spaces	0
Roads	100
Arable land	0
Permanent crops	0
Semi-Natural areas	40
Water bodies	100
Forest & natural areas	80
Natura 2000 protected areas	**+20**

Table 6: Exclusion layer classes and resistance values for BAU scenario

For the APR scenario, this study followed the compact city approach to create zones of development for controlling urban sprawl. Furthermore, this scenario suggests that agricultural areas should be protected considering, Law 4277/2014, Chapter 4, Article 12 (Greek government, 2014). Due to lack of data on Local Spatial Plans, the accurate extend of areas for urbanization could not be defined based on published plans. Therefore, an approach used by Huang et. al. 2008 was decided to be followed. According to that two buffer zones of 1 and 2 km distant from the existing urban areas were created. Areas inside the first buffer zone are fully developable, while areas between the first and the second buffer zone have a 50% resistance to urbanization. All other areas outside the 2km buffer zone are fully excluded. To adjust this approach on this study the following steps had to be followed. First the GHSL_BUILT(2015) urban layer was used to derive the buffer zones. This process included several steps of data transformation and reclassification. On the same time the BAU excluded layer, created in the previous step, was redeveloped to include resistance values for agricultural classes too. Table 7, shows the values assigned on the APR excluded layer classes. The development zones are finally merged with the resistance layer to derive the final outcome.

Exclusion layer classes	**Resistance Value %**
Built up areas	0
Roads	100
Arable land	40
Permanent crops	60
Semi-Natural areas	40
Water bodies	100
Forest & natural areas	80
Natura 2000 protected areas	+20
Zone 1000m	**+0**
Zone 1000m to 2000m	**+50**
Areas outside the 2000m zone	**+100**

Table 7: exclusion layer resistance values for the APR scenario

It should be noted that the calibration of the model was conducted only for the BAU scenario excluded layer, as it is assumed that this perspective follows the historic growth patterns. SLEUTH applications in their majority use only one excluded layer in calibration. Next, they simulate different scenarios of change, using different excluded layers. (Akın et.al. 2014).

4 Results and discussion

4.1 Calibration results

In general, each calibration phase yielded higher OSM values (coarse >0.7, fine > 0.8 and final > 0.9) than the previous one (Table 9). The high OSM values in each calibration phase indicate the success of the model in mimicking the trend of urban growth in the study area. Therefore, the best-fit coefficients (Table 8) can be reliably used for simulating future scenarios of change.

The diffusion coefficient of 40% shows, that new detached urban cells are simulated, while the low breed coefficient 1%, shows that those detached areas are not expanding further. Moreover, the spread coefficient of 8% is an indication that existing urban centers or clusters of urban cells, generate new cells on their edges but not extensively. The slope coefficient of 23% indicates that urban areas on steeper slopes are not expanding further, but up to a certain point (i.e critical slope of 51%), growth is expected to occur. Finally, the road gravity coefficient is very low as roads will probably attract minimum growth.

As described by (Houet, et.al. 2016) the model simulates future changes by mimicking past trends derived from the internal model’s functionality during the calibration phase. A drawback related to this in the scenario implementation is that the calibration is possible to limit the effect of a pattern breaking scenario, by consistently replicating past trends, especially in terms of magnitude. This happens due to the fact that SLEUTH is calibrated with the use of only one exclusion layer Another drawback in the implementation of SLEUTH is the time-consuming calibration phase, which is critical for the model’s performance. Furthermore, it is proven that in terms of accuracy assessment, the uncertainty increases in long-term simulations. (Chaudhuri & Clarke, 2014).

Coefficient	*Coarse*	*Fine*	*Final*	*Best-fit value*
Diffusion	{0 - 100, 25}	{0 - 50, 10}	{10 - 40, 6}	40
Breed	{0 - 100, 25}	{0 - 50, 10}	{0 - 50, 10}	1
Spread	{0 - 100, 25}	{0 - 20, 5}	{0 - 10,2}	8
Slope	{0 - 100, 25}	{15 - 35, 4}	{10 - 50, 8}	23
Road gravity	{0 - 100, 25}	{0 - 100, 20}	{0 - 100, 20}	1

Table 8: Results of SLEUTH's calibration for the period 1975-2015. Coefficient ranges selection after sorting on the OSM metric, for all calibration phases (coarse, fine and final) and the deriving best-fit coefficient values.

Coarse calibration results					
OSM	*Diffusion*	*Breed*	*Spread*	*Slope*	*Road gravity*
0.76910025	1	50	1	25	1
0.76910025	1	50	1	25	25
0.73566127	50	1	1	25	1
0.73566127	50	1	1	25	25
0.73004967	1	1	1	25	50
0.73004967	1	1	1	25	75
Fine calibration results					
0.86927617	10	50	5	19	40
0.86225563	30	1	5	27	1
0.86225563	30	1	5	27	20
0.8560881	40	10	5	35	80
0.8560881	40	10	5	35	100
Final calibration results					
0.90395153	40	1	8	23	1

Table 9: Top scores of OSM values during each calibration phase. The table shows the selection of the top 3 scores during the "coarse" and "fine" calibration step together with the top score of the "final calibration step"

4.2 Evaluation of SLEUTH's performance

The comparison of the modelled with the actual urban growth for the period 1975 to 2015 showed that the model performed well for the purpose of this study. The contingency table, which resulted after the comparison of the actual and modelled maps describes quantitatively the amount of agreement and disagreement in cell number between the two datasets (Table 12). All maps can be viewed in Appendix B.

K-transition and K-transloc are 0.73 and 0.36, respectively, which is way above 0 and an indication that SLEUTH explains both the number of land-use transitions and the allocation of these transitions better than can be expected by chance, given the total number of transitions. K-simulation scores above 0 does not necessary indicate a good simulation of urban growth, but for this study the results will be accepted. K-simulation of 0.25 will be accepted in this research, as it showed that the model explains past changes relative well.

More specifically the value of K-transition 0.73 is high, approaching 1, which is an indication that the amount of each class transition is explained well by the model. On the other hand, the low value of K-transloc indicates that the simulated changes were not correctly allocated in their majority during the model simulation. K-simulation does not usually provide high scores such as Kappa, because it accounts for the fractional agreement of class transitions and not just class sizes (Van Vliet et. al, 2011).

SLEUTH's results were not independent validated. In order to assess the model's performance, independent observational data must be compared with the ones simulated by the model (Van Vliet et. al, 2011). Because all data were used during the calibration, K-simulation results with the use of independent comparison data could be much different. Another remark is that K-simulation results were affected by the selection of all outputs higher than 50% probability. Selecting outputs based on higher probabilities than 90% for example could have different results in SLEUTH's assessment

Map categories

Actual map 2015 \ Modelled map 2015	**Non-urban cells**	**Urban cells**	**Sum Map 1**
Non-urban cells	228185	11484	239669
Urban cells	5279	3443	8722
Sum Map 2	233464	14927	248391

Table 12: Contingency table of actual and modelled map for year 2015.The table shows urban and non-urban land use that exist in the actual and not the modelled map and vice versa. The diagonal indicates cells that have the same land-use in both maps.

K-simulation	0.2583
K-transloc	0.35605
K-transition	0.72545

Table 13: K-simulation results

4.3 Simulation results and Impact Assessment

4.3.1 Simulation from 2015 to 2050

Urban growth in both scenarios occurred on the peri-urban fringe of existing urban centers and did not have any particular difference in terms of growth patterns. Both scenarios showed that during their 35-year simulation, urban growth was more extensive than it used to be for the past 40 years (1975 - 2015). The BAU scenario showed 82% and the APR scenario 46% more growth than observed in the past for about the same time span (Table 14). Another characteristic of both scenarios is that they didn't show diffusive growth with exception of some minor cases in the BAU scenario. BAU simulated almost 20% more growth than the APR (Table 14). Furthermore, existing and newly created urban areas in the BAU scenario become far denser (Figure 3). BAU produced relative more growth in the western and eastern areas of the region, while both APR and BAU simulations show similar results on the peri-urban fringe of Athens (Figure 3).

The implementation of resistance values in both scenarios prevented growth on certain areas as planned, but it should be mentioned that those values were randomly selected. Other approaches direct towards Multi-Criteria-Evaluation (MCE) for assigning resistance to urbanization values to LULC classes, in an effort to create urban growth suitability maps (de Noronha et. al 2012, Asgarian et. al 2018)

In the APR scenario agricultural areas included increased resistance values to urbanization and an additional zoning criterion was implemented, which was selected to partially or fully exclude areas on a certain distance from the existing urban centers as described by (Huang et. al. 2008). The zoning criterion secured certain areas in the APR scenario but did not change the pattern of growth or the total amount noticeably. This is explained due to lack of information on different zoning systems that may exist in different parts of the region.

The scenario development in this study was based on the Master Plans of Athens and therefore both BAU and APR shared similar characteristics. The exclusion layers were created using a free representation of certain policies included in the Master Plans such as resistance to urbanization values, protection and enhancement policies and zoning criteria. Because Master Plans only provide a vision for the region with arbitrary spatial characteristics, this study suggests the use of more specific plans for describing spatial planning policies and strategies such as the “Local Spatial Plans”. Those are the urban plans of each municipality in the region and include local characteristics for development and specific zoning tools to be applied with respect to local characteristics (Asprogerakas, 2016).

Past change			**Future simulated change**		**Past/Future change**		**APR/BAU change**
Urban area in year 1975	Urban area year 2015	Observed change 1975-2015 (40 years)	BAU simulation for 2015 - 2050 (35 years)	APR simulation for 2015 – 2050 (35 years)	Percentage difference of past observed and simulated change for BAU scenario	Percentage difference from past and simulated change for APR scenario	Percentage difference of APR with BAU scenario
43748 ha	52625 ha	8877 ha	16141 ha	12941 ha	82 %	46%	20%

Table 14: Output results of the BAU and APR scenarios for the year 2050. The table shows urban growth in hectares between two time periods, namely 1975-2015 and 2015 – 2050. The first period indicates the actual growth that occurred during this 40-year span and acts as a reference point for comparison with the second period. The second period is referring to the simulated by the model future growth and expands for 35 years. Those two periods are compared for both scenarios, showing percentagewise the increased growth that occurred in the BAU an APR scenarios in relation to past growth.

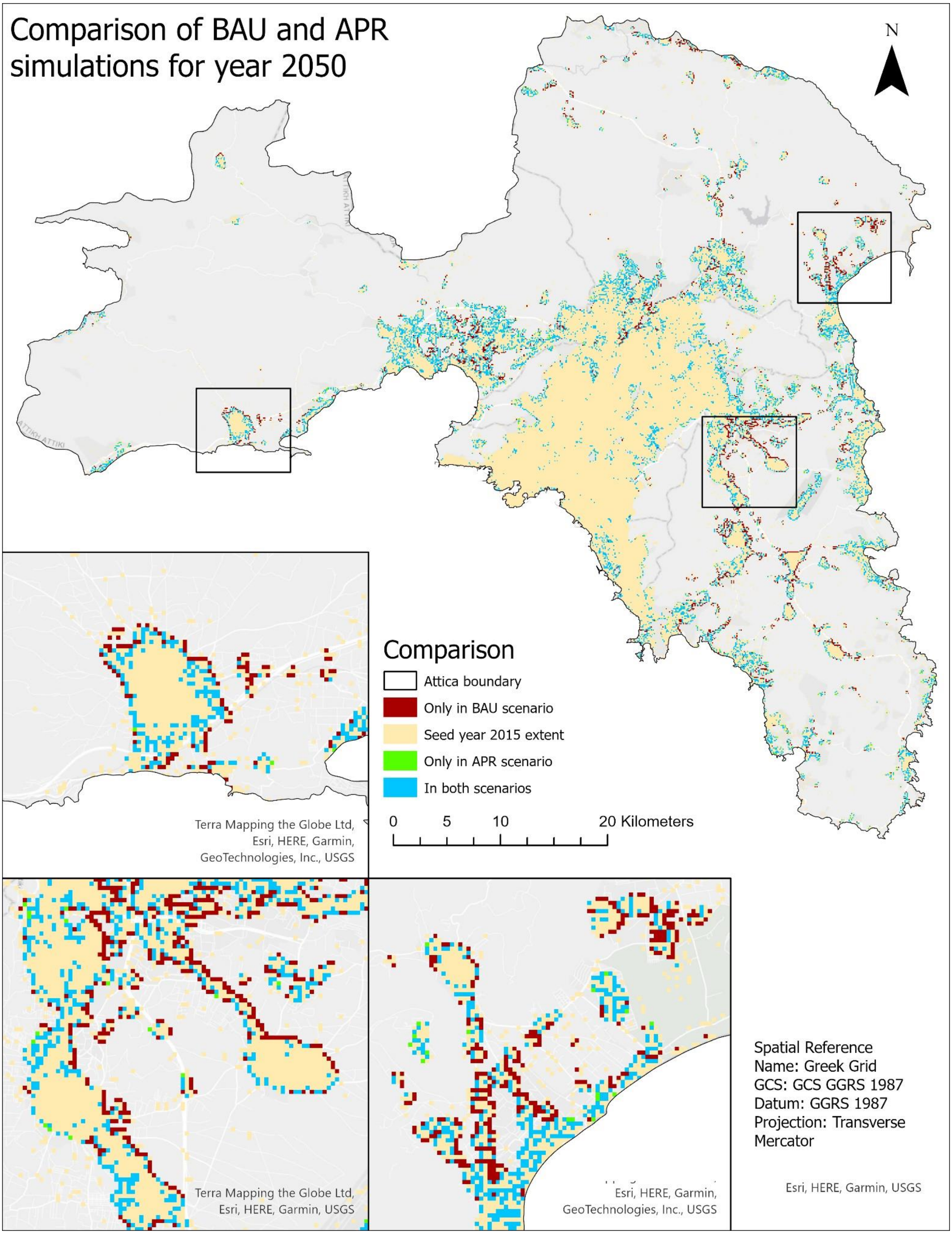

Figure 3: Comparison of simulated results for the BAU and APR scenario for 2050. Each cell is 1 ha of urban area. Red cells indicate areas of urban growth that occurred only in the BAU scenario. On the other hand, green cells indicate urban growth that occurred only during the APR simulation. Urban areas that expanded in both scenarios have the blue color, while cells that indicate the seed year (2015) have yellow color. Areas of the eastern and western parts of the region were selected to indicate noticeable differences between the two scenarios

4.3.2 Impact Assessment

In year 2015, the total harvested for the 12 selected crops is estimated at about 29675 ha, while the total production at about 267898.9 tonnes (Table 15). As expected for both scenarios the harvested area is reducing over time, but there are some differences. The BAU scenario simulated more urban growth and therefore, the amount of harvested area loss was higher than in the APR scenario.

More specifically the harvested area was reduced by 1905 ha and 1452 ha for the BAU and APR scenarios respectively (Table 15). This accounted to 6.5 % for the BAU scenario and 4.9% for the APR scenario of the total harvested area in year 2015 (Table 15). The total production loss can also be explained in a similar way. The total production loss during the simulation is 17805.6 tonnes and 13207.7 tonnes for the BAU and APR scenarios respectively (Table 15). These results to 6.7 % and 4.9 % of the total production in 2015 for the BAU and APR scenarios accordingly (Table 15).

The APR scenario loses almost 453 ha of harvested area and 4597.9 tonnes of crops less than the BAU scenario and seems to perform better overall. This is an indication that both the zoning system and the resistance values that were applied in the APR scenario protected around 20 % of harvested areas and saved 25% of total crop production in comparison to BAU. Areas that accounted a total production of more than 1.5 tonnes per hectare of harvested area for the 12 crops selected in the research area, were considered valuable agricultural areas. Those are allocated mostly on the western and eastern parts of the region (Figure 5). As diffusive growth was mostly absent in both scenarios, the most valuable agricultural areas were lost on the peri-urban areas on the eastern and western part of the region. Urban growth on the peri-urban fringe of Athens is considered high, but showed low production values per harvested area, not exceeding 0.5 tonnes per hectare for the 12 crops selected (Figure 5).

Results	BAU simulation	APR simulation
Total harvest area for 12 selected crops for 2015 (based on GAEZv4 data)	29675 ha	
Total harvested area loss	1905 ha	1452 ha
Relative harvested area loss compared to total harvested area of 2015	6,5%	4,9%
Mean harvested area loss	54,4 ha/year	41,5 ha/year
Total production for 12 selected crops for 2015 (based on GAEZv4 data)	267898.9 tonnes	
Total production loss	17805.6 tonnes	13207.7 tonnes
Relative production loss compared to total production of 2015	6.7%	4.9%
Mean production loss	508.7 tonnes/year	377.4 tonnes/year

Table 15: Comparison of BAU and APR impact. The table shows the results of the impact assessment for the BAU and APR scenario and provides a statistical overview of the outcome.

Moreover, the food supply quantity for the selected 12 crops is 0.389 tonnes per capita (FAO,2015). Given the total production in the region of Attica is around 3.8 million, the total production of the selected 12 crops should be around 1487147 tonnes to exclusively cover the regional population needs (Table 17). The corresponding values for the selected 12 crops of both the national statistical data and the GAEZv4 data indicated that the region produces far less, 198017 and 267898.9 tonnes respectively (Table 16). As a result, the total population supplied is accounted around 688686 based on GAEZv4 data, while 4897 and 3732 people are expected to lose supply by 2050 based on the BAU and APR scenarios respectively. In the APR scenario 1164 less, people lose supplies than in the BAU scenario, which is the size of a city neighborhood or village (Table 17).

The impact assessment was based on the total production of all 12 crops and therefore it cannot reveal further information on individual crop production values. It is suggested here for further research to take this into account and follow the same method for individually assessing the impact of each crop. This would reveal which crops are dominant and important for the local production and which will be affected more due to urban growth.

Food supply quantity (FAO 12 selected crops Greece 2015, tonnes/capita/year)	Total population 2015	Total food supply per capita needed	Total Population supplied from regional production based on National statistical data in 2015	Total Population supplied from regional production based on GAEZv4 data in 2015	Total population to lose supply based on BAU in year 2050	Total population to lose supply based on APR	Total population that is saved from supply loss due to APR scenario
0.389 tonnes / capita	3823000	1487147 tonnes	509041	688686	4897	3732	1164

Table 17: The table shows the Food supply quantity per capita as described in FAO statistics for Greece in year 2015. Further estimations are made given the total population of the region and the production estimated at the beginning and end of the simulation for both scenarios.

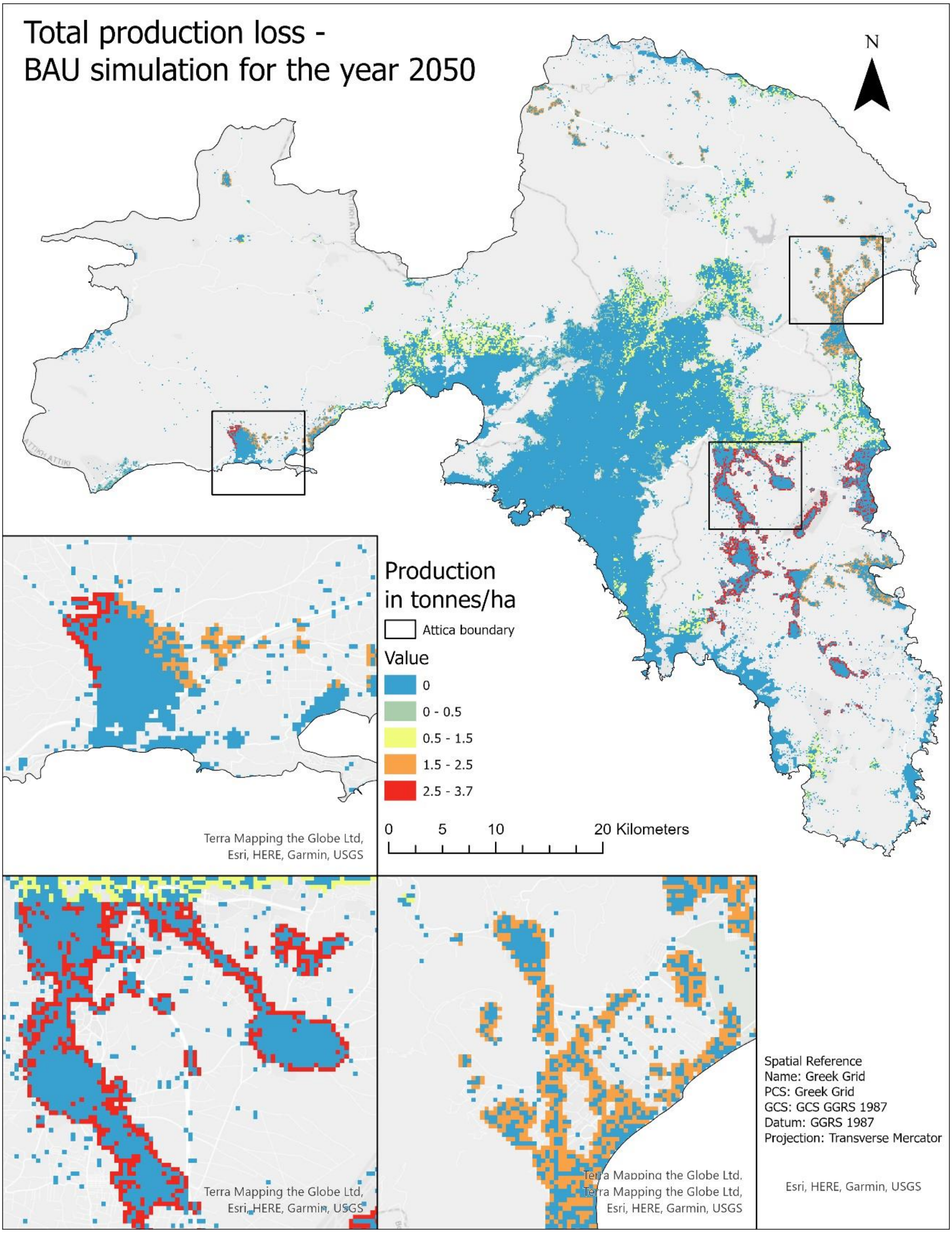

Figure 4: Total production loss per hectare for the BAU scenario. The total production is the weighted sum of all 12 crops selected for this study (Barley, Cotton, crops NES, Fodder crops, Maize, Olives, Other cereals, Potato & sweet potato, pulses, sugar beet, vegetables, Wheat). Areas with values higher than 1.5 tones/hectares are considered valuable agricultural areas for the research areas as they indicate both high yield and harvested area.

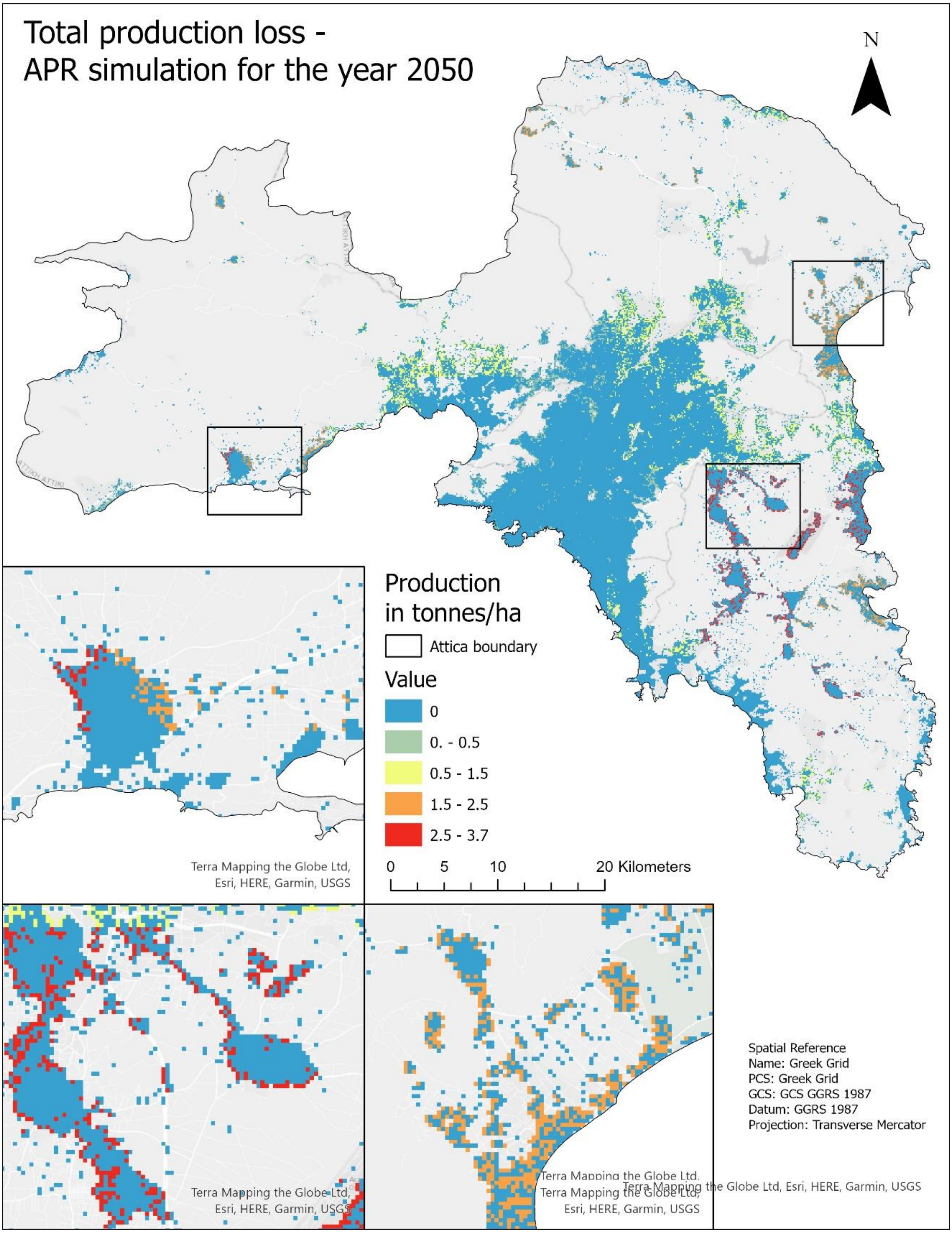

Figure 5: Total production loss per hectare for the APR scenario. The total production is the weighted sum of all 12 crops selected for this study (Barley, Cotton, crops NES, Fodder crops, Maize, Olives, Other cereals, Potato & sweet potato, pulses, sugar beet, vegetables, Wheat). Areas with values higher than 1.5 tones/hectares are considered valuable agricultural areas for the research areas as they indicate both high yield and harvested area.

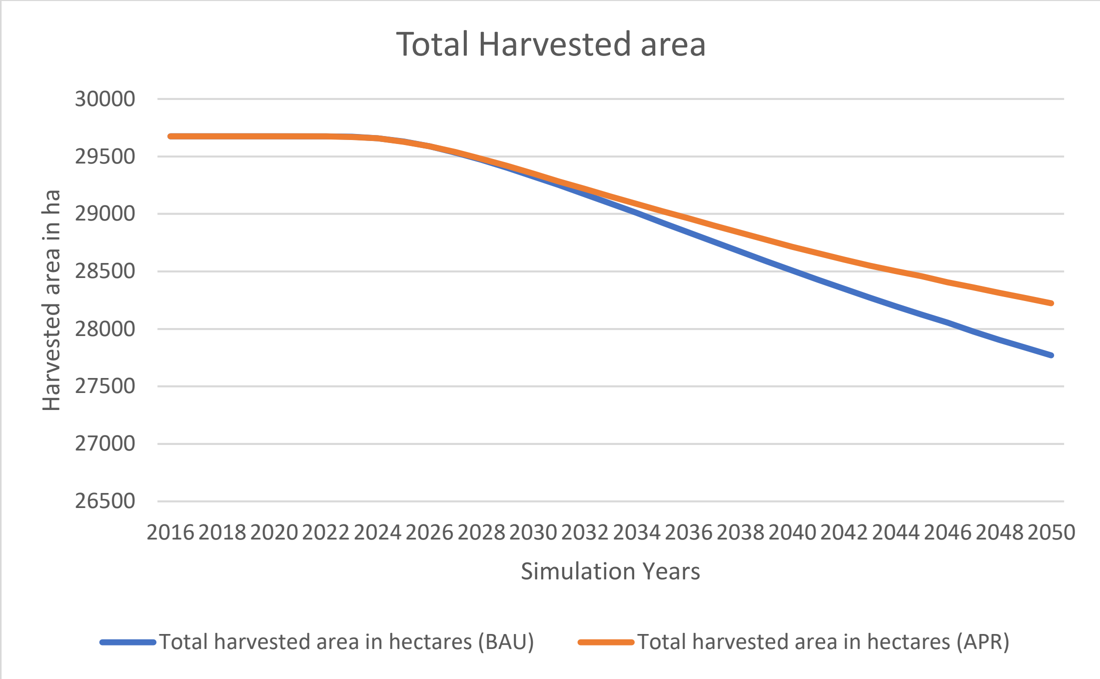

Figure 6: Total harvested area of 12 selected crops (Barley, Cotton, crops NES, Fodder crops, Maize, Olives, Other cereals, Potato & sweet potato, pulses, sugar beet, vegetables, Wheat) in the research area over the simulation time period.

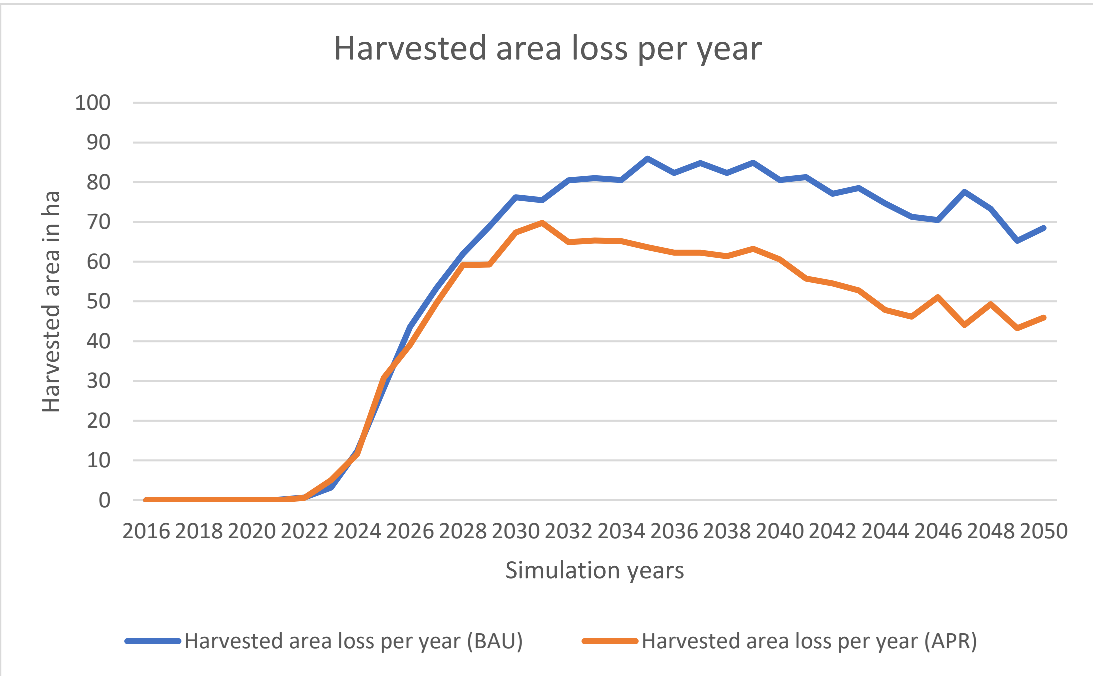

Figure 7: Yearly loss of total harvested area for 12 crops (Barley, Cotton, crops NES, Fodder crops, Maize, Olives, Other cereals, Potato & sweet potato, pulses, sugar beet, vegetables, Wheat) in the research area over the simulation time.

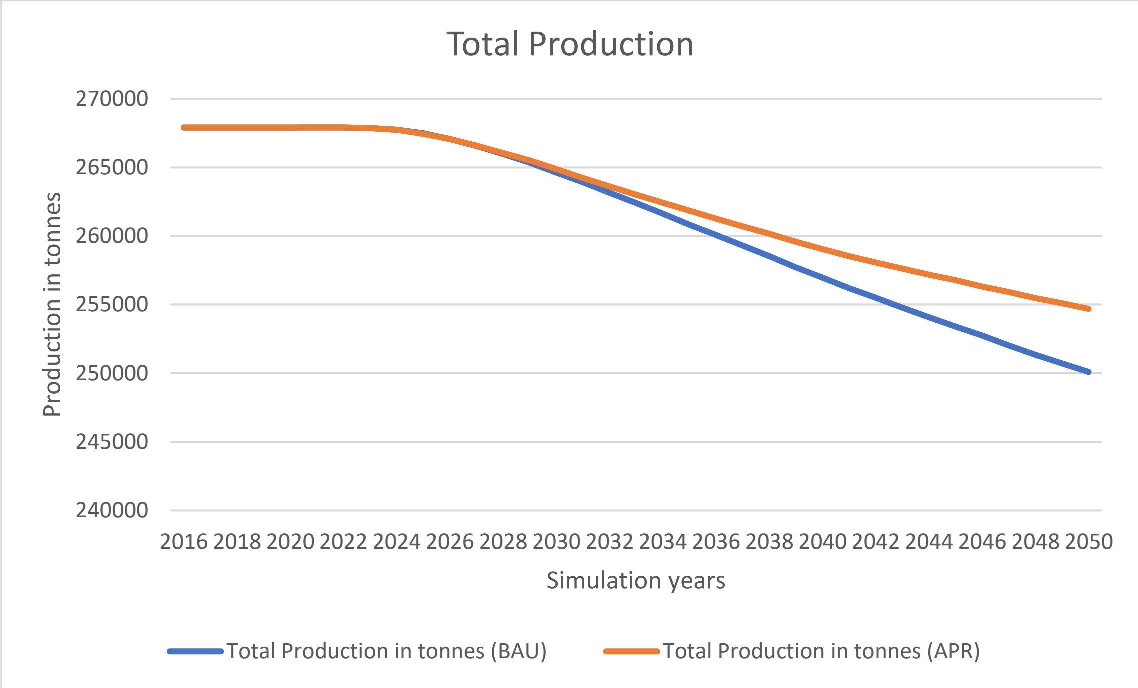

Figure 8: Weighted sum of total production in tonnes for 12 crops (Barley, Cotton, crops NES, Fodder crops, Maize, Olives, Other cereals, Potato & sweet potato, pulses, sugar beet, vegetables, Wheat) in the research area over the simulation time.

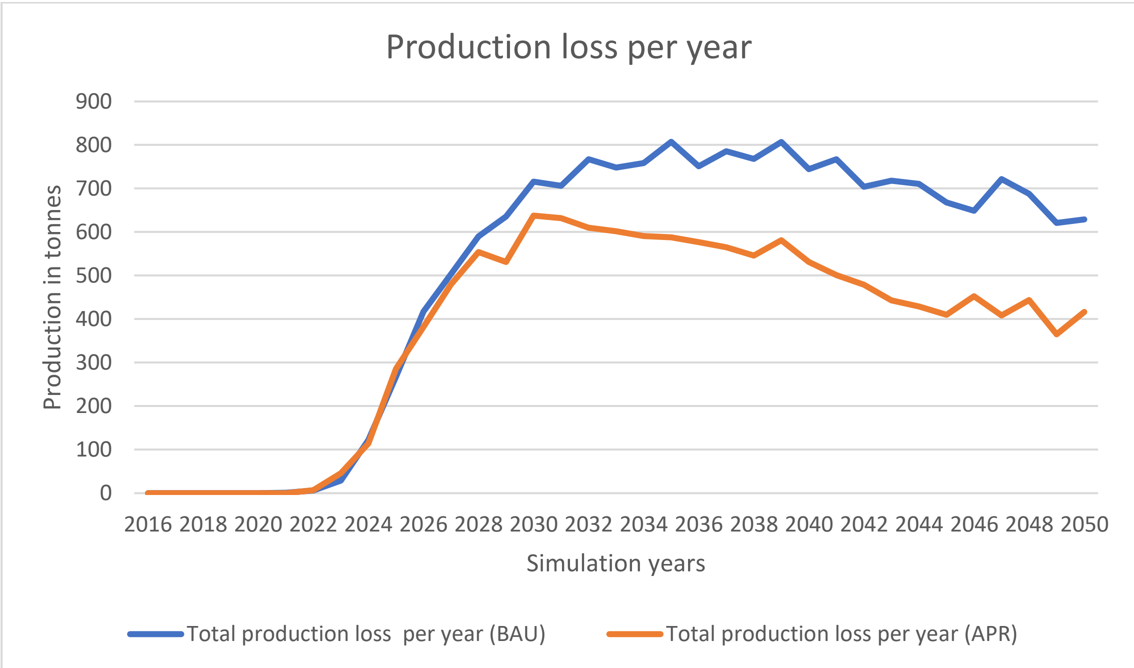

Figure 9: Yearly weighted sum production loss for 12 crops in tonnnes (Barley, Cotton, crops NES, Fodder crops, Maize, Olives, Other cereals, Potato & sweet potato, pulses, sugar beet, vegetables, Wheat) in the research area over the simulation time.

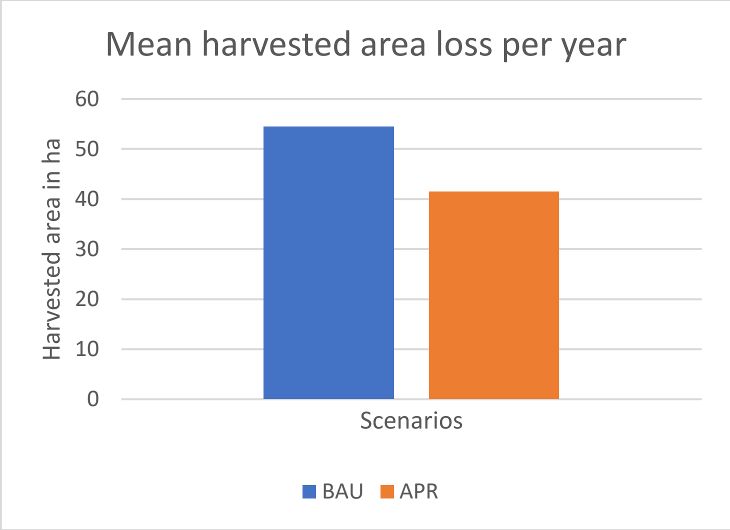

Figure 10: The bar chart shows the mean harvested area loss per year for both scenarios in ha.

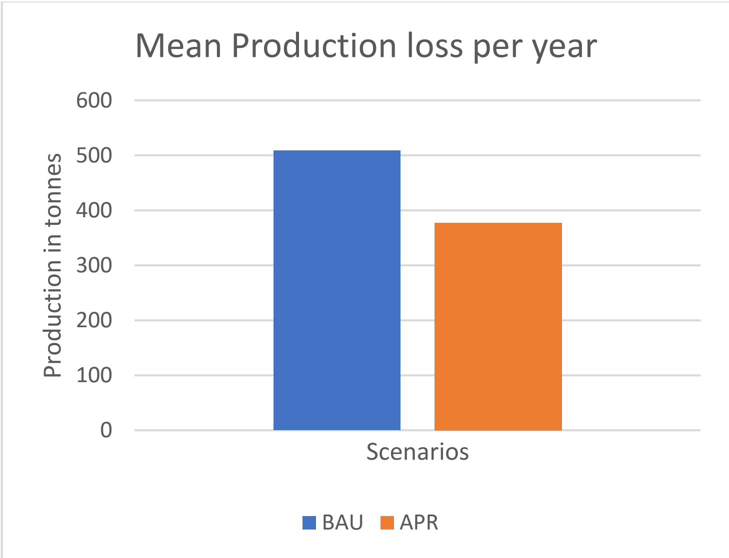

Figure 11: The bar chart shows the mean production loss per year for both scenarios in tonnes.

4.4 Limitations and drawbacks for discussion

Data and preprocessing played a defining role in modelling urban growth using SLEUTH and then assess its impact on the crop production of 12 different crop products for two scenarios of change. For the input data of SLEUTH, four different datasets were used for the urban, excluded and road layers. The selection of different datasets has happened due to lack of consistent spatial and temporal data involving the beforementioned layer data requirements of the model's calibration. As a result, the inconsistencies between those four datasets had a negative effect on the calibration of SLEUTH and thus in the future simulated outcomes. A way to have a better consistency between the input data would be by supervised classification of remote sensing imagery or using a preprocessed classified dataset such as the Corine landcover dataset (Copernicus,2018). The latter was not used as the GHSL (Corbane et.al., 2018) urban dataset has been found to be more precise than Corine in capturing built-up areas on the research area than Corine, while it provides temporal data since 1975. Supervised classification of satellite imagery could solve this problem and has been used in numerous studies (Chaudhuri & Clarke,2014, Cui et.al., 2019, Gounaridis et.al., 2018), but would require a considerable amount of time to derive accurate classified data for different time periods. Including more time periods in the calibration phase, for the urban, exclusion and road layers could improve the predictive accuracy of the model, as those are basically related with the simulated growth.

For the selection of crop related data, the GAEZv4, 2015 (Frolking et.al, 2020) dataset was selected, which uses FAO statistics, landcover, topographic and other data to spatially aggregate harvested area and yield values of 26 crops in 5-arcminuted global gridded layers. This selection was made due to lack of regional spatial and temporal crop data. A drawback found in this dataset, was that certain coastal areas were completely missing yield and harvested area data

After examining the data, 12 out of the 26 crop classes included in the GAEZv4 dataset, were selected for this study as they were present in regional statistics too (Hellenic Statistical Authority, 2015). The total harvested area was computed by simply merging the harvested area values of all 12 crops into a single layer. Given the individual yield and harvested area values for each crop is known in the dataset, the weighted total production of all crops was computed into a single layer. Using the weighted total value for the production, does provide a holistic view of the total production of those crops together and provides spatial information on areas with high production values in the region, but cannot reveal individual information of each crop. To counter this problem, using the GAEZv4 data, every crop production layer of the 12 crop classes should be assessed independently. To be able to monitor crops at a regional level with better results, data of higher spatial and temporal resolution are needed. An example is the crop-type map of the Netherlands, published by ESA (ESA,2017).

For the reasons mentioned before, the impact assessment of potential urban growth on crop production lacks of accuracy in certain aspects and therefore it can only be considered as an indication of potential loss. Yield is not possible to remain stable for a 35-year span, as it is highly dependent on methods used for growing and harvesting crops, agroclimatic and environmental parameters. Furthermore, aggregating the 5-arcminute values of harvested area into hectares was necessary for simulating cell by cell changes using SLEUTH's outputs. By resampling the data into 100 m grid cell, each grid inside a 5-arcminute area was assigned with equally distributed per-hectare (100m*100m) values for yield and harvested area. This does not allow the spatial allocation of those crops at a regional scale of analysis with high spatial resolution. Last but not least, production loss is not validated due to lack of crop data and therefore the results should only be examined based on the impact of different policy implementations.

5 Conclusion

The main research question for this study was formulated as it follows:

"What is the impact of future urban growth in the Attica region up to 2050 on the potential total production of different crops under two scenarios of change: a business-as-usual scenario (BAU) and an agriculture preservation scenario (APR)?"

Concluding on this research results, urban growth in Attica region is expected to continue at a high rate for both scenarios of change. In comparison to the past observed change between 1975 and 2015 the simulated by the model urban growth indicated 82% more growth for the BAU scenario and 46% more growth for the APR between 2015 and 2050. The impact of urban growth in the potential total crop production of 12 selected crops for the BAU scenario was about 2% higher than in the APR in comparison to the total amount of production for the year 2015.The results of this study indicate that by implementing zoning and protection strategies in the APR scenario, potential production loss of 4597.9 tonnes for the 12 selected crops can be avoided and valuable peri-urban space of 453 ha of harvested area can be conserved for agricultural activities instead of urban expansion. Accordingly, it is estimated that 1164 people will not lose their food supply by 2050. In comparison to the BAU scenario, the APR scenario conserved 24% more harvested area and saved 26 % more production. The results indicated that the western and eastern parts of Attica region are affected more by urban growth as they concentrate high production values for the 12 crops selected. Therefore, it is suggested that those areas must be considered carefully in future plans of urban expansion by goverment authorities.

The first sub-question was formulated as it follows:

"What are the drivers of change and how can spatial strategies and policies be integrated into an UGM?"

The drivers of change for urban growth were related with the best-fit, growth coefficients of SLEUTH's model, that derived from the calibration with historic data and the exclusion layers, which acted as policy layers for the UGM. The diffusion coefficient of 40 % indicates the probability of newly created urban areas detached from existing urban centers. The low breed of 1% on the other hand, shows that those newly detached urban areas will probably not expand much further. The spread coefficient of 8% shows that existing urban areas are expected to have some expansion on their edges. The low road gravity coefficient shows that roads will not attract much growth, while the slope resistance of 23% indicates that urban growth o steeper slopes is more unlikely to occur than on flat surfaces. The exclusion layers of SLEUTH are used to integrate different policies and measures for the two scenarios of change into the UGM. The BAU scenario represents growth based on past trends and is partially related with the former Master Plan of Athens, while the APR scenario represents growth based on the new Master Plan of Athens together with zoning criteria for controlling growth and protecting agricultural areas. In the BAU scenario, resistance to urbanization values were applied on landcover classes to protect forests and natural areas while agricultural areas received no protection at all. The development of this scenarios was based Article 11, Law 1515/1985 (Greek Government, 1985), which indicates that natural protected and forest areas are fully protected. On the APR scenario agricultural areas were assigned with resistance to urbanization values and a zoning policy was implemented, which completely or partially prevented growth. The APR scenario was based on Law 4277/2014 (Greek government, 2014), which promotes the compact city approach and for protection of peri-urban space and related activities such as agricultural.

The second sub-question was formulated as it follows:

"What measures can be taken to protect and enhance peri-urban agriculture?"

In this study measures to protect peri-urban agriculture are associated with spatial interventions in the peri-urban space. Those are usually related with changing the existing land use zoning systems, creating green corridors, developing sustainable activities, promoting the awareness of ecosystem services and their protection and others (Spyra et.al 2021). The APR scenario implements a zoning system based on the study of Huang et.al 2008. Zoning systems have different forms and functions depending on the area of application and the scale of analysis and they have been used in many cases to protect and enhance agricultural areas and related activities (Sarker et.al.2019). For the APR scenario two zones of 1 and 2 km were created. Areas inside of 1 km distance from existing urban centers had no restrictions, while areas between 1 and 2 km were assigned with 50% resistance to urbanization values. Areas above 2km distance from existing urban centers were completely excluded from urbanization. Furthermore, agricultural areas have been assigned with increased resistance to urbanization values in this scenario. The results indicated that although the APR scenario successfully prevented growth in certain agricultural areas due to the increased resistance to urbanization values, the growth patterns did not change significantly from the BAU scenario. This is an indication that the zoning system used in the APR scenario for this study case does not apply well enough to become a pattern breaking intervention, but still has positive effect in completely preventing diffusive growth and preserve harvested area and production. In addition to the measures applied in this study, several densification, regeneration and containment interventions are discussed in chapter 2.3 such as the "Huerta de Valencia Spatial Plan" (2018) in Spain, which enhanced the protection of traditional vegetable production areas by combining the protection of rural areas in plans, with support for agricultural activities.

Peri-urban space and agriculture is gaining more attention all over the world and its importance in sustainable development is mentioned (Wynne et. al 2016). As alternative ways to organize and use peri-urban space, such as peri-urban agriculture, are implemented more frequently, evidence show that those interventions usually contribute positively in the local and regional development when considered in the decision making and planning processes.

6 References

Abdullahi, S., & Pradhan, B. (2018). Land use change modeling and the effect of compact city paradigms: integration of GIS-based cellular automata and weights-of-evidence techniques. Environmental Earth Sciences, 77(6), 1–15. https://doi.org/10.1007/s12665-018-7429-z

Aburas, M. M., Ho, Y. M., Ramli, M. F., & Ash'aari, Z. H. (2016). The simulation and prediction of spatio-temporal urban growth trends using cellular automata models: A review. *International Journal of Applied Earth Observation and Geoinformation*, *52*, 380-389.

Akın, A., Clarke, K. C., & Berberoglu, S. (2014). The impact of historical exclusion on the calibration of the SLEUTH urban growth model. *International Journal of Applied Earth Observation and Geoinformation*, *27*, 156-168.

Ana Paula García-Nieto, Ilse Geijzendorffer, Francesc Baró, Philip Roche, Alberte Bondeau, et al.. Impacts of urbanization around Mediterranean cities: changes in ecosystem service supply. Ecological Indicators, Elsevier, 2018, 91, pp.589-606. ffhal-01744748f

Asgarian, A., Soffianian, A., Pourmanafi, S., & Bodaghabad, M. B. (2018). Evaluating the spatial effectiveness of alternative urban growth scenarios in protecting cropland resources: A case of mixed agricultural-urbanized landscape in central Iran. *Sustainable cities and society*, *43*, 197-207.

Asprogerakas, E. (2016, May). Strategic planning and urban development in Athens. The current attempt for reformation and future challenges. In *Keynote speech at Sustainable Urban Planning and Design Symposium, Nicosia, May13*.

Barbosa, A., Vallecillo, S., Baranzelli, C., Jacobs-Crisioni, C., Batista e Silva, F., Perpiña-Castillo, C., ... & Maes, J. (2017). Modelling built-up land take in Europe to 2020: An assessment of the Resource Efficiency Roadmap measure on land. *Journal of Environmental Planning and Management*, *60*(8), 1439-1463.

Berling-Wolff, S., & Wu, J. (2004). Modeling urban landscape dynamics: a case study in Phoenix, USA. *Urban ecosystems*, *7*(3), 215-240.

Bihamta, N., Soffianian, A., Fakheran, S., & Gholamalifard, M. (2015). Using the SLEUTH urban growth model to simulate future urban expansion of the Isfahan metropolitan area, Iran. *Journal of the Indian Society of Remote Sensing*, *43*(2), 407-414.

Caswell, H., & Etter, R. J. (1993). Ecological Interactions in Patchy Environments: From Patch-Occupancy Models to Cellular Automata. In S. A. Levin, T. M. Powell, & J. W. Steele (Eds.), Patch Dynamics (pp. 93–109). Springer Berlin Heidelberg.

Cecchini, M., Zambon, I., Pontrandolfi, A., Turco, R., Colantoni, A., Mavrakis, A., & Salvati, L. (2019). Urban sprawl and the ‘olive’landscape: Sustainable land management for ‘crisis’ cities. *GeoJournal*, *84*(1), 237-255.

Chaudhuri, G., & Clarke, K. (2013). The SLEUTH land use change model: A review. *Environmental Resources Research*, *1*(1), 88-105.

Chaudhuri, G., & Clarke, K. C. (2014). Temporal accuracy in urban growth forecasting: A study using the SLEUTH model. *Transactions in GIS*, *18*(2), 302-320.

Chen, Q., Mynett, A.E. & Minns, A.W. (2002). Application of cellular automata to modelling competitive growths of two underwater species Chara aspera and Potamogeton pectinatus in Lake

Chen, Y., & Lin, J. (2009). Modeling the self-affine structure and optimization conditions of city systems using the idea from fractals. *Chaos, Solitons & Fractals*, *41*(2), 615-629.

Clarke, K. C. (1997, June). Land transition modeling with deltatrons. In *Web Paper at: http://www. ncgia. ucsb. edu/conf/landuse97*.

Clarke, K. C., Hoppen, S., & Gaydos, L. (1997). A self-modifying cellular automaton model of historical urbanization in the San Francisco Bay area. *Environment and planning B: Planning and design*, *24*(2), 247-261.

Cohen, J. (1960). A coefficient of agreement for nominal scales. *Educational and psychological measurement*, *20*(1), 37-46.

Colantoni, A., Grigoriadis, E., Sateriano, A., Venanzoni, G., & Salvati, L. (2016). Cities as selective land predators? A lesson on urban growth, deregulated planning and sprawl containment. *Science of the Total Environment*, *545*, 329-339.

Coulthard, T. J., & Van De Wiel, M. J. (2013). Numerical Modeling in Fluvial Geomorphology. In Treatise on Geomorphology (Vol. 9). Elsevier Ltd. https://doi.org/10.1016/B978-0-12-374739-6.00261-X

Cui, Y., Liu, J., Xu, X., Dong, J., Li, N., Fu, Y., ... & Xiao, X. (2019). Accelerating cities in an unsustainable landscape: Urban expansion and cropland occupation in China, 1990–2030. Sustainability, 11(8), 2283.

d'Amour, C. B., Reitsma, F., Baiocchi, G., Barthel, S., Güneralp, B., Erb, K. H., ... & Seto, K. C. (2017). Future urban land expansion and implications for global croplands. *Proceedings of the National Academy of Sciences*, *114*(34), 8939-8944.

de Noronha Vaz, E., Nijkamp, P., Painho, M., & Caetano, M. (2012). A multi-scenario forecast of urban change: A study on urban growth in the Algarve. *Landscape and Urban Planning*, *104*(2), 201-211.

Dietzel, C., & Clarke, K. C. (2004, October). Replication of spatio-temporal land use patterns at three levels of aggregation by an urban cellular automata. In International conference on cellular automata (pp. 523-532). Springer, Berlin, Heidelberg.

Dietzel, C., & Clarke, K. C. (2007). Toward optimal calibration of the SLEUTH land use change model. *Transactions in GIS*, *11*(1), 29-45.

El Bilali, H., Berjan, S., Simic, J., Despotovic, A., Cadro, S., & Kulina, M. (2013). Urban and peri-urban agriculture in Sarajevo region: an exploratory study. *Journal of Central European Agriculture*, *14*(4), 1602-1614.

Feng, Y., & Tong, X. (2017). Using exploratory regression to identify optimal driving factors for cellular automaton modeling of land use change. Environmental Monitoring and Assessment, 189(10). https://doi.org/10.1007/s10661-017-6224-8

Feng, Y., Wang, R., Tong, X., & Shafizadeh-Moghadam, H. (2019). How much can temporally stationary factors explain cellular automata-based simulations of past and future urban growth?. *Computers, Environment and Urban Systems*, *76*, 150-162.

Follmann, A., Willkomm, M., & Dannenberg, P. (2021). As the city grows, what do farmers do? A systematic review of urban and peri-urban agriculture under rapid urban growth across the Global South. *Landscape and Urban Planning*, *215*, 104186.

Francesco, B. & Tagliabue, J. (2021). "Cellular Automata", The Stanford Encyclopedia of Philosophy (Spring 2021 Edition), Edward N. Zalta (ed.), URL: https://plato.stanford.edu/archives/spr2021/entries/cellular-automata/

Gardi, C., Panagos, P., Van Liedekerke, M., Bosco, C., & De Brogniez, D. (2015). Land take and food security: assessment of land take on the agricultural production in Europe. *Journal of Environmental Planning and Management*, *58*(5), 898-912.

Goodarzi, M. S., Sakieh, Y., & Navardi, S. (2017). Scenario-based urban growth allocation in a rapidly developing area: a modeling approach for sustainability analysis of an urban-coastal coupled system. *Environment, Development and Sustainability*, *19*(3), 1103-1126.

Gounaridis, D., Chorianopoulos, I., Symeonakis, E., & Koukoulas, S. (2019). A Random Forest-Cellular Automata modelling approach to explore future land use/cover change in Attica (Greece), under different socio-economic realities and scales. *Science of the Total Environment*, *646*, 320-335.

Gounaridis, D., Symeonakis, E., Chorianopoulos, I., & Koukoulas, S. (2018). Incorporating density in spatiotemporal land use/cover change patterns: The case of Attica, Greece. *Remote Sensing*, *10*(7), 1034.

Hagen, A. (2002, April). Multi-method assessment of map similarity. In *Proceedings of the 5th AGILE Conference on Geographic Information Science* (pp. 171-182). Palma, Spain: Universitat de les Illes Balears.

Hogeweg, P. (1988). Cellular automata as a paradigm for ecological modeling. Applied Mathematics and Computation, 27(1), 81–100. https://doi.org/10.1016/0096-3003(88)90100-2

Hope, K. R. (1998). Urbanization and urban growth in Africa. *Journal of Asian and African Studies*, *33*(4), 345-358.

Houet, T., Aguejdad, R., Doukari, O., Battaia, G., & Clarke, K. (2016). Description and validation of a "non path-dependent" model for projecting contrasting urban growth futures. *Cybergeo: European Journal of Geography*.

Hu, X., Li, X., & Lu, L. (2018). Modeling the land use change in an arid oasis constrained by water resources and environmental policy change using cellular automata models. Sustainability (Switzerland), 10(8). https://doi.org/10.3390/su10082878

Huang, J., Zhang, J., & Lu, X. X. (2008). Applying SLEUTH for simulating and assessing urban growth scenario based on time series tm images: Referencing to a case study of Chongqing, China. *The international archives of the photogrammetry, remote sensing and spatial information sciences*, *37*(2), 598-606.

Ilachinski, Andrew, 2001, Cellular Automata, Singapore: World Scientific Publishing.

Islam, K., Rahman, M. F., & Jashimuddin, M. (2018). Modeling land use change using Cellular Automata and Artificial Neural Network: The case of Chunati Wildlife Sanctuary, Bangladesh. Ecological Indicators, 88(May 2017), 439–453. https://doi.org/10.1016/j.ecolind.2018.01.047

Jabareen, Y. R. (2006). Sustainable urban forms: Their typologies, models, and concepts. *Journal of planning education and research*, *26*(1), 38-52.

Jat, M. K., Garg, P. K., & Khare, D. (2008). Monitoring and modelling of urban sprawl using remote sensing and GIS techniques. *International journal of Applied earth Observation and Geoinformation*, *10*(1), 26-43.

Kyparissas, N. & Dollas, A. (2020). Large-scale Cellular Automata on FPGAs: A New Generic Architecture and a Framework. ACM Transactions on Reconfigurable Technology and Systems. 14. 10.1145/3423185.

Kyparissas, N. & Dollas, A. (2019). An FPGA-Based Architecture to Simulate Cellular Automata with Large Neighborhoods in Real Time, 2019 29th International Conference on Field Programmable Logic and Applications (FPL), 2019, pp. 95-99, doi: 10.1109/FPL.2019.00024.

Lavalle, C., Barbosa, A. L., Mubareka, S., Jacobs-Crisioni, C., Baranzelli, C., & Castillo, C. P. (2013). Land Use Related Indicators for Resource Efficiency-Part I Land Take Assessment. *Luxembourg. doi*, *10*, 94223.

Li, X., & Gong, P. (2016). Urban growth models: progress and perspective. *Science bulletin*, *61*(21), 1637-1650.

Liang, Y., Liu, L., & Huang, J. (2020). Modeling Urban Growth with CA Model at Regional Scale. In *Integrated Modelling of Ecosystem Services and Land-Use Change* (pp. 19-38). Springer, Singapore.

Lin, F. T., & Tseng, W. Y. (2010). Using cellular automata model to simulate the impact of urban growth policy on environment in danshuei township, Taiwan. Lecture Notes in Computer Science (Including Subseries Lecture Notes in Artificial Intelligence and Lecture Notes in Bioinformatics), 6016 LNCS(PART 1), 77–88. https://doi.org/10.1007/978-3-642-12156-2_6

López, E., Bocco, G., Mendoza, M., & Duhau, E. (2001). Predicting land-cover and land-use change in the urban fringe: A case in Morelia city, Mexico. *Landscape and urban planning*, *55*(4), 271-285.

Maithani, S., Jain, R. K., & Arora, M. K. (2007). An artificial neural network based approach for modelling urban spatial growth. *ITPI Journal*, *4*(2), 43-51.

Martellozzo, F., Amato, F., Murgante, B., & Clarke, K. C. (2018). Modelling the impact of urban growth on agriculture and natural land in Italy to 2030. *Applied Geography*, *91*, 156-167.

Mohan, M., Pathan, S. K., Narendrareddy, K., Kandya, A., & Pandey, S. (2011). Dynamics of urbanization and its impact on land-use/land-cover: a case study of megacity Delhi. *Journal of Environmental Protection*, *2*(09), 1274.

Moissidis, A., & Duquenne, M. N. (1997). Peri‐Urban Rural Areas in Greece: The Case of Attica. *Sociologia ruralis*, *37*(2), 228-239.

Moran Alonso, N., Obeso Muniz, I., Hernandez Aja, A., & Fernandez Garcia, F. (2017). Challenges for the revitalisation of peri-urban agriculture in Spain: Territorial analysis of the Madrid and Oviedo metropolitan areas. *Moravian Geographical Reports*.

Musa, S. I., Hashim, M., & Reba, M. N. M. (2017). A review of geospatial-based urban growth models and modelling initiatives. *Geocarto International*, *32*(8), 813-833.

Oguz, H., Klein, A. G., & Srinivasan, R. (2007). Using the SLEUTH urban growth model to simulate the impacts of future policy scenarios on urban land use in the Houston-Galveston-Brazoria CMSA. *Research Journal of Social Sciences*, *2*(1), 72-82.

Opitz, I., Berges, R., Piorr, A., & Krikser, T. (2016). Contributing to food security in urban areas: differences between urban agriculture and peri-urban agriculture in the Global North. *Agriculture and Human Values*, *33*(2), 341-358.

Pan, Y., Roth, A., Yu, Z., & Doluschitz Reiner, R. (2010). The impact of variation in scale on the behavior of a cellular automata used for land use change modeling. In Computers, Environment and Urban Systems (Vol. 34, Issue 5, pp. 400–408). https://doi.org/10.1016/j.compenvurbsys.2010.03.003

Patra, S., Sahoo, S., Mishra, P., & Mahapatra, S. C. (2018). Impacts of urbanization on land use/cover changes and its probable implications on local climate and groundwater level. *Journal of urban management*, *7*(2), 70-84.

Perrin, C., Clément, C., Melot, R., & Nougarèdes, B. (2020). Preserving farmland on the urban fringe: A literature review on land policies in developed countries. *Land*, *9*(7), 223.

PŁONKA, A., & SROKA, W.(2021). FOOD STRATEGIES AND RESTITUTION OF URBAN AGRICULTURE ILLUSTRATED BY THE CASE OF SELECTED SOLUTIONS OF METROPOLITAN AREAS.

Population and Development | UNEPMAP QSR. Medqsr.org. (2021). Retrieved 30 September 2021, from https://www.medqsr.org/population-and-development.

Qiu, B., Li, H., Tang, Z., Chen, C., & Berry, J. (2020). How cropland losses shaped by unbalanced urbanization process?. *Land Use Policy*, *96*, 104715.

Rajan, K. S., & Shibasaki, R. (2001, November). A GIS based integrated land use/cover change model to study agricultural and urban land use changes. In *22nd Asian Conference on Remote Sensing* (Vol. 9).

Ritchie, H., & Roser, M. (2018). Urbanization. *Our world in data*.Hu, X., Li, X., & Lu, L. (2018). Modeling the land use change in an arid oasis constrained by water resources and environmental policy change using cellular automata models. Sustainability (Switzerland), 10(8). https://doi.org/10.3390/su10082878

Sakieh, Y., Amiri, B. J., Danekar, A., Feghhi, J., & Dezhkam, S. (2015). Simulating urban expansion and scenario prediction using a cellular automata urban growth model, SLEUTH, through a case study of Karaj City, Iran. *Journal of Housing and the Built Environment*, *30*(4), 591-611.

Sakieh, Y., Salmanmahiny, A., Jafarnezhad, J., Mehri, A., Kamyab, H., & Galdavi, S. (2015). Evaluating the strategy of decentralized urban land-use planning in a developing region. *Land use policy*, *48*, 534-551.

Salvia, R., Halbac-Cotoara-Zamfir, R., Cividino, S., Salvati, L., & Quaranta, G. (2020). From Rural Spaces to Peri-Urban Districts: Metropolitan Growth, Sparse Settlements and Demographic Dynamics in a Mediterranean Region. *Land*, *9*(6), 200.

Sandamali, S. P. I., Kantakumar, L. N., & Sivanantharajah, S. U. N. D. A. R. A. M. O. O. R. T. H. Y. (2018). Remote sensing data and SLEUTH urban growth model: As decision support tools for urban planning. *中国地理科学*, *28*(2), 274.

Santé, I., García, A. M., Miranda, D., & Crecente, R. (2010). Cellular automata models for the simulation of real-world urban processes: A review and analysis. *Landscape and urban planning*, *96*(2), 108-122.

Sarker, A. H., Bornman, J. F., & Marinova, D. (2019). A framework for integrating agriculture in urban sustainability in Australia. *Urban Science*, *3*(2), 50.

Saxena, A., & Jat, M. K. (2019). Capturing heterogeneous urban growth using SLEUTH model. *Remote Sensing Applications: Society and Environment*, *13*, 426-434.

Sayas, J. P. (2006). Urban sprawl in the periurban coastal zones of Athens. *Επιθεώρηση Κοινωνικών Ερευνών*, *121*, 71-104.

Sekovski, I., Mancini, F., & Stecchi, F. (2015, June). Application of SLEUTH model to predict urbanization along the Emilia-Romagna coast (Italy): Considerations and lessons learned. In *International Conference on Computational Science and Its Applications* (pp. 426-439). Springer, Cham.

Shafizadeh-Moghadam, H., Asghari, A., Tayyebi, A., & Taleai, M. (2017). Coupling machine learning, tree-based and statistical models with cellular automata to simulate urban growth. *Computers, Environment and Urban Systems*, *64*, 297-308.

Shaw, B. J., van Vliet, J., & Verburg, P. H. (2020). The peri-urbanization of Europe: A systematic review of a multifaceted process. *Landscape and Urban Planning*, *196*, 103733.

Silva, E. A., & Clarke, K. C. (2002). Calibration of the SLEUTH urban growth model for Lisbon and Porto, Portugal. *Computers, environment and urban systems*, *26*(6), 525-552.

Skayannis, P. (2013). The (master) plans of Athens and the challenges of its re-planning in the context of crisis. *ArchNet-IJAR: International Journal of Architectural Research*, *7*(2), 192.

Skordili, Sophia. "Economic crisis as a catalyst for food planning in Athens." *International Planning Studies* 18.1 (2013): 129-141

Spyra, M., Kleemann, J., Calò, N. C., Schürmann, A., & Fürst, C. (2021). Protection of peri-urban open spaces at the level of regional policy-making: Examples from six European regions. *Land Use Policy*, *107*, 105480.

Syphard, A. D., Clarke, K. C., & Franklin, J. (2005). Using a cellular automaton model to forecast the effects of urban growth on habitat pattern in southern California. *Ecological Complexity*, *2*(2), 185-203.

Tong, X., & Feng, Y. (2020). A review of assessment methods for cellular automata models of land-use change and urban growth. In International Journal of Geographical Information Science (Vol. 34, Issue 5, pp. 866–898). https://doi.org/10.1080/13658816.2019.1684499

Torrens, P. M. (2009). The Advantages of Cellular Automata. Environmental Monitoring and Assessment, 1–4.

Triantakonstantis, D., & Mountrakis, G. (2012). Urban growth prediction: a review of computational models and human perceptions.

Triantakonstantis, D., & Stathakis, D. (2015). Urban growth prediction in Athens, Greece, using artificial neural networks. *International Journal of Architectural and Environmental Engineering*, *9*(3), 234-238.

Van Veenhuizen, R., & Danso, G. (2007). *Profitability and sustainability of urban and periurban agriculture* (Vol. 19). Food & Agriculture Org., p.14

van Vliet, J., Bregt, A. K., & Hagen-Zanker, A. (2011). Revisiting Kappa to account for change in the accuracy assessment of land-use change models. *Ecological modelling*, *222*(8), 1367-1375.

van Vliet, J., Eitelberg, D. A., & Verburg, P. H. (2017). A global analysis of land take in cropland areas and production displacement from urbanization. *Global environmental change*, *43*, 107-115.

Veldkamp, A., & Fresco, L. O. (1996). CLUE: a conceptual model to study the conversion of land use and its effects. *Ecological modelling*, *85*(2-3), 253-270.

Verzandvoort, S., Rietra, R., Hack, M., & Alterra, W. U. (2009). Pressures on prime agricultural land in Europe. *Wageningen UR*, *17*.

Visser, H., & De Nijs, T. (2006). The map comparison kit. *Environmental Modelling & Software*, *21*(3), 346-358.

Visser, H., & De Nijs, T. (2006). The map comparison kit. *Environmental Modelling & Software*, *21*(3), 346-358.

Watkiss, B. M. (2008). *The SLEUTH urban growth model as forecasting and decision-making tool* (Doctoral dissertation, Stellenbosch: Stellenbosch University).

Wu, X., Hu, Y., He, H., Xi, F., & Bu, R. (2010). Study on forecast scenarios for simulation of future urban growth in Shenyang City based on SLEUTH model. *Geo-Spatial Information Science*, *13*(1), 32-39.

Wynne, L., Cordell, D., Chong, J., & Jacobs, B. (2016). Planning Tools for strategic management of peri-urban food production.

Yang, J., Su, J., Chen, F., Xie, P., & Ge, Q. (2016). A local land use competition cellular automata model and its application. In ISPRS International Journal of Geo-Information (Vol. 5, Issue 7). https://doi.org/10.3390/ijgi5070106

Yang, X., Zheng, X. Q., & Lv, L. N. (2012). A spatiotemporal model of land use change based on ant colony optimization, Markov chain and cellular automata. Ecological Modelling, 233, 11–19. https://doi.org/10.1016/j.ecolmodel.2012.03.011

Yeh, A. G., Li, X., & Xia, C. (2021). Cellular automata modeling for urban and regional planning. *Urban Informatics. BATTY, M. GOODCHILD, MF SHI, W. editors. Springer*.

Yin, H., Kong, F., Yang, X., James, P., & Dronova, I. (2018). Exploring zoning scenario impacts upon urban growth simulations using a dynamic spatial model. *Cities*, *81*, 214-229.

Zaitsev, D. A. (2017). A generalized neighborhood for cellular automata. In Theoretical Computer Science (Vol. 666, pp. 21–35). https://doi.org/10.1016/j.tcs.2016.11.002

Zambon, I., Serra, P., Salvia, R., & Salvati, L. (2018). Fallow land, recession and socio-demographic local contexts: Recent dynamics in a Mediterranean urban fringe. *Agriculture*, *8*(10), 159.

Zhang, B., & Wang, H. (2021). A new type of dual-scale neighborhood based on vectorization for cellular automata models. In GIScience and Remote Sensing. https://doi.org/10.1080/15481603.2021.1883946

Zhou, Y., Varquez, A. C., & Kanda, M. (2019). High-resolution global urban growth projection based on multiple applications of the SLEUTH urban growth model. *Scientific data*, *6*(1), 1-10.

Zitti, M., Zambon, I., Mavrakis, A., & Salvati, L. (2018). The Way Toward Dispersed Metropolitan Growth: Land-use Efficiency and the Abandonment of a Mediterranean Compact Tradition. *Int. J. Ecol. Dev*, *33*, 108-124.

Online reference

Crop-type map of the Netherlands (2017). Available at : https://www.esa.int/ESA_Multimedia/Images/2018/05/Crop_map (Accessed at 22 February of 2022)

EEA , 2019. Land take in Europe. Available at https://www.eea.europa.eu/data-an d-maps/indicators/land-take-2/assessment-1 (Accessed at 16 November 2021)

GAEZ v4 Data Portal. (2021)., Available at: https://gaez.fao.org/ Accessed at 13 October 2021

SUPER - Sustainable Urbanization and land-use Practices in European Regions (2020). Available at https://www.eea.europa.eu/data-an d-maps/indicators/land-take-2/assessment-1 (Accessed at 16 November 2021)

Project Gigalopolis. (2005). Retrieved 16 November 2021, Available at: http://www.ncgia.ucsb.edu/projects/gig/index.html

Cygwin. Retrieved 19 November 2021, from https://www.cygwin.com/

Data and Dataset sources

Copernicus. (2021). Retrieved 9 October 2021, from https://www.copernicus.eu/en

Corbane, Christina; Florczyk, Aneta; Pesaresi, Martino; Politis, Panagiotis; Syrris, Vasileios (2018): GHS built-up grid, derived from Landsat, multitemporal (1975-1990-2000-2014), R2018A. European Commission, Joint Research Centre (JRC) doi: 10.2905/jrc-ghsl-10007 PID: http://data.europa.eu/89h/jrc-ghsl-10007

Database - Eurostat. (2021). Retrieved 9 October 2021, from https://ec.europa.eu/eurostat/web/main/data/database

Food and Agriculture Organization (FAO) of the United Nations. FAOSTAT statistical database [Greece][Crops and livestock products][Year 2015]. Retrieved 20 October 2021, from https://www.fao.org/faostat/en/#data/TCL

Food and Agriculture Organization (FAO) of the United Nations.(2015) FAOSTAT statistical database [Greece][Food supply quantity (kg/capita/year), 12 selected crops][Year 2015]. Retrieved 20 October 2021, from https://www.fao.org/faostat/en/#data/FBS

Frolking, S., Wisser, D., Grogan, D., Proussevitch, & Glidden, S. (2020). *GAEZ+_2015 Crop Yield* [Data set]. Harvard Dataverse. https://doi.org/10.7910/DVN/NNNFNR

Frolking, S., Wisser, D., Grogan, D., Proussevitch, A., & Glidden, S. (2020). *GAEZ+_2015 Crop Harvest Area* [Data set]. Harvard Dataverse. https://doi.org/10.7910/DVN/KAGRFI

Geodata - GISCO - Eurostat. (2021). Retrieved 9 October 2021, from https://ec.europa.eu/eurostat/web/gisco/geodata

Global Human Settlement - Download - European Commission. (2021). Retrieved 9 October 2021, from https://ghsl.jrc.ec.europa.eu/download.php

Hellenic Statistical Authority. (2015). Areas *and production* (Table 01-Table 07). Retrieved 15 February 2022, from https://www.statistics.gr/en/statistics/-/publication/SPG06/2015

Natura 2000 data and maps - Environment - European Commission. (2021). Retrieved 9 October 2021, from https://ec.europa.eu/environment/nature/natura2000/data/index_en.htm

Schiavina, Marcello; Freire, Sergio; MacManus, Kytt (2019): GHS population grid multitemporal (1975, 1990, 2000, 2015) R2019A. European Commission, Joint Research Centre (JRC)DOI: 10.2905/42E8BE89-54FF-464E-BE7B-BF9E64DA5218 PID: http://data.europa.eu/89h/0c6b9751-a71f-4062-830b-43c9f432370f

Greek cited regulations and laws

Greek government Law 1515/1985, *Regulatory and environmental protection Plan of wider Athens Region*, Government Gazette of the Hellenic Republic (18/A/18.2.1985) (in Greek)

Greek government Law 4277/2014, *New Regulatory Plan of Athens Attica*, Government Gazette of the Hellenic Republic (156/A/1.8.2014) (in Greek)

Appendix A (Preprocessing of SLEUTH and crop data)

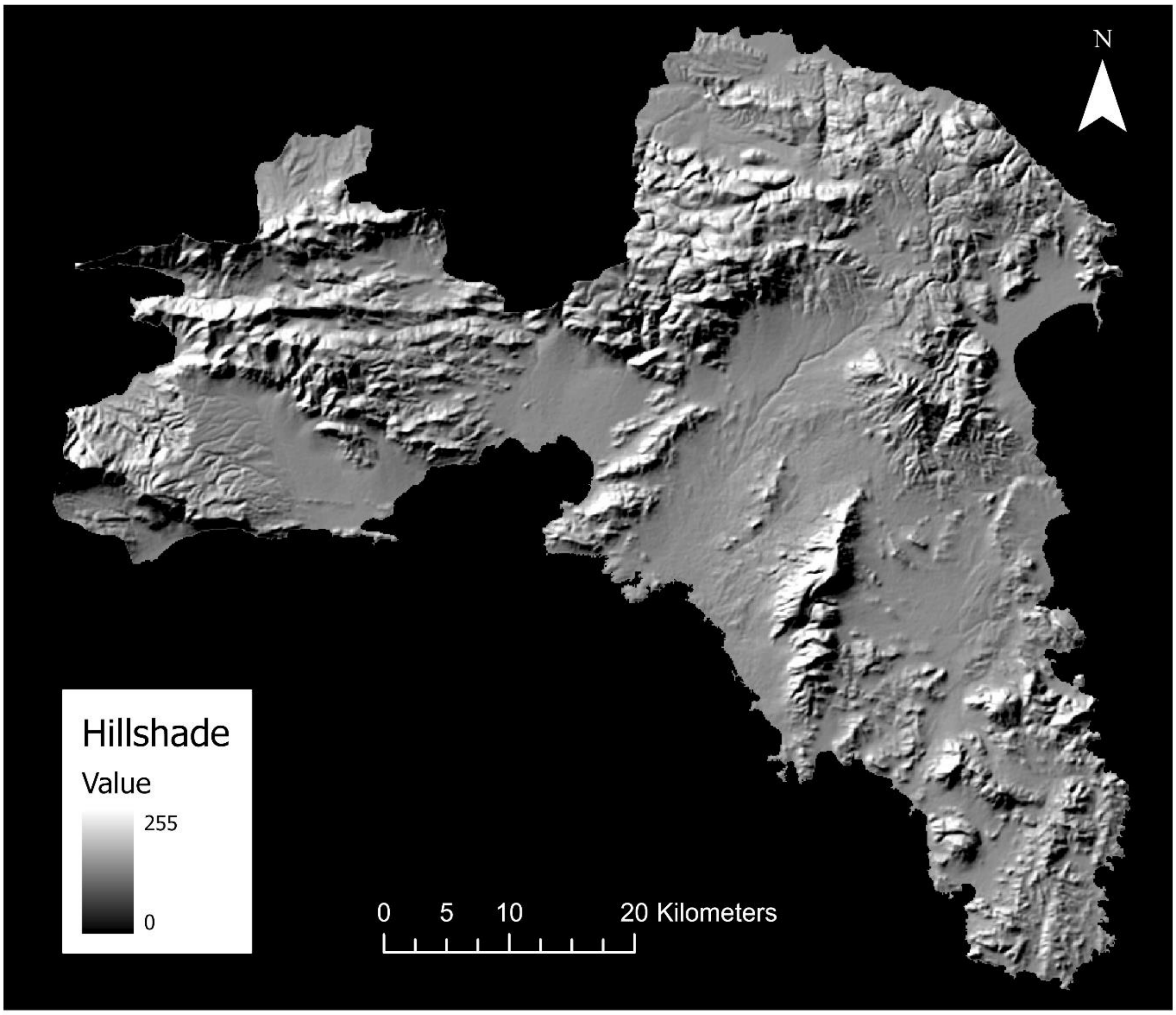

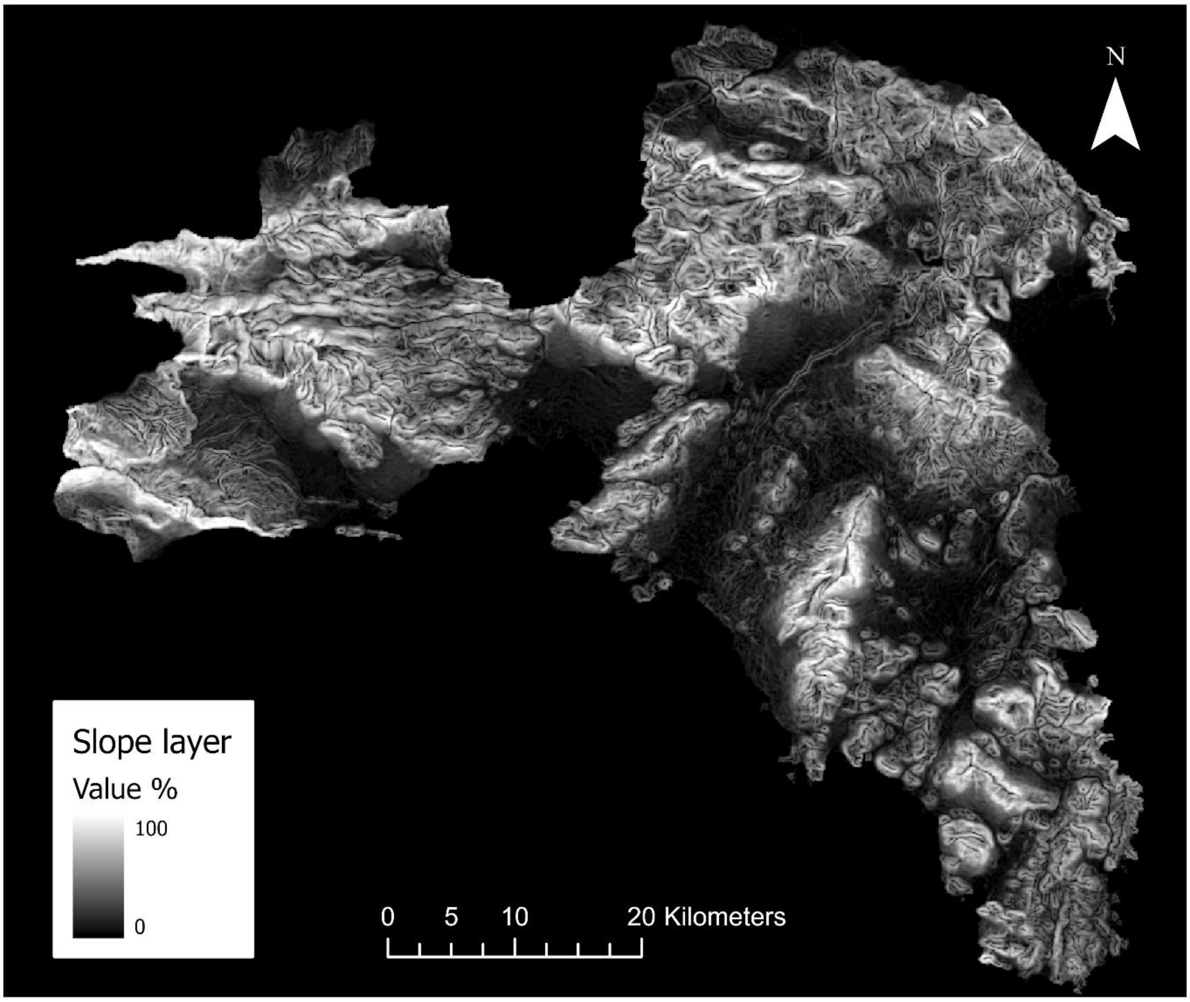

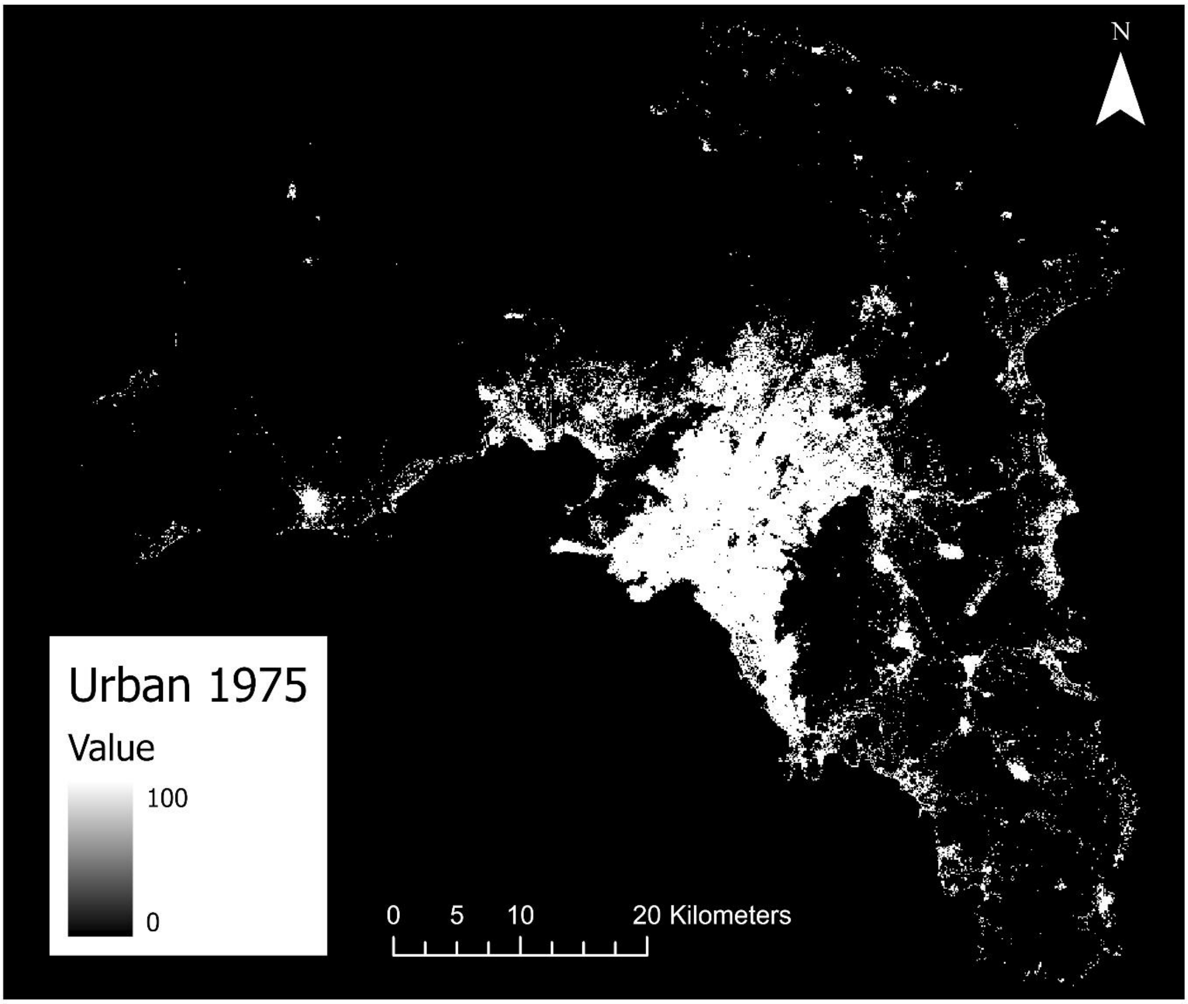
N
Urban 1975
Value
100
0
0 5 10 20 Kilometers

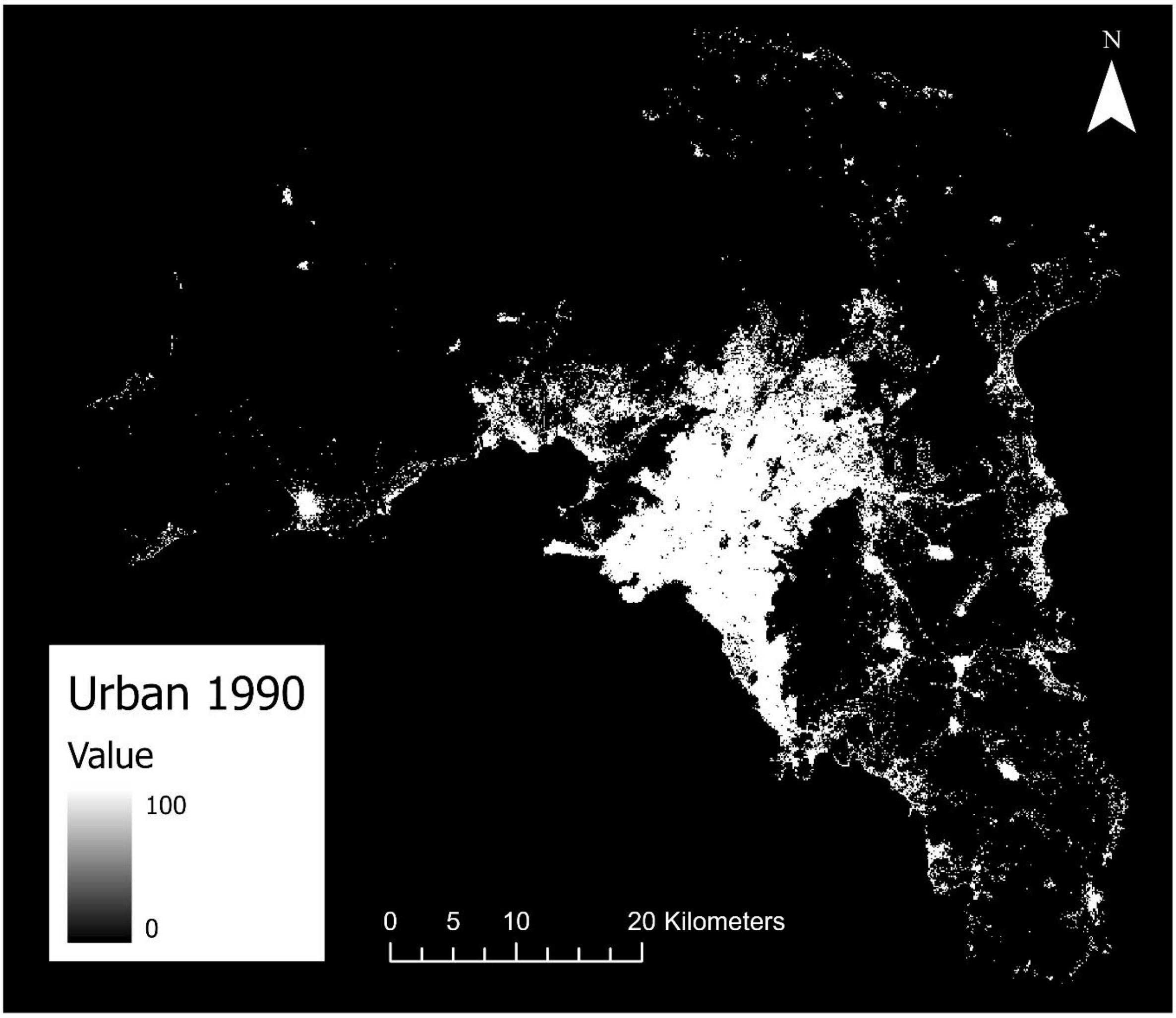
N
Urban 1990
Value
100
0
0 5 10 20 Kilometers

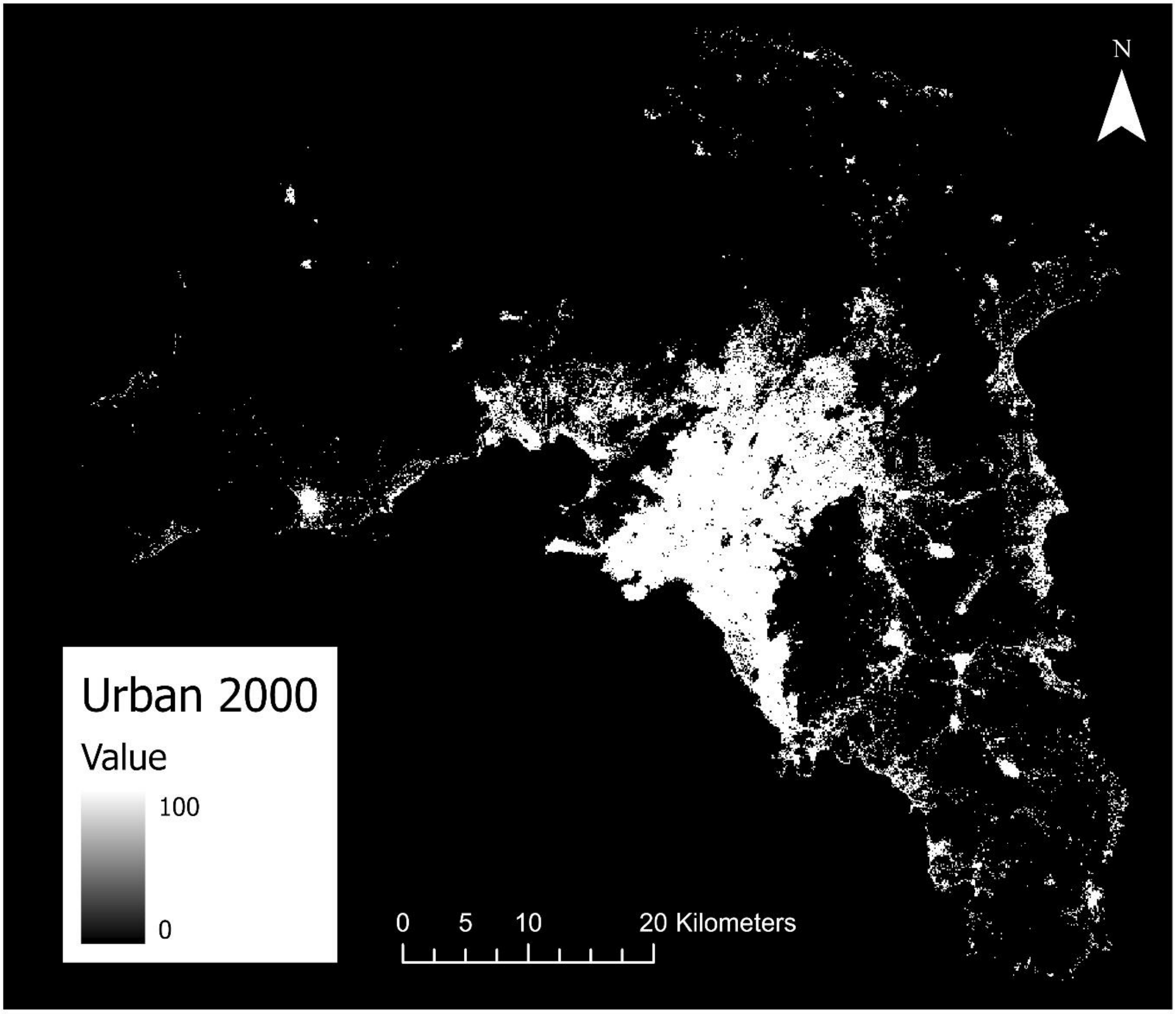
N
Urban 2000
Value
100
0
0 5 10 20 Kilometers

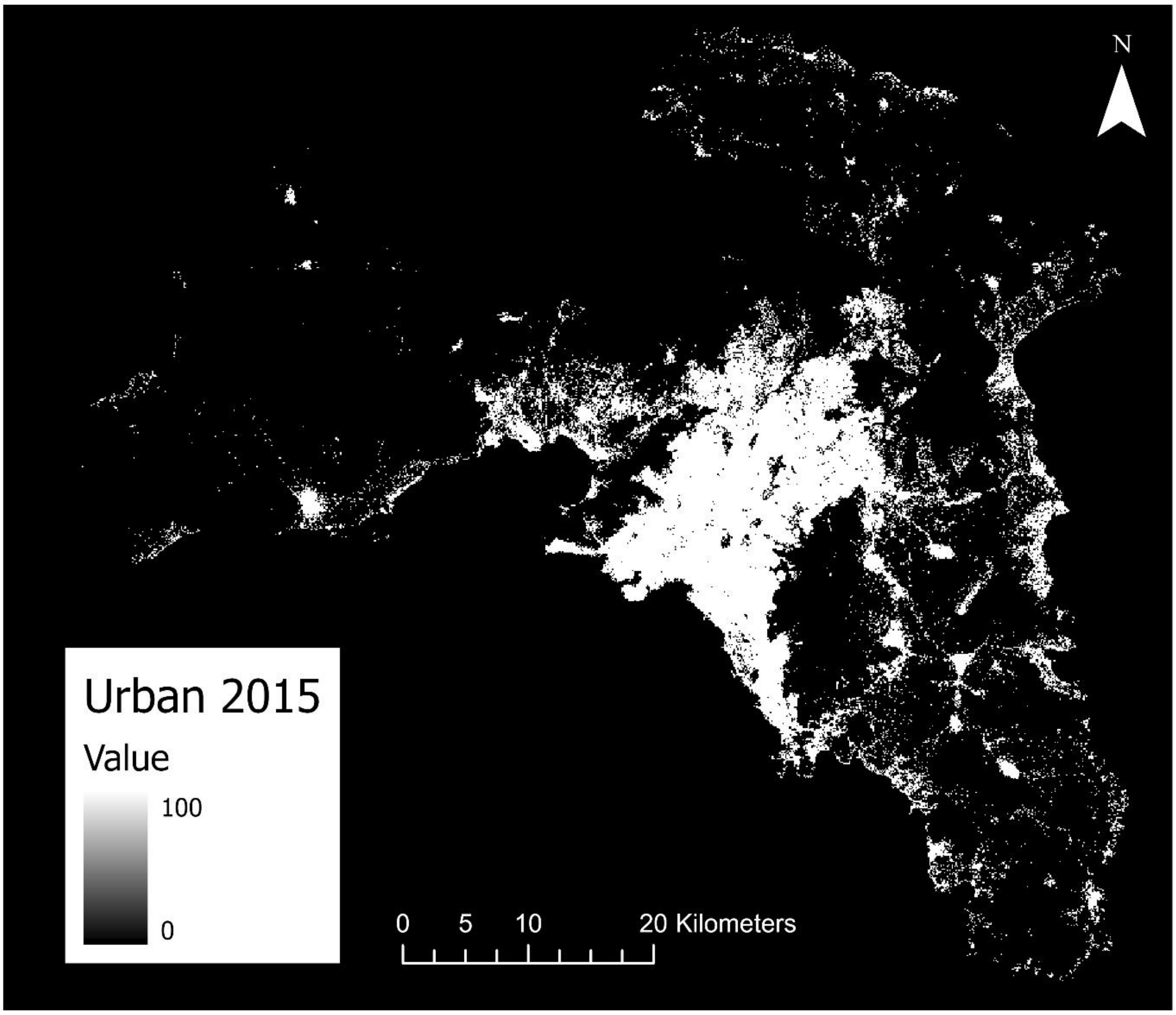
N
Urban 2015
Value
100
0
0 5 10 20 Kilometers

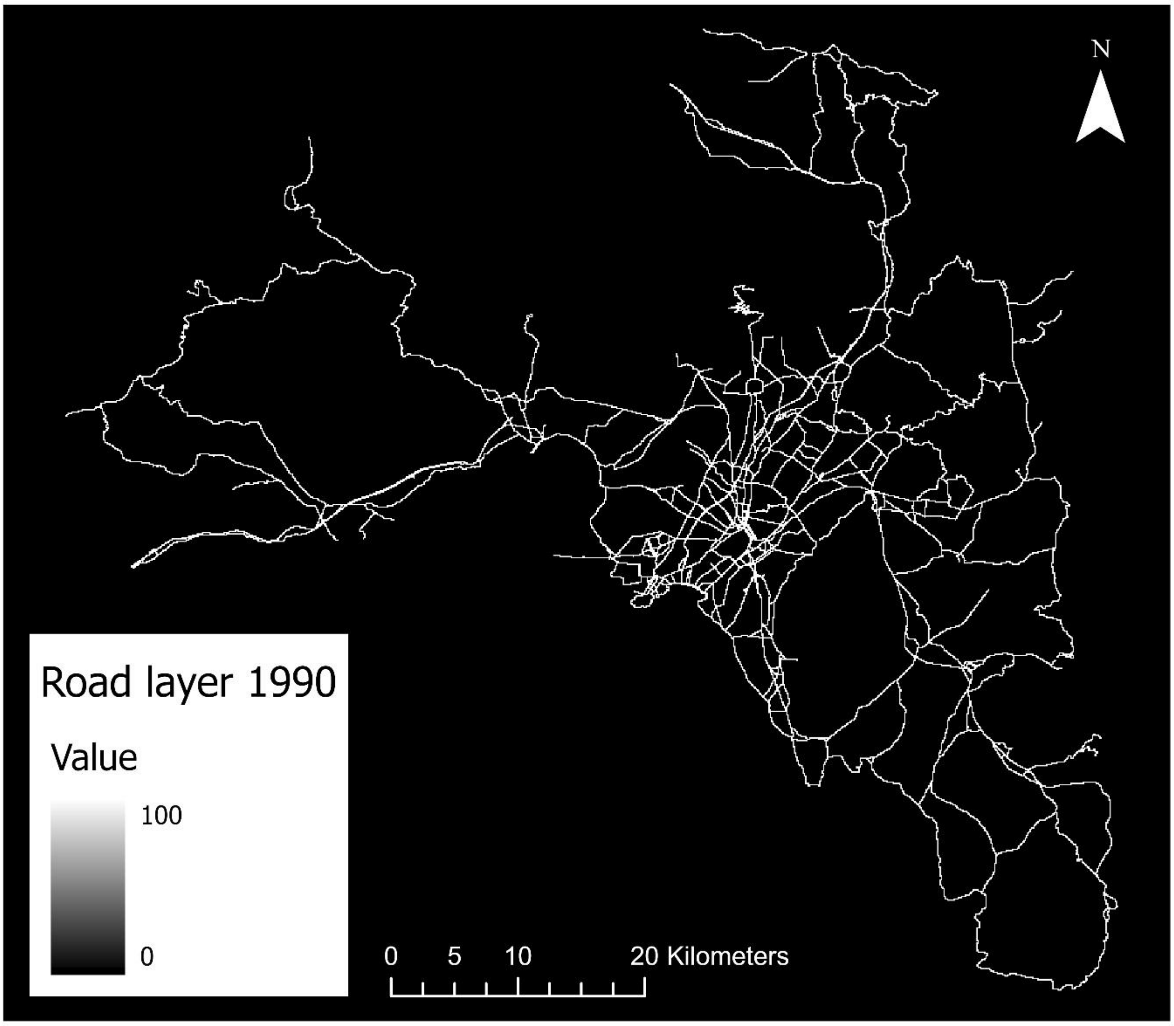
N
Road layer 1990
Value
100
0
0 5 10 20 Kilometers

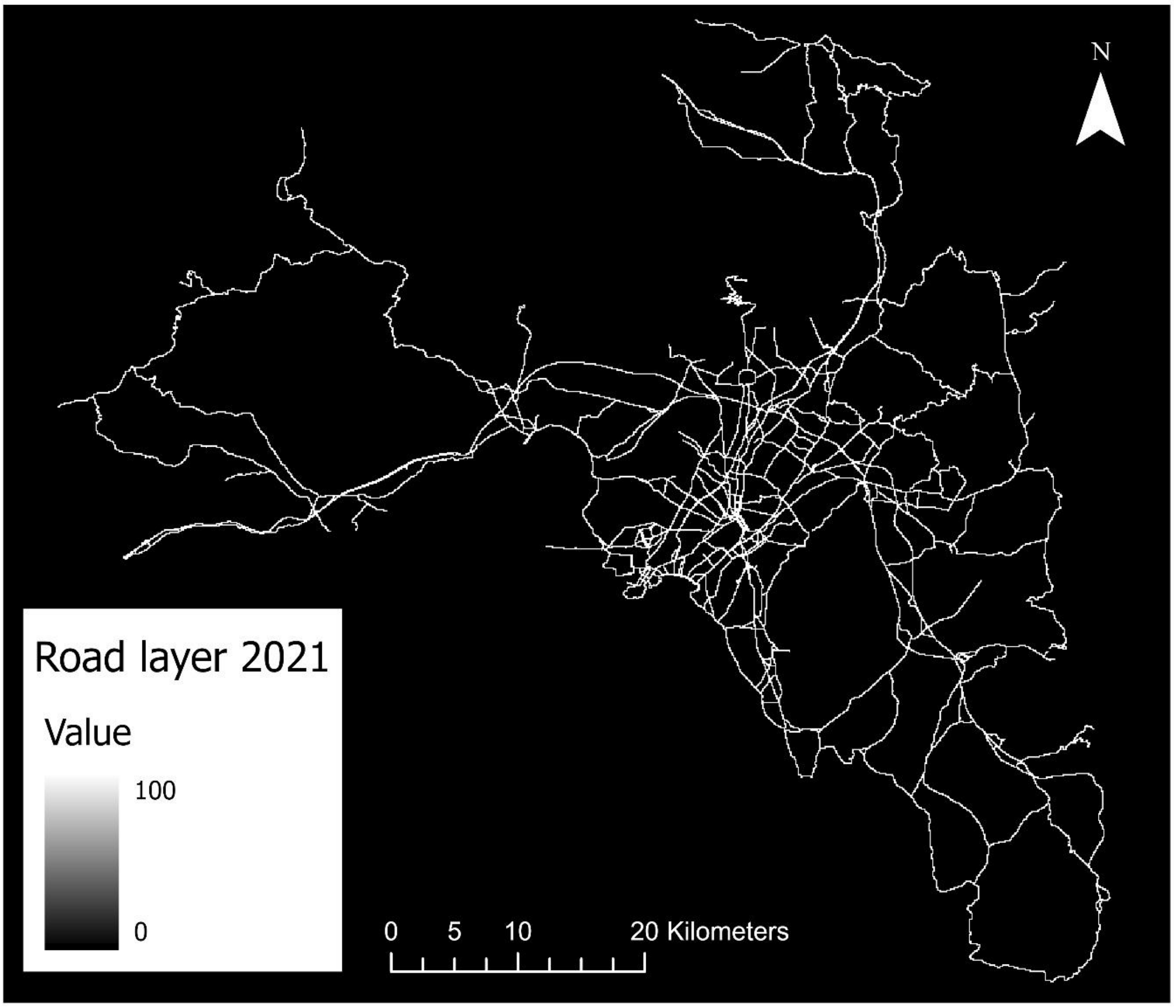
N
Road layer 2021
Value
100
0
0 5 10 20 Kilometers

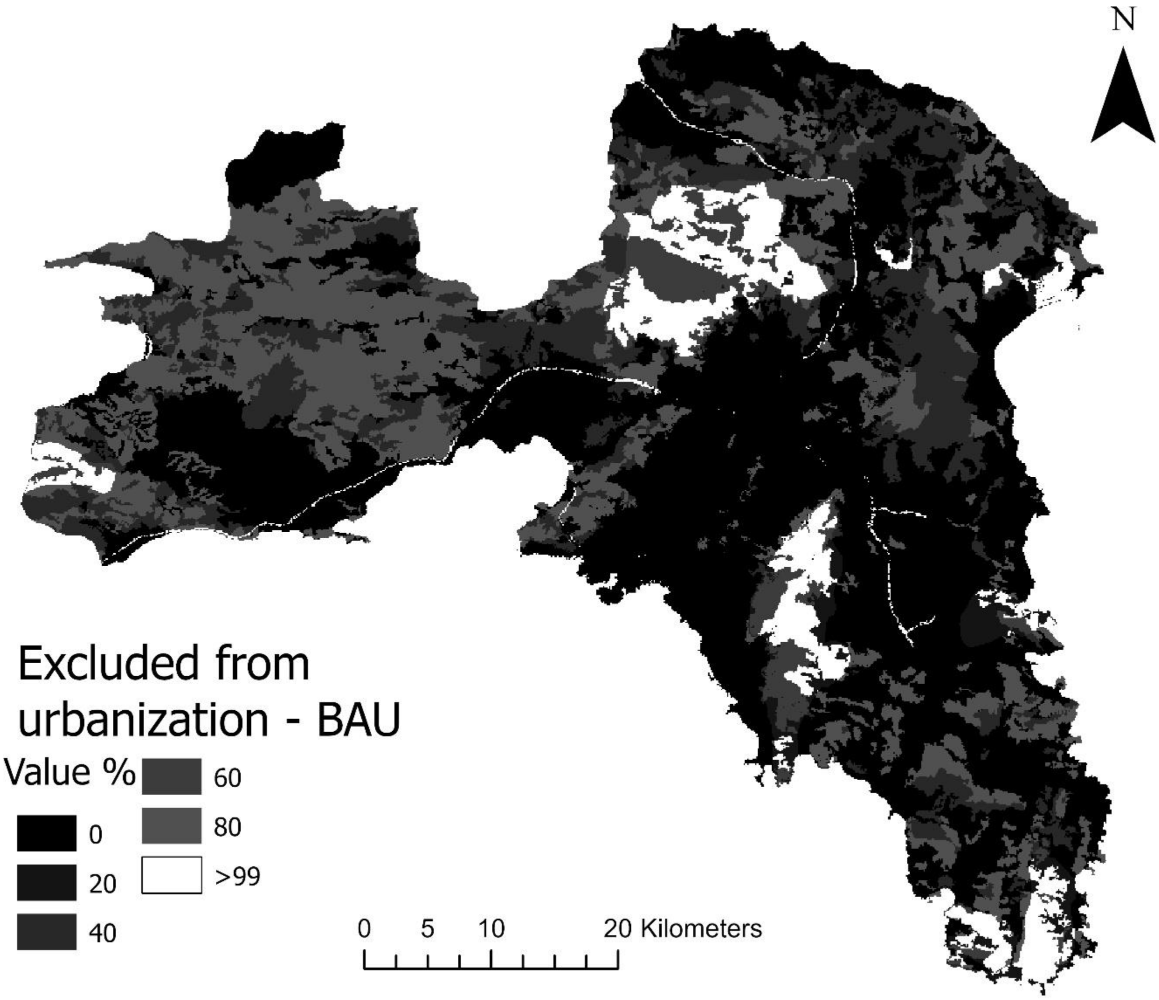
N
Excluded from urbanization - BAU
Value %
0
20
40
60
80
>99
0 5 10 20 Kilometers

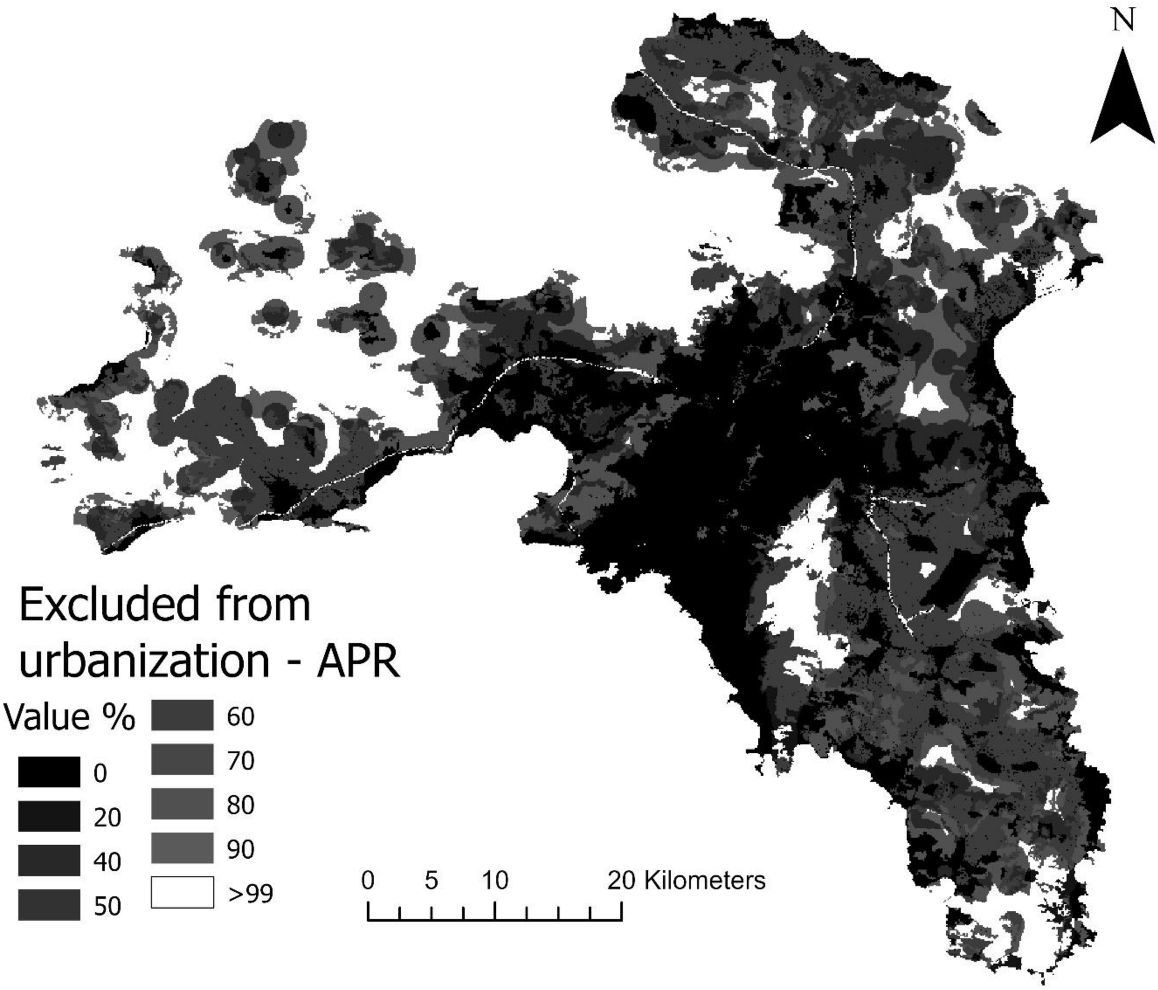
N
Excluded from urbanization - APR
Value %
0
20
40
50
60
70
80
90
>99
0 5 10 20 Kilometers

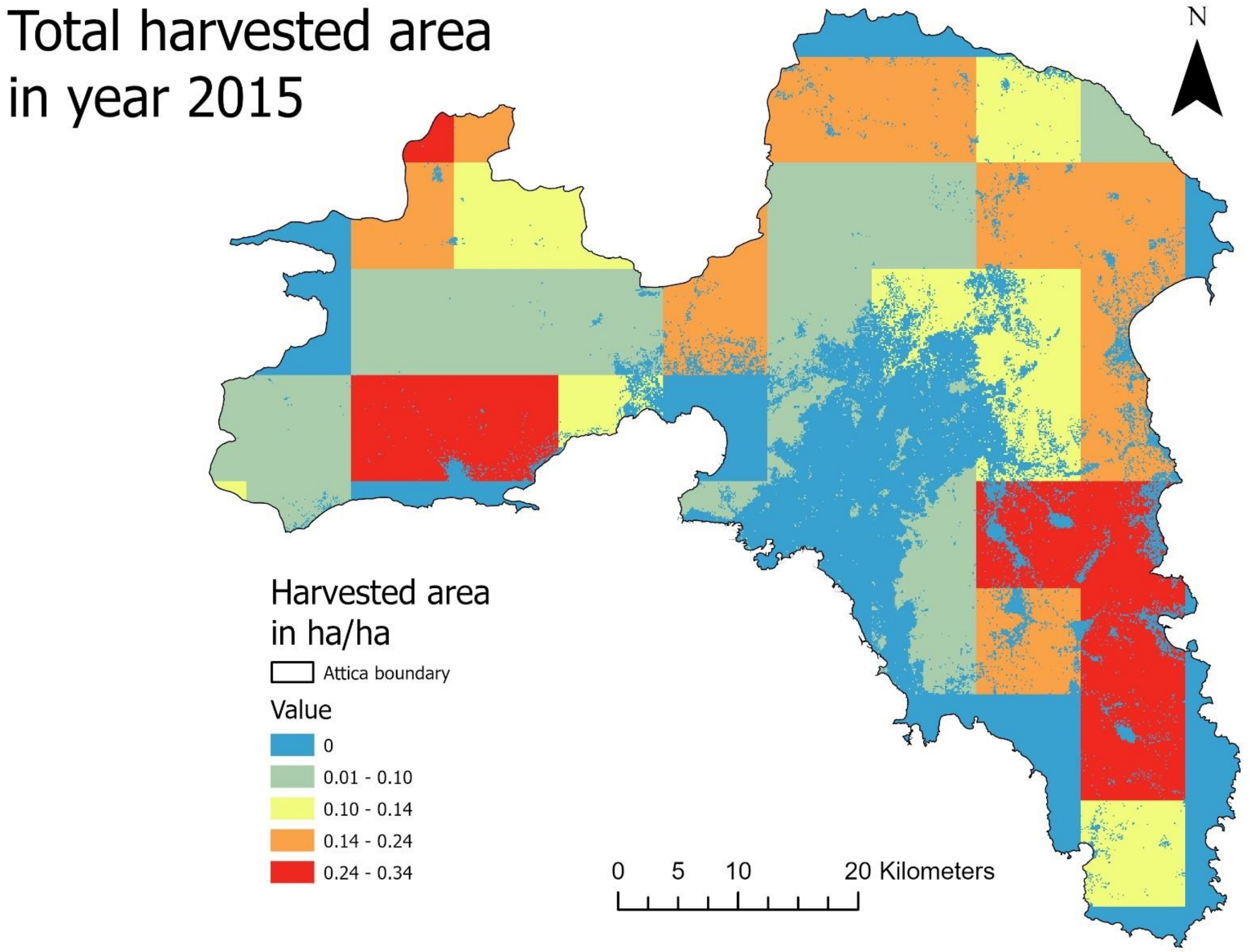
Total harvested area
in year 2015
N
Harvested area
in ha/ha
Attica boundary
Value
0
0.01 - 0.10
0.10 - 0.14
0.14 - 0.24
0.24 - 0.34
0 5 10 20 Kilometers

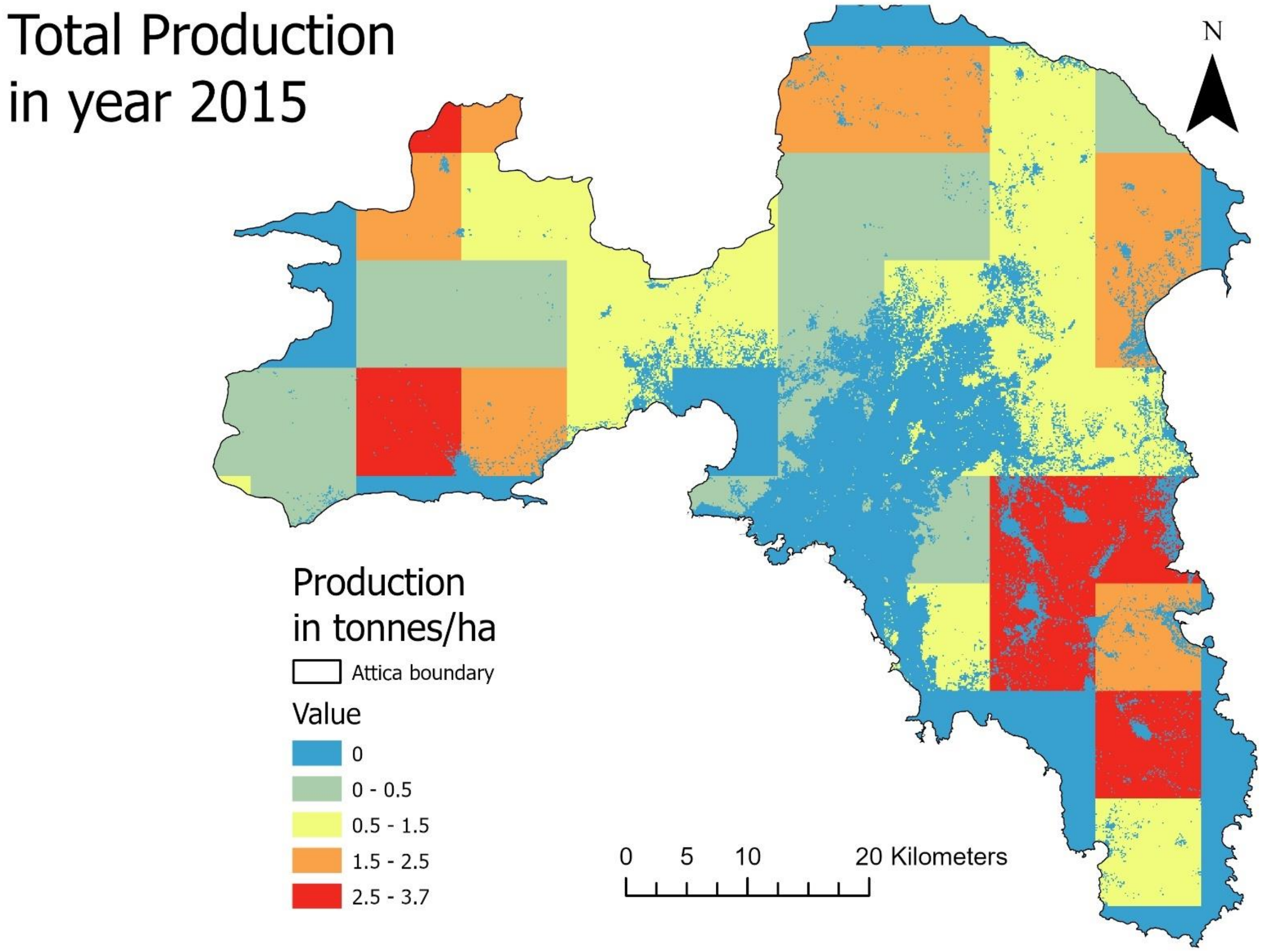
Total Production
in year 2015
N
Production
in tonnes/ha
Attica boundary
Value
0
0 - 0.5
0.5 - 1.5
1.5 - 2.5
2.5 - 3.7
0 5 10 20 Kilometers

Appendix B (Evaluation of SLEUTH's performance)

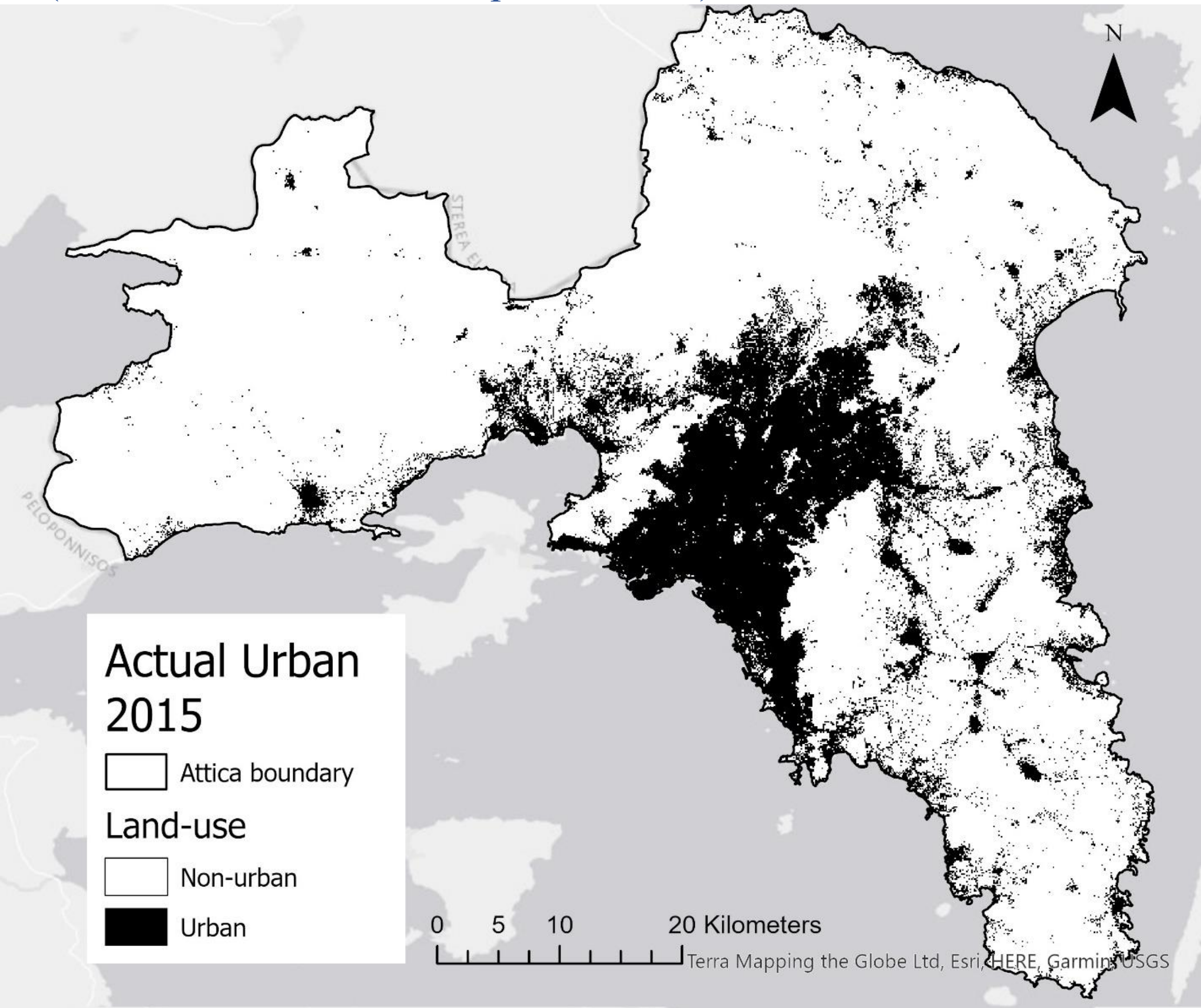

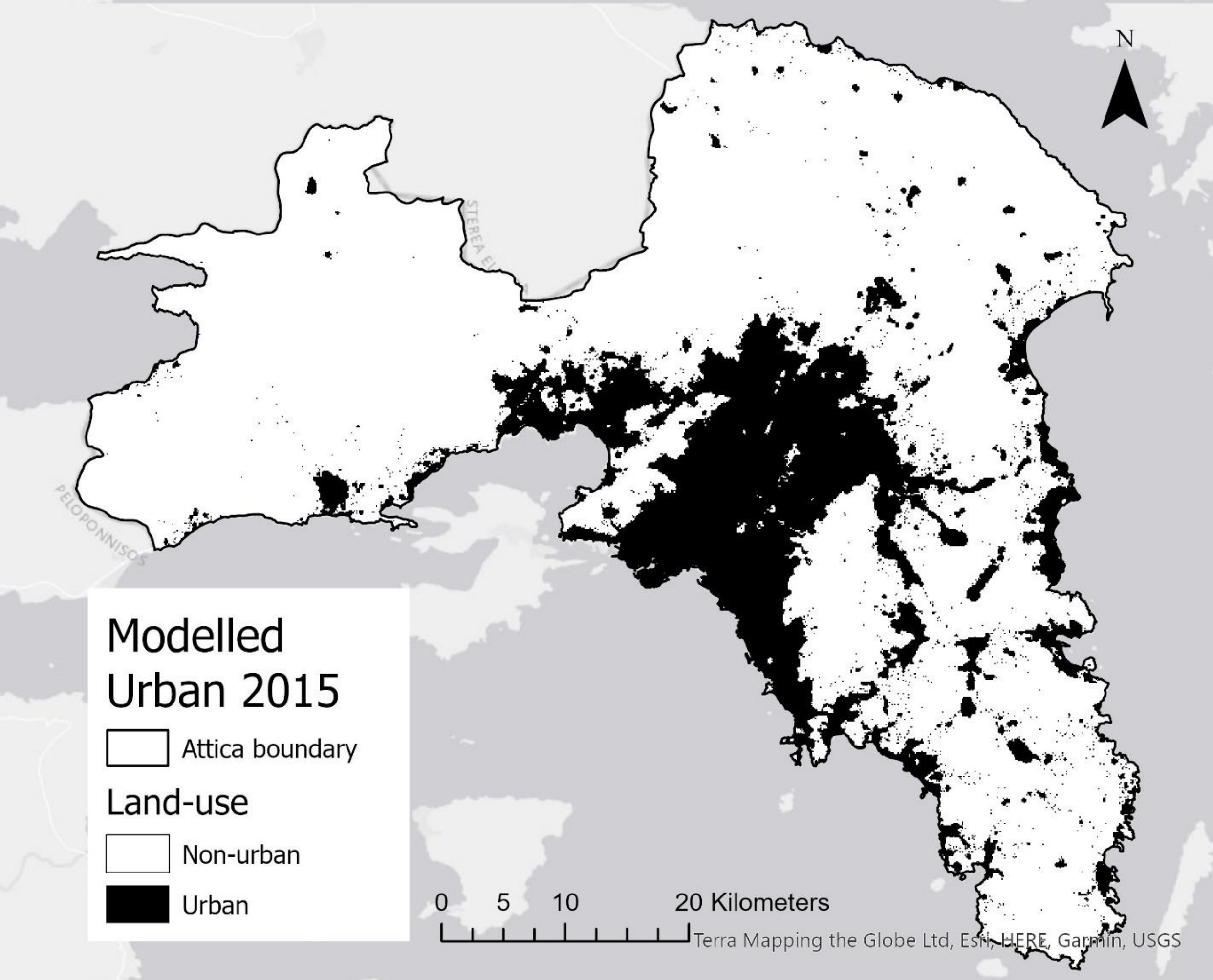

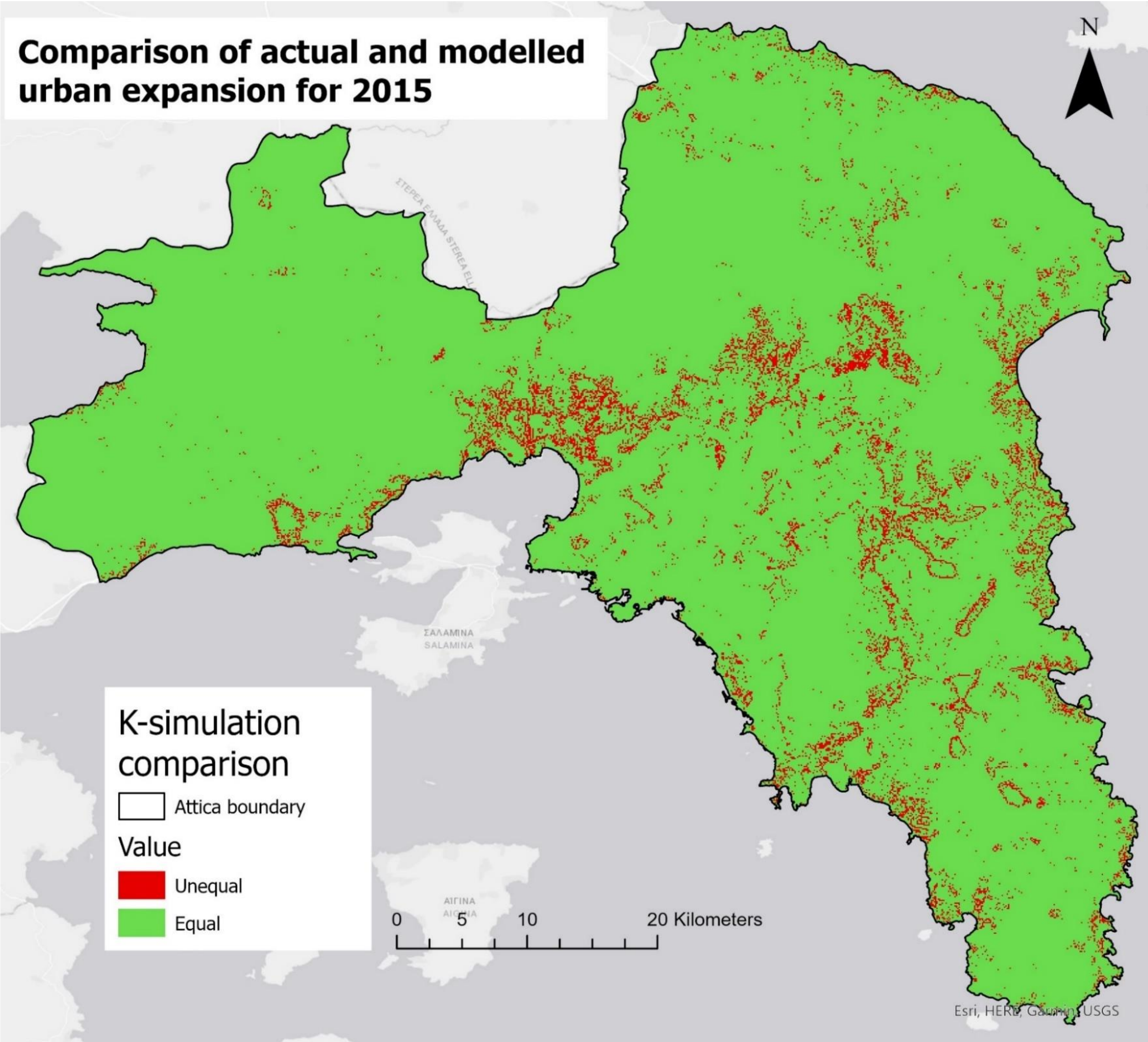

Comparison of actual and modelled urban expansion for 2015
N
ΣΤΕΡΕΑ ΕΛΛΑΔΑ STEREA ELL
ΣΑΛΑΜΙΝΑ
SALAMINA
K-simulation comparison
Attica boundary
Value
Unequal
Equal
ΑΙΓΙΝΑ
0 5 10 20 Kilometers
Esri, HERE, Garmin, USGS

Appendix C (Simulation results and impact assessment)

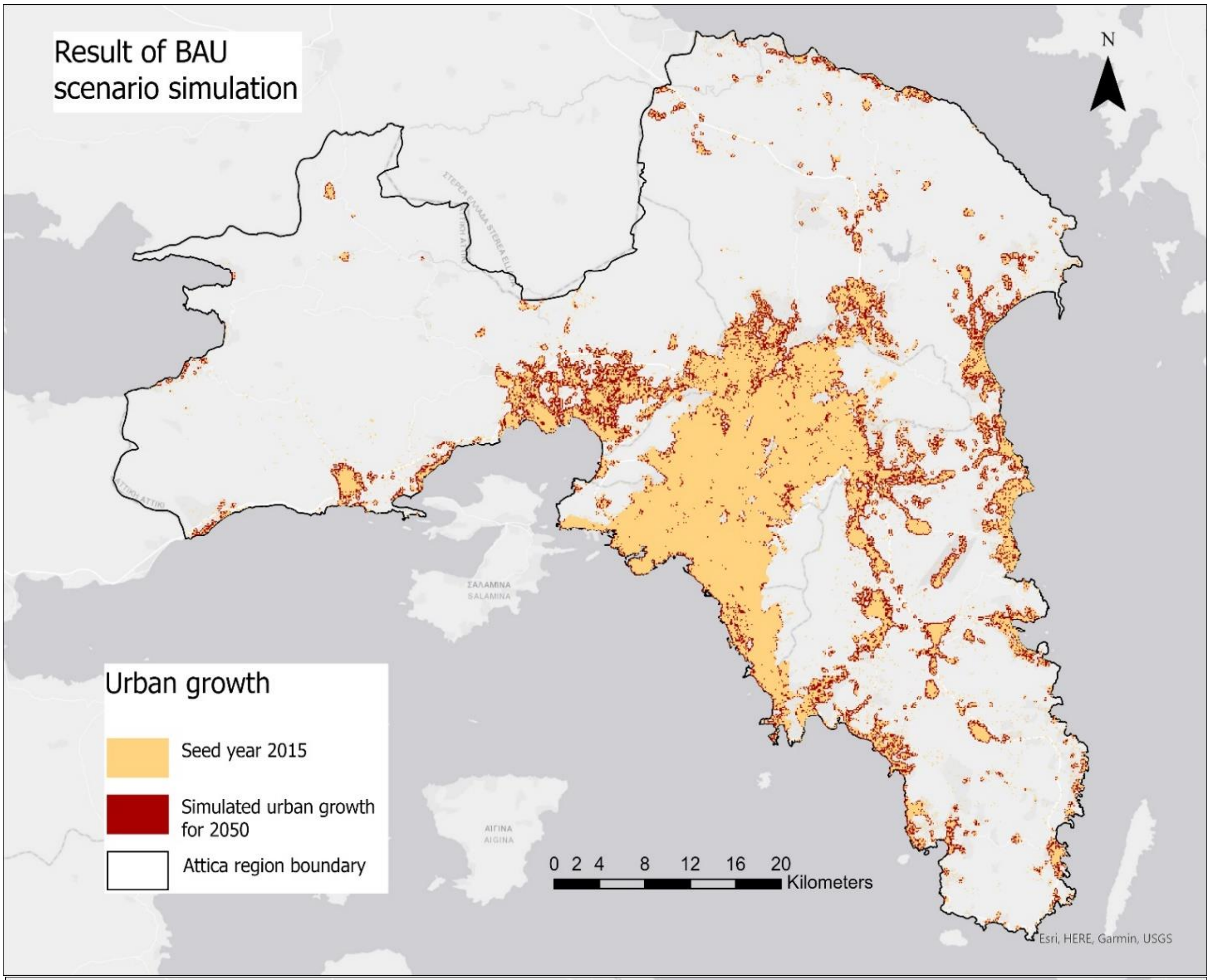

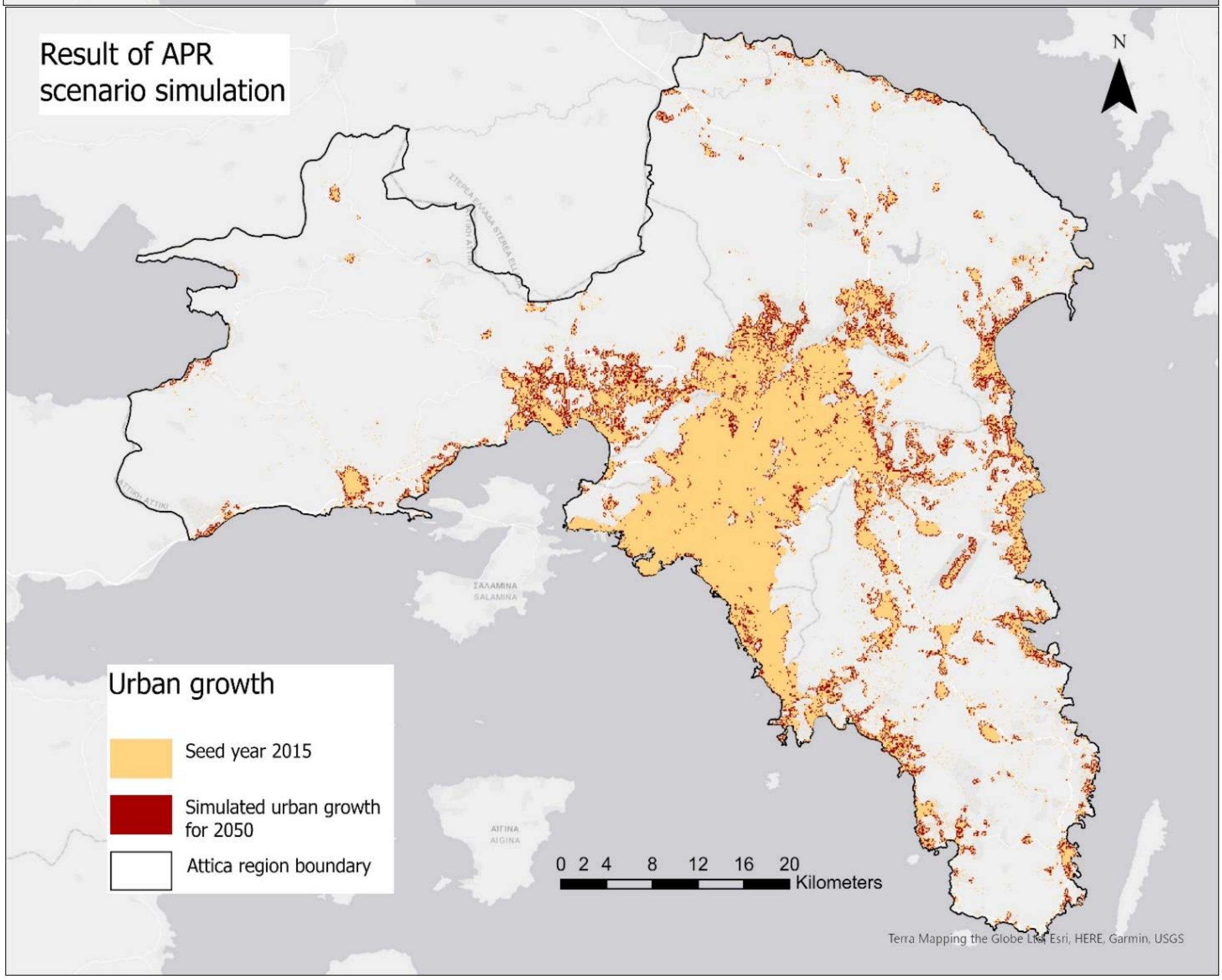

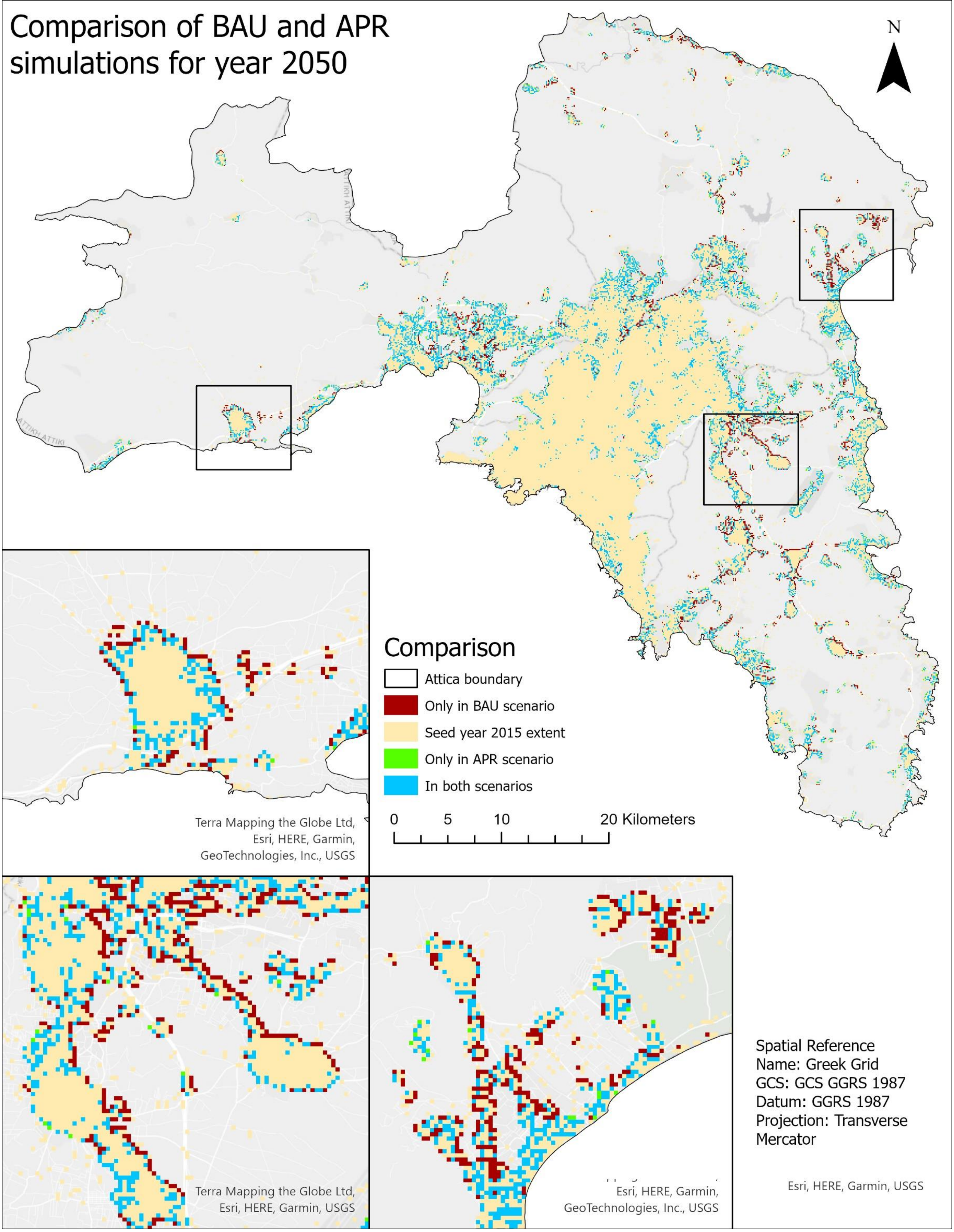
Comparison of BAU and APR simulations for year 2050
N
Comparison
Attica boundary
Only in BAU scenario
Seed year 2015 extent
Only in APR scenario
In both scenarios
0 5 10 20 Kilometers
Terra Mapping the Globe Ltd, Esri, HERE, Garmin, GeoTechnologies, Inc., USGS
Terra Mapping the Globe Ltd, Esri, HERE, Garmin, USGS
Esri, HERE, Garmin, GeoTechnologies, Inc., USGS
Spatial Reference
Name: Greek Grid
GCS: GCS GGRS 1987
Datum: GGRS 1987
Projection: Transverse Mercator
Esri, HERE, Garmin, USGS

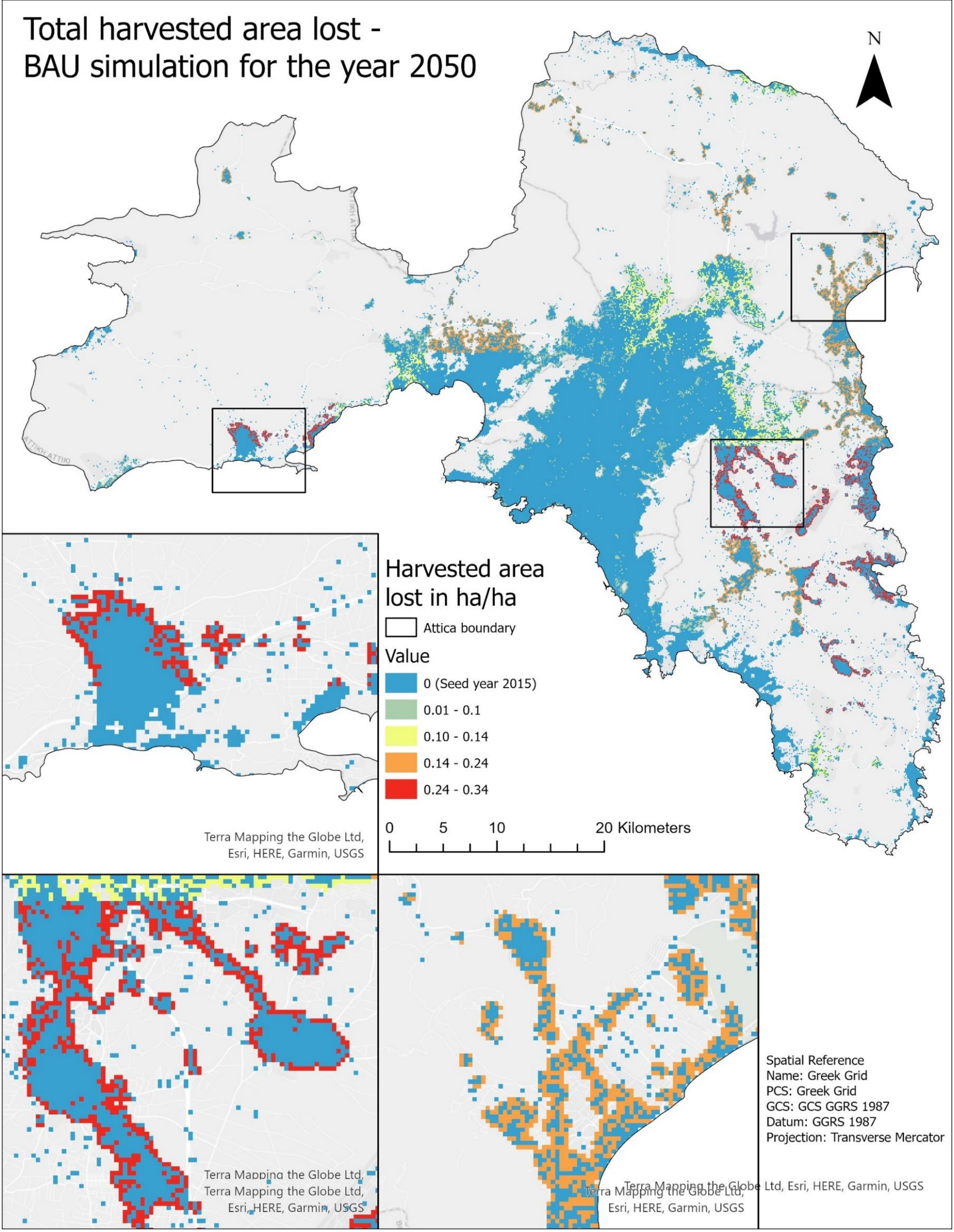
Total harvested area lost -
BAU simulation for the year 2050
N
Harvested area
lost in ha/ha
Attica boundary
Value
0 (Seed year 2015)
0.01 - 0.1
0.10 - 0.14
0.14 - 0.24
0.24 - 0.34
0
5
10
20 Kilometers
Terra Mapping the Globe Ltd,
Esri, HERE, Garmin, USGS
Spatial Reference
Name: Greek Grid
PCS: Greek Grid
GCS: GCS GGRS 1987
Datum: GGRS 1987
Projection: Transverse Mercator
Terra Mapping the Globe Ltd, Esri, HERE, Garmin, USGS

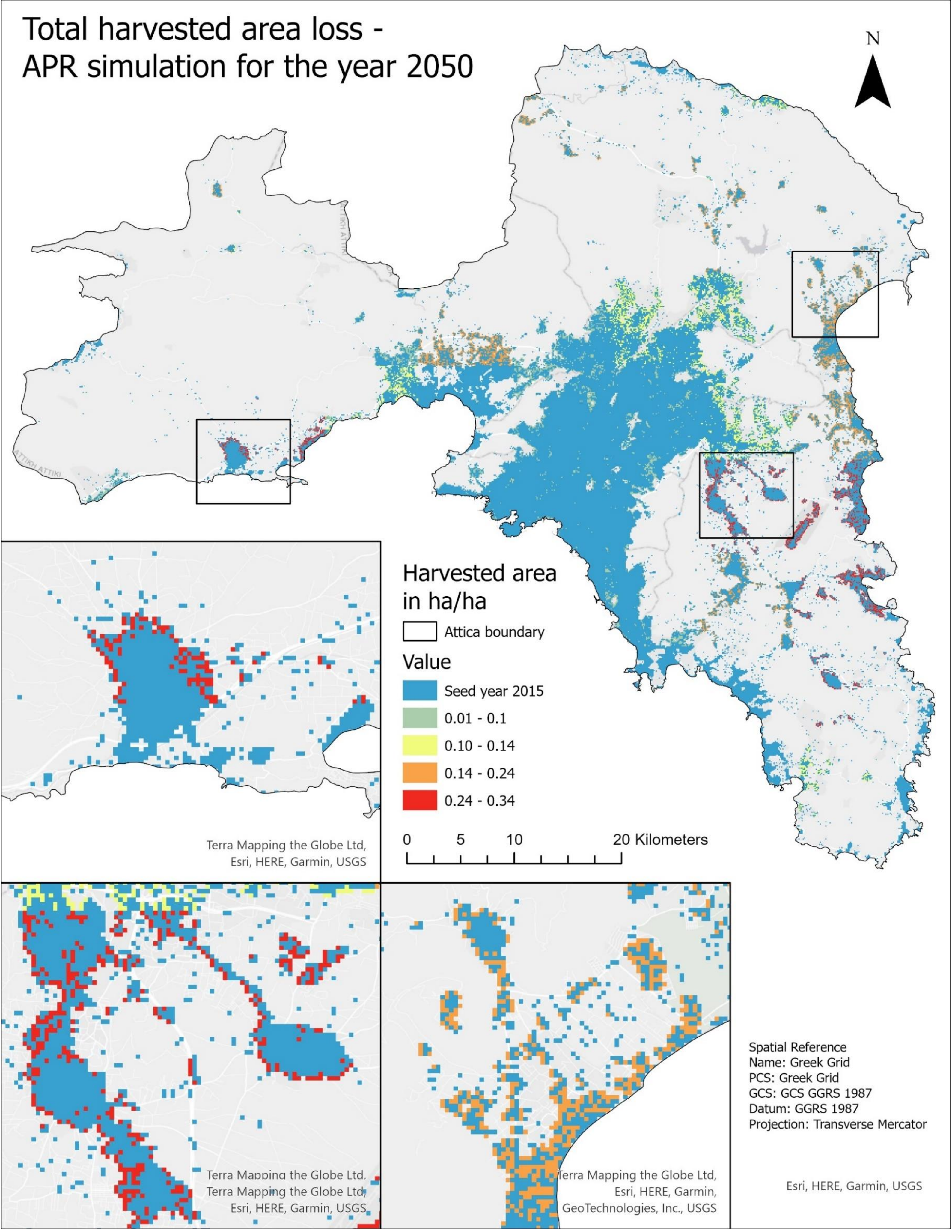
Total harvested area loss -
APR simulation for the year 2050
N
Harvested area
in ha/ha
Attica boundary
Value
Seed year 2015
0.01 - 0.1
0.10 - 0.14
0.14 - 0.24
0.24 - 0.34
0
5
10
20 Kilometers
Terra Mapping the Globe Ltd,
Esri, HERE, Garmin, USGS
Terra Mapping the Globe Ltd,
Terra Mapping the Globe Ltd,
Esri, HERE, Garmin, USGS
Terra Mapping the Globe Ltd,
Esri, HERE, Garmin,
GeoTechnologies, Inc., USGS
Spatial Reference
Name: Greek Grid
PCS: Greek Grid
GCS: GCS GGRS 1987
Datum: GGRS 1987
Projection: Transverse Mercator
Esri, HERE, Garmin, USGS

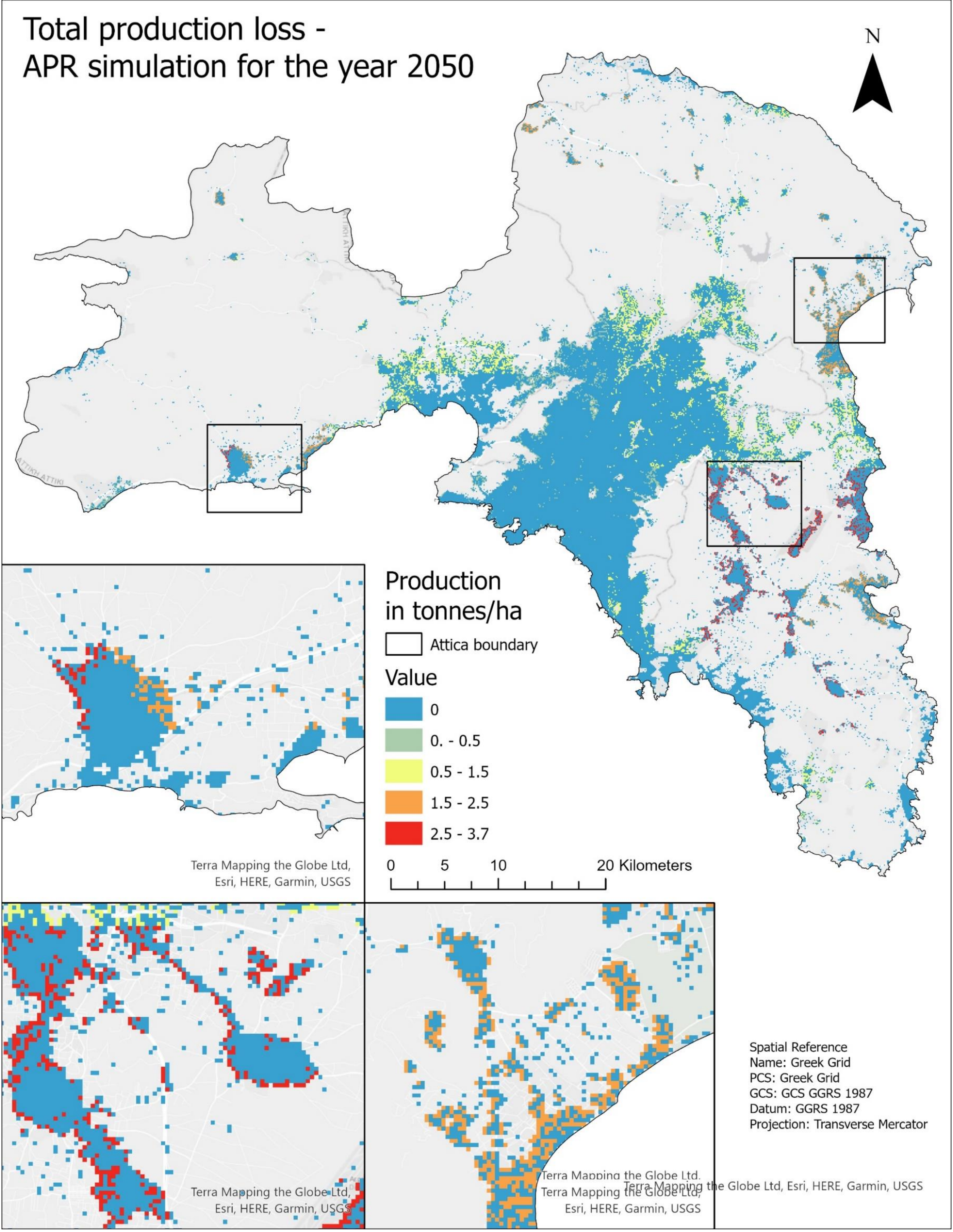
Total production loss -
APR simulation for the year 2050
N
Production
in tonnes/ha
Attica boundary
Value
0
0. - 0.5
0.5 - 1.5
1.5 - 2.5
2.5 - 3.7
0
5
10
20 Kilometers
Terra Mapping the Globe Ltd,
Esri, HERE, Garmin, USGS
Terra Mapping the Globe Ltd,
Esri, HERE, Garmin, USGS
Terra Mapping the Globe Ltd,
Terra Mapping the Globe Ltd,
Esri, HERE, Garmin, USGS
Terra Mapping the Globe Ltd, Esri, HERE, Garmin, USGS
Spatial Reference
Name: Greek Grid
PCS: Greek Grid
GCS: GCS GGRS 1987
Datum: GGRS 1987
Projection: Transverse Mercator

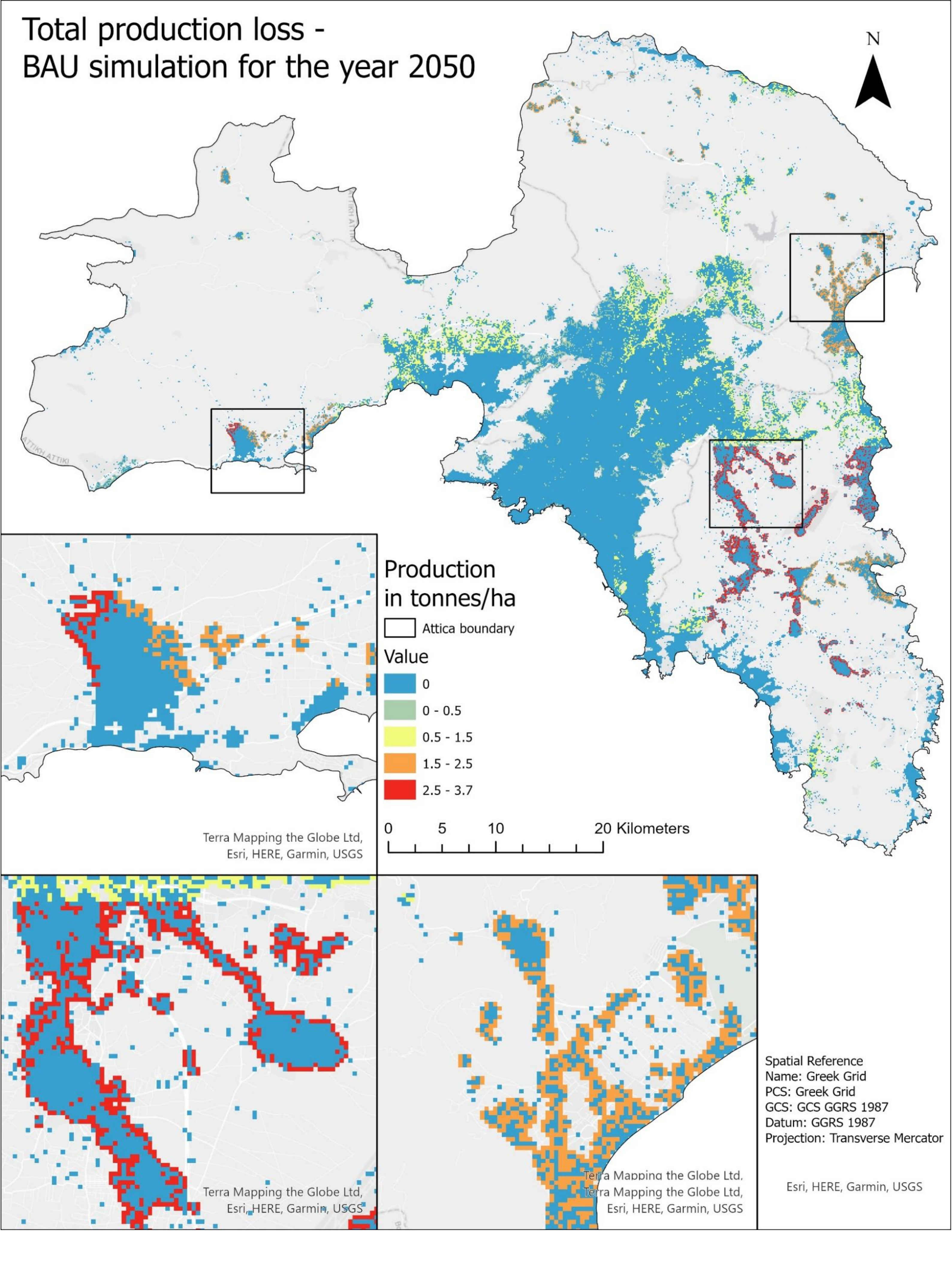
Total production loss -
BAU simulation for the year 2050
N
Production
in tonnes/ha
Attica boundary
Value
0
0 - 0.5
0.5 - 1.5
1.5 - 2.5
2.5 - 3.7
0 5 10 20 Kilometers
Terra Mapping the Globe Ltd,
Esri, HERE, Garmin, USGS
Spatial Reference
Name: Greek Grid
PCS: Greek Grid
GCS: GCS GGRS 1987
Datum: GGRS 1987
Projection: Transverse Mercator
Esri, HERE, Garmin, USGS